

OPTIMIZATION OF REFRIGERATION CYCLE

NANDHINI BALAJI

School of Electrical and Electronic Engineering

A thesis submitted to the Nanyang Technological University
in partial fulfillment of the requirement for the degree of
Master of Engineering

2010

Acknowledgements

First and foremost, I express my sincere gratitude to my supervisor, Associate Professor Dr. Cai Wenjian, for his tremendous support, and invaluable guidance throughout the course of my research work. His easy nature has always encouraged me to approach him for any research clarifications and he has been forever enthusiastic to clarify them.

I particularly thank Dr. Ding Xudong for his continuous guidance and for the help that I have received from him throughout the duration of my research. I am sincerely obliged to him for answering my questions and correcting my mistakes whenever I have erred.

I also thank my colleagues and seniors in the Process Instrumentation Laboratory and laboratory incharge Mr. Yock for their help during the course of my study.

I owe my degree to my family from whom I have received steadfast support and understanding. Thanks also to my friends for their presence and their help to complete my research.

Table of Contents

Acknowledgements	i
Table of Contents	ii
Summary	v
List of Figures	vi
List of Tables	ix
Nomenclature	x
1. Introduction	1
1.1 Background and Motivation.....	1
1.2 Objective	6
1.3 Contributions.....	6
1.4 Thesis Outline	8
2. Fundamentals of VCC and GA	10
2.1 Vapour Compression Cycle	10
2.1.1 Working Principle	11
2.2 Genetic Algorithms.....	15
2.2.1 Characteristics of Genetic Algorithms	16
2.2.2 Population Initialization and Encoding.....	17
2.2.3 Objective Function and Fitness Function.....	18

2.2.4 Genetic Algorithm Methodology and Flowchart.....	19
3. Modelling of vapour compression cycle.....	24
3.1 Evaporator Modelling.....	24
3.2 Modelling of Condenser.....	29
3.3 Modelling of Expansion Valve.....	34
3.4 Modelling of Compressor.....	35
3.5 Modelling of Evaporator and Condenser fans.....	37
4. VCC and Optimization Implementation.....	40
4.1 Problem Definition.....	40
4.1.1 Mechanical constraints.....	41
4.1.2 Operational constraints.....	42
4.1.3 Other Important Constraints.....	44
4.2 Variable Relationships.....	45
4.3 Model based Optimization-Vapour Compression Cycle.....	50
4.3.1 Optimization Algorithms.....	52
4.3.2 Subroutine.....	55
4.3.3 VCC Optimization Flowcharts.....	57
4.3.4 Explanation of penalty functions.....	60
5. Implementation and Results.....	62
5.1 Basic Optimization Results.....	62

5.1.1 Initialization and Assumptions.....	62
5.1.2 GA implementation and Results	65
5.2 Comparison with ON-OFF Control	73
5.2.1 Comparison Base - Input Profile.....	74
5.2.2 ON-OFF Control – Base Case Study	76
5.2.3 GA optimization Control.....	81
5.2.4 Comparison	89
6. Conclusion and Future Scope.....	92
6.1 Conclusion.....	92
6.2 Discussions and Future Scope.....	94
Bibliography	96
Appendix A	99
A.1 Component Models.....	99
A.2 Parameter Models.....	101

Summary

This thesis presents the development of optimization technology for the vapour compression cycle. The steady state mathematical models for heat transfer, mass flow rate, power consumption and other intermediary parameters associated with the vapour compression cycle for different cooling loads are formulated. These models are developed using manufacturers' catalogue and data from a simulated refrigeration cycle. Later, genetic algorithm is adopted to get steady state energy optimization of vapour compression cycle. The objective function used for this purpose is summation of power consumed by the components of vapour compression cycle, while the control objective is to maintain the room temperature or to satisfy the cooling load demand. The energy optimization technique is then simulated for different cooling loads, room temperature and outside air temperature. Finally, to get a picture of the amount of savings the optimization technique can result in, the genetic algorithm based optimization technique is compared with a simulated on-off control of vapour compression cycle. The evaluation is done on the basis of a common cooling load and temperature profile for 24 hours. The results show that in comparison to on-off control, optimization control of vapour compression cycle can result in significant amount of energy savings. Summarizing the above, the thesis contributes in developing a simple and straightforward energy optimization technique using hybrid modelling of evaporator and condenser as the basis of mathematical model for vapour compression cycle.

List of Figures

Figure 1.1: Optimal Control – set-point and dynamic optimizing control	3
Figure 1.2: Block diagram of a typical HVAC system.....	4
Figure 2.1: Layout of Vapour Compression Cycle	12
Figure 2.2: Pressure enthalpy diagram of vapour compression cycle. $h - \log(p)$ diagram.	13
Figure 2.3: Example of Roulette Wheel Selection.....	20
Figure 2.4: Simple Genetic Algorithm Flowchart	23
Figure 3.1: Basic Structure of Evaporator	26
Figure 3.2: Representation of Heat transfer in Evaporator	27
Figure 3.3: Basic Structure of condenser.....	30
Figure 3.4: Representation of heat transfer in condenser	31
Figure 3.5: Mass flow rate Vs Differential pressure for different valve openings .	35
Figure 3.6: Compressor Power consumption – varying P_e	36
Figure 3.7: Compressor Power Consumption - varying P_c	37
Figure 3.8: Evaporator fan Power Consumption	38
Figure 3.9: Condenser fan Power Consumption	39
Figure 4.1: Temperature Vs Pressure Diagram.....	42
Figure 4.2: Saturation temperature T_c Vs Saturation pressure P_c	46

Figure 4.3: Saturation temperature T_e Vs Saturation pressure P_c	47
Figure 4.4: Enthalpies Involved in evaporation.....	47
Figure 4.5: Vapour enthalpy of refrigerant in evaporator.....	48
Figure 4.6: Liquid Enthalpy $H_{e,i}$ Vs Saturation pressure P_c	48
Figure 4.7: Enthalpy of liquid-vapour mixture in Condenser.....	49
Figure 4.8: Control Structure for Optimization	51
Figure 4.9: VCC with parameters	55
Figure 4.10: Flowchart for application of GA on optimization problem.....	58
Figure 4.11: Subroutine – VCC Model and objective function.....	59
Figure 4.12: Heat flow diagram in VCC.....	60
Figure 5.1a: Input profile 1, T_{SFe1} , T_{SFc1} , Q_{load}	63
Figure 5.1b: Input profile 2, T_{SFe2} , T_{SFc2}	64
Figure 5.2: Heat transfer in evaporator	68
Figure 5.3: Heat transfer in condenser.....	69
Figure 5.4a: Objective Function Convergence – Q_{load} – 0.95 kW to 1.1 kW	70
Figure 5.4b: Objective Function Convergence – Q_{load} – 1.15 kW to 1.3 kW	71
Figure 5.5: Vapour compression cycle power consumption.....	72
Figure 5.6: Power consumption – Compressor, Condenser fan, Evaporator fan...	73
Figure 5.7: Outside Air temperature profile	74
Figure 5.8: Cooling load requirement of room for outside air temperature 23°C....	75

Figure 5.9: Explanation for ON-OFF Control	76
Figure 5.10: Difference in heat content between 27°C and 23°C	78
Figure 5.11: Time taken for temperature to change, with VCC on and off.....	78
Figure 5.12: Power consumption of VCC in 24 hours.....	80
Figure 5.13: VCC energy consumption in 24 hours	81
Figure 5.14: Cooling load profiles for varying room temperature.....	82
Figure 5.15: Cooling load profile for TSP = 25 °C, in 24 hours.....	83
Figure 5.16: Flowchart for optimization based control of VCC for one whole day	85
Figure 5.17: VCC power consumption for 24 hours.....	86
Figure 5.18: Room temperature in the course of 24 hours	87
Figure 5.19: Calculated Cooling load for 24 hours.....	87
Figure 5.20: Manipulated variables values- P_e , P_c , u , m_{SFc} , m_{SFe} for 24 hours.....	88
Figure 5.21: Energy consumption of VCC (optimized control) in 24 hours	89
Figure 5.22: VCC Energy consumption– for every 3 hours (on-off Vs optimization)	90
Figure 5.23: VCC Energy consumption for 24 hours duration, in kWh.....	91

List of Tables

Table 2.1 Comparison of Binary and Gray Code	18
Table 2.2 Example of two point crossover	21
Table 5.1 Genetic Algorithm Constants.....	65
Table 5.2a: Input profile 1 - Variable values for optimized operation of VCC.....	66
Table 5.2b: Input profile 2 - Variable values for optimized operation of VCC.....	66

Nomenclature

Symbols

A	Area (m^2)
B	Constant coefficient derived from Reynolds and Prandl number
c_n, d_n	Constant coefficients
C	Constant involved in heat transfer
C_p	Specific heat capacity at constant pressure (kJ/kg/K)
ef, cf	Evaporator and condenser Fan constant coefficients
E	Energy consumed (kW)
f_q	Heat Loss factor
f_v	Expansion Valve coefficient
h_{ad}	Specific enthalpy at compressor outlet, adiabatic compression
H/h	Specific enthalpy (kJ/kg)
$HVAC$	Heating, Ventilation and Air Conditioning
J	Cost Function
K	Thermal conductivity (kW/m/K)
m	Mass flow rate (kg/s)
$ObjF$	Objective Function
P	Pressure (kPa)
Q	Heat transfer rate (kW)
Q_{23}	Heat content of room at 23°C (kW)
Q_{27-23}	Heat content difference, when temperature rises from 23 to 27°C

S	Entropy
SF_m	Metal tube and secondary flow junction
t	Time
T	Temperature ($^{\circ}\text{C}$)
T_{room}	Temperature of room ($^{\circ}\text{C}$)
U	Percentage opening of valve (%)
VCC	Vapour Compression Cycle
W	Power consumed (kW)
W_{com}	Power consumed by compressor (kW)
W_{comp}	Actual work done by the compressor (kW)
W_f	Fitness function value (kW)
$W_{penalty}$	Penalty value
W_{total}	Total power consumption (kW)
W_q	Maximum heat removal capacity (kW)

Subscripts

c	Condensation
cf	Condenser Fan
cl	Heat load in condenser
cr	Cold Storage Room / Cold reservoir
$comp$	Compressor(When represented for energy consumed)
C	Condenser
dec	Decrease
ef	Evaporator Fan

<i>e</i>	Evaporation
<i>E</i>	Evaporator
<i>f</i>	Liquid
<i>g</i>	Vapour
<i>i</i>	In
<i>inc</i>	Increase
<i>load</i>	Cooling load
<i>max</i>	Maximum
<i>min</i>	Minimum
<i>nom</i>	Nominal
<i>o</i>	Out
<i>ref</i>	Reference
<i>rel</i>	Relative
<i>sat</i>	Saturation
<i>sc</i>	Sub-cool
<i>sh</i>	Superheat
<i>SF / sf</i>	Secondary Fluid / Secondary Flow
<i>SP</i>	Set point
<i>T</i>	Temperature
<i>Troom</i>	Temperature of room
<i>v</i>	Valve
<i>WF / wf</i>	Working Fluid / Working Flow
<i>Whour</i>	Work hour

Superscripts

e_n Constant coefficient

INTRODUCTION

Chapter 1

Introduction

1.1 Background and Motivation

The vapour compression refrigeration cycle is a system widely used in industries. It basically removes heat from a cold reservoir and transfers it to a hot reservoir, by circulating a refrigerant functioning as a common working fluid between an evaporator and a condenser that act as heat exchangers.

The vapour refrigeration cycles have extensive applications in our day-to-day life and therefore play an indispensable role in sustainable development. They are used in the food processing industry, to retain freshness of perishable items for a longer time from post-harvest to consumption. In building segment, the vapour compression cycle is used for air conditioning to provide comfortable surroundings for people dwelling and working in the building. In Singapore, the four main categories of energy intensive buildings are shopping malls, hotels, office buildings and hospitals [3]; and air-conditioning contributes to 52% of electricity consumed in buildings [2]. The widespread use of refrigeration systems has hugely contributed to global warming. It

INTRODUCTION

has been estimated that a very high percentage of the global warming results from emission of CO₂ originating from the production of the energy used by the heating ventilation and air-conditioning (HVAC) processes, in the forms of electricity or other energy sources like fuel. Thus, the reduction of energy consumed in HVAC systems has been a major concern amongst researchers, environmentalists, and governments all across the world. The Building and Construction Authority, in Singapore, champions the cause of environment wherein energy efficiency of buildings is a major target [2 & 3]. Being the most important part in HVAC, energy minimization of vapour compression cycles is a major study area.

1.1.1 Overview of Optimization

Energy savings is already part of strategy in every major refrigeration company. Traditionally, the control of vapour refrigeration systems (equipped with Variable speed drives) in the industry, is mainly by a number of distributed controllers which ignore the interactions and cross-couplings between the sub loops. The supervisory control is mostly done by skilled operators. They are trained to adjust the parameters affecting the operation of the system so as to regulate system performance under different operating conditions. The more traditional approach for a simple vapour refrigeration system is to maintain the temperature of an area by on-off control. The on-off method or the manual method, both do not consider the energy consumption as the major concern.

To integrate the energy consumption factor in the control of vapour refrigeration system, a control method can be devised from the perspective of optimization. The basis of optimization can be described as follows.

INTRODUCTION

Set point and Dynamic optimization: For process plants with complexities, it is important to design a control system which helps the plant to attain the control objective. For an optimal control system, the two most important aspects are the controller properties, and the set points given for control. Figure (1.1) shows a generic control scheme.

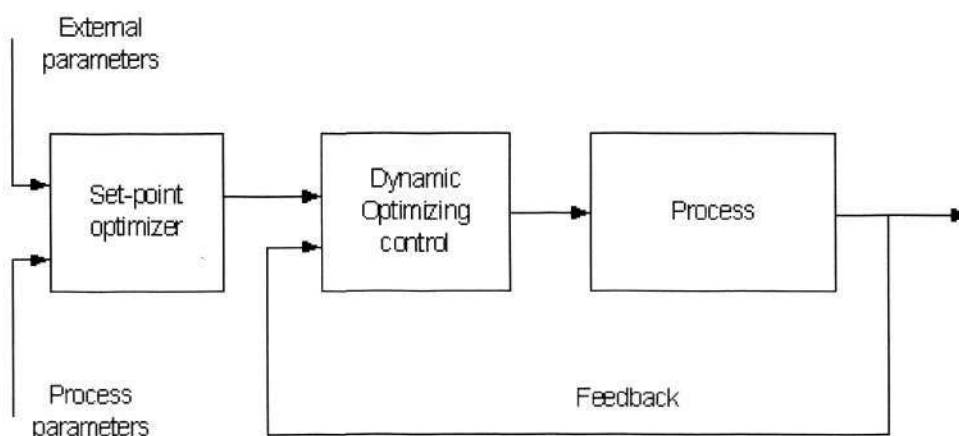


Figure 1.1: Optimal Control – set-point and dynamic optimizing control

The typical feedback control system consists of a controller, which outputs the control signal for the process. The output of the process is taken as a feedback, compared with the set-point and given as an input to the controller.

The purpose of the set-point optimizer is to observe the environmental conditions, and appropriately predict the set-points to be given to the controller so that the control objective is achieved, and to minimize the objective function so as to ensure energy savings. The set-point optimizer also has to work within certain constraints. The control objective has to be met while the given constraints are never violated.

INTRODUCTION

Dynamical optimizing control takes charge of the control system performance in the transient stage. In the transient phase, the system has to remain within the system limitations, and for this, dynamic optimizing control is required which would restrict the transient performance of the process while driving it to the set-point. The dynamical optimizing ensures that each step of the control action is limited by the constraints and most importantly, reaches the steady state in the least possible time.

1.1.2 Previous work on Vapour compression system and optimization

Since the vapour compression cycle is a part of the HVAC system, optimization techniques applied on other sub-loops of HVAC [13 & 14] was studied before beginning VCC optimization.

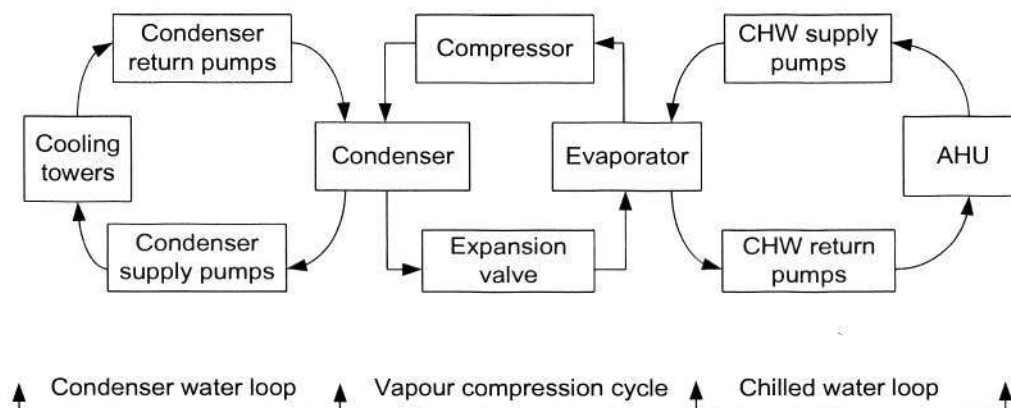


Figure 1.2: Block diagram of a typical HVAC system

1. Optimization of the condenser water loop section as shown in Figure (1.2) has already been established in [15]. Theoretically, about 10% of energy savings was achieved by implementing genetic algorithm on a simplified condenser water loop mathematical model. This was also tested on a pilot HVAC plant.

INTRODUCTION

2. A simulation study was also done on the chilled water section shown in Figure (1.2) to optimize the energy consumed by this segment, wherein the implementation of the optimization algorithm was simple and the results were considerable [16].

The conclusions taken from various references for the purpose of VCC are:

1. The preference of multi-input multi-output (MIMO) control over single input single output (SISO) control is because the SISO control has limited performance for VCC which has many interactions within the loop [9]. Model based controls can be implemented for co-ordinated modulation of expansion valve and airflow rate over evaporator as established in [22].
2. The inclusion of VSD for compressor and the control of electronic expansion valve (EEV) increase the degrees of freedom for multivariable control. The simultaneous control of compressor and EEV has been studied in [4 & 19].
3. The inclusion of variable-speed condenser fan and evaporator fan, adds flexibility to control design of VCC thus widening the scope of improvement of control; this has been presented in [28].

The optimization techniques were first explored before settling on use of genetic algorithm. The numerical methods for optimization as discussed in [24 & 25], require descriptive mathematical analysis; and implementing the numerical methods for purpose of VCC can complicate the optimization problem. Thus, Genetic algorithm is studied for optimization purpose as discussed in [7]. A model-based predictive control of vapour compression cycle has also been studied by [11].

INTRODUCTION

1.2 Objective

The main objective of this thesis is to investigate and develop a feasible and practical model-based set-point optimization technique for a single evaporator- single-condenser vapour compression cycle. The need for optimizing the vapour compression cycle is to achieve energy savings of considerable amount in comparison to the traditional control solutions used commonly in the industry. This thesis examines genetic algorithm based optimization strategy on a simulated environment.

The scope of this thesis is limited to set-point optimization in a simulated environment. Here, we explore how we can achieve the optimal set-points for energy minimization while using a simplified mathematical model of vapour compression cycle with a set of constraint equations. The simplified model is a combination of compressor equipped with VSD, electronic expansion valve, and evaporator and condenser fans with VSD. These models are studied in Chapter 3.

1.3 Contributions

The contributions made by this thesis are as follows:

1. Simple formulation of vapour compression cycle, with R134 as the circulating refrigerant. The VCC is formulated for steady-state operation, with a set of equations that define,
 - Heat transfer at evaporator side (range 0.95 to 1.3kW), that is, the heat absorbed by the refrigerant in the evaporator, from the air in the control room.

INTRODUCTION

- Heat transfer at condenser side, that is, the heat rejected by the refrigerant in the condenser, to the outside air.
- Mass flow rate of refrigerant and mass flow rate of air in control room and surroundings.
- Saturation temperature for condensation and evaporation and secondary parameters like enthalpy of vapour, liquid and vapour-liquid mixture.
- Power consumption of major energy consuming devices, i.e., compressor, evaporator fan and condenser fan.
- Constraints on amount of heat transfer, pressure, temperature, enthalpy, and mass flow rate values.

The above formulation is done for the vapour compression cycle with R-134 refrigerant, assuming that there are no inherent losses in the system.

2. Development of genetic algorithm based steady-state set-point energy-optimization strategy for vapour compressions cycle. The aforementioned VCC formulation is adapted to make it convenient to devise an algorithm for power and energy optimization. The GA based optimization accomplishes the following,
 - It ensures that the control objective is reached, that is, control of room temperature and meeting the cooling load demand.
 - It ensures that none of the constraints are defied.
 - While meeting the control objective and conforming to the constraints, it minimizes the power consumed by the vapour compression cycle. The optimization algorithm searches for the combination of manipulated variables for which the minimization is done effectively.

INTRODUCTION

3. Testing of optimization algorithm. The GA based optimization algorithm is tested for its effectiveness by comparing it with the traditional on-off method. As the thesis is limited to the simulated environment, the inputs and requirements for 24 hours, from midnight to midnight, are assumed and fixed for both on-off and optimization control. The comparison is done as follows,

- On-off control is implemented on the stipulated inputs, for a room of predefined volume with known specific heat of air and air density. Energy consumed in 24 hours is calculated.
- The optimization strategy is then implemented, and the VCC control is assumed to follow the set-points recommended by the optimization algorithm. For the same predefined parameters taken in on-off control, the energy consumed in 24 hours is calculated.

The above two methods are compared and it is concluded that relative to on-off control, the energy consumed by the vapour compression cycle when optimized, can be reduced by nearly 17%.

1.4 Thesis Outline

The thesis is divided into 5 main chapters. Chapter 2 discusses the basics of vapour compression cycle and genetic algorithms. It also discusses optimization and the type of optimization implemented in the thesis. Chapter 3 explores the mathematical model that will represent the vapour compression cycle in further sections for implementation of optimization strategy. Chapter 4 expounds on the development and execution of genetic algorithm based optimization method on the vapour compression

INTRODUCTION

cycle representation. Chapter 5 is divided into two main sections. The first section discusses the results of optimization for various input parameters. The second section compares the optimization technique with a traditional control method. Chapter 6 is the conclusion of the thesis. The future scope and work that can be carried out is also discussed in this chapter.

Chapter 2

Fundamentals of VCC and GA

2.1 Vapour Compression Cycle

The vapour compression cycle works on the principle of the laws of thermodynamics. The following section will briefly elucidate the “Laws of Thermodynamics”, before progressing to the working of cycle [5 & 20].

First law: This is also called as law of conservation of matter. It states that energy can neither be created nor be destroyed. It can be only transferred from one form to another. Mathematically it states that the change in internal energy is equal to the difference in heat transfer (Q) into the system and the work done (W) by the system.

$$E_2 - E_1 = Q - W \quad (2.1)$$

Derived from the above equation, we also get the equation for specific enthalpy,

$$h_2 - h_1 = c_p(T_2 - T_1) \quad (2.2a)$$

$$q - w = h_2 - h_1 \quad (2.2b)$$

FUNDAMENTALS OF VCC AND GA

where, c_p is specific capacity of heat for constant pressure.

$(E_2 - E_1)$ is change in internal energy of matter.

h is the specific enthalpy and T is temperature

All lower cases indicate the specific values of the variables i.e. independent of mass.

Second law: The second law of thermodynamics relates to entropy. Entropy is defined as disorderliness or chaos in a closed system.

This law states that “Energy stored as heat cannot be completely used to do work, or cannot be completely converted to equivalent work”. Thus the second law deals with the efficiency of a system, i.e. how much energy that is stored can actually be converted to work.

From the point of view of refrigeration, the second law of thermodynamics restricts the direction of heat transfer, which in turn states that heat can flow freely without any work only from a hot reservoir to cold reservoir. Thus, this rules out the possibility of a perfect refrigerator.

$$\Delta S = (dQ/T) \quad (2.3)$$

dQ is the heat absorbed in an isothermal and reversible process.

ΔS is the change in entropy.

2.1.1 Working Principle

The vapour compression cycle is used in refrigeration systems. The purpose of the process is to remove heat from a lower temperature (cold reservoir) to an environment of high temperature (hot reservoir). This cannot be achieved by a simple heat exchanger, where the flow of heat is always from the fluid with higher heat content to the fluid with lower heat content.

FUNDAMENTALS OF VCC AND GA

The vapour compression cycle [5] has basically four components – *Evaporator*, *Compressor*, *Condenser*, and *Expansion Valve* as shown in Figure (2.1). These four components are connected in a closed loop so that the working fluid (refrigerant R134) is continuously circulated in the cycle. Starting from the evaporator side of the cycle; the temperature T inside the evaporator is lower than the cold reservoir temperature T_{cr} .

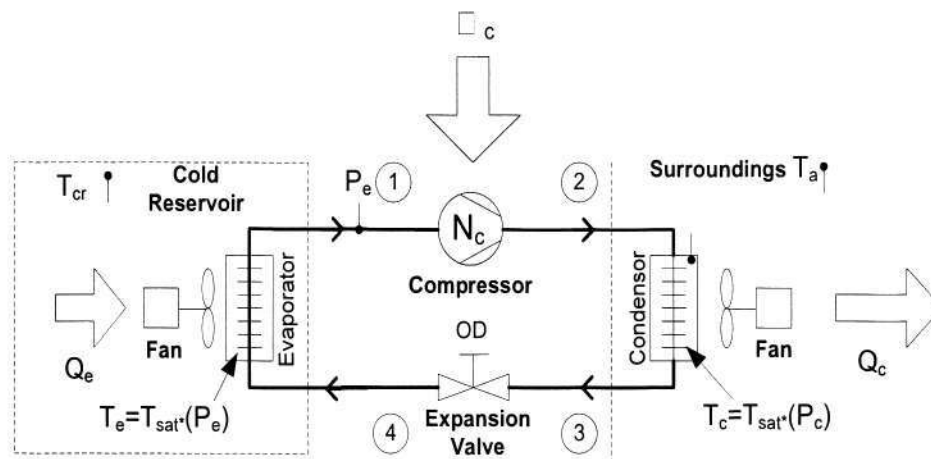


Figure 2.1: Layout of Vapour Compression Cycle

This results in heat being transferred from the cold reservoir to the refrigerant in the cycle. The ensuing high temperature refrigerant is compressed by the compressor to an extent that the saturated vapour is in a much higher temperature than the temperature at compressor inlet (The saturation temperature T_{sat} of a refrigerant is distinctively dependent on the vapour pressure). The compressor thus enables easy heat transfer in the condenser. In the condenser, the high temperature high pressure saturated vapour gives away its heat to the outside environment (hot reservoir).

This condensed liquid refrigerant is then passed through the expansion valve which drastically reduces the pressure of refrigerant from P_c to P_e . The reduction in pressure

FUNDAMENTALS OF VCC AND GA

also ensures that the low evaporator pressure P_e reduces the saturation temperature of refrigerant in the evaporator. Thus the refrigerant is flash evaporated as it enters the evaporator.

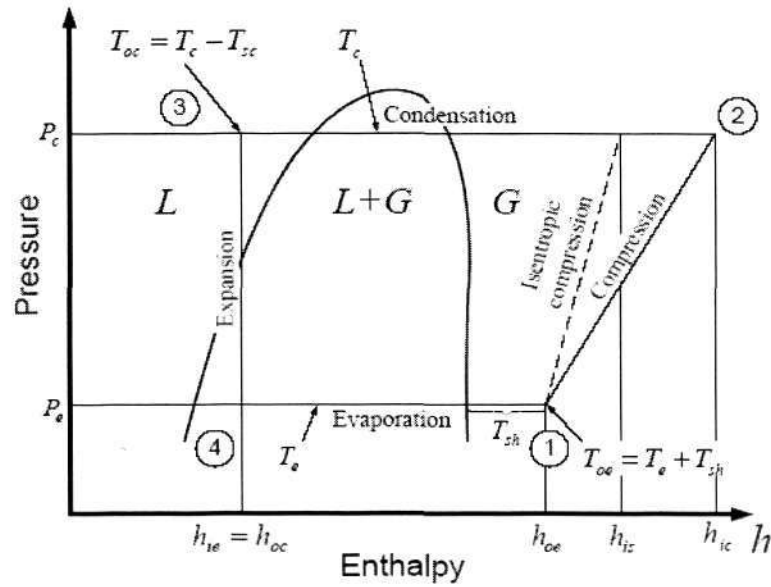


Figure 2.2: Pressure enthalpy diagram of vapour compression cycle. $h - \log(p)$ diagram.

Referring to Figure (2.2), the flow of cycle [12] can be explained as below.

1. Refrigerant starts from state 1, inlet of compressor in gas state at low pressure and temperature. As the refrigerant exits the compressor or reaches state 2, it is in gas state and in high pressure (saturation pressure for condensation) and high temperature.

For an adiabatic process,

$$W_c = m(h_{ad} - h_{oe}) \quad (2.4)$$

Practically, there is some heat loss due to which $h_{ad} \approx h_{ie}$. Thus we have to include a heat loss factor f_q [23].

FUNDAMENTALS OF VCC AND GA

$$f_q = \frac{h_{ad} - h_{ie}}{h_{ad} - h_{oe}} \quad (2.5)$$

The heat rejected by the compressor is $f_q W_c$. Thus, W_c becomes

$$W_c = \frac{1}{1 - f_q} m_c (h_{ic} - h_{oe}) \quad (2.6)$$

From state 2, the superheated vapour refrigerant enters the condenser where a secondary fluid is also circulated. The secondary fluid or the surroundings is at lower temperature compared to the refrigerant in the condenser. Thus heat Q_c is transferred from the working fluid to secondary fluid. The refrigerant is in liquid plus gas state inside the condenser. As it exits the condenser, it is in state 3 in liquid state. The high pressure P_c ensures that, when the refrigerant exits the condenser after transferring the heat to the surroundings, the temperature is brought below the condensing temperature. Thus the refrigerant is fully condensed and sub cooled at exit.

The absence of gas bubbles guarantees that the mass flow rate through the valve remains constant. It also helps in minimizing the wear and tear of the valve.

From the first law of thermodynamics,

$$Q_c = Q_e + W_c - f_q W_c. \quad (2.7)$$

2. The refrigerant in liquid state enters the expansion valve in the state 3-4. The expansion valve is just a throttle valve which decreases the pressure of the fluid. The sudden decrease in the pressure of the refrigerant causes it to partially evaporate. This further drives the saturation temperature T_e to reduce; thus when the refrigerant exits the valve it is in low pressure and low temperature and in liquid plus gas state ($L+G$).

FUNDAMENTALS OF VCC AND GA

No work is done in this process, nor is any heat rejected or absorbed. Thus $W = 0$ and $Q = 0$;

3. In state 4-1, i.e. while entering the evaporator, the refrigerant in $L+G$ (Liquid and gas mix) state is in low temperature and low pressure. This temperature is lower than the cold reservoir's temperature. Thus the $L+G$ refrigerant completely evaporates at a constant temperature T_e during the heat transfer. The fans help in increasing the heat transfer rate. At the exit of the evaporator, the temperature is slightly above T_e ; it is superheated to T_{sh} . The refrigerant exiting the evaporator is totally evaporated. This is important for the safety of compressor which can fail in presence of any liquid.

$$Q_c = m(h_{oe} - h_{oc}) \quad (2.8)$$

2.2 Genetic Algorithms

Genetic algorithms (also called evolutionary algorithm) are adaptive heuristic search methods which find solutions for problems within a defined search space. The genetic algorithm was first proposed by Holland [10] and later consolidated and developed by Goldberg [8]. It has been widely studied and used in the fields of engineering and management for complex problems such as planning and automatic programming.

Genetic Algorithm is called so because it uses the same laws as that of evolution namely encoding, selection, reproduction, mutation, crossover and most importantly the rule of survival of the fittest. The edge that GA has over other traditional methods

FUNDAMENTALS OF VCC AND GA

is that it does not require detailed mathematical analysis of a problem to reach the solution. The terminology used in genetic algorithm is explained as following.

Chromosome: Chromosome matrix consists of the variables to be modified in the program. They are represented in gray code in a specified number of bits. All the variables are included in a single row of the matrix. Each row indicates a new individual of the population.

Population: Chromosome matrix is called a population. Defined by the user, it in fact indicates the number of rows of the chromosome matrix.

Variables in chromosome: These are the variables that can be changed, i.e. manipulated by the user, which affects the fitness function/ objective function of the optimization problem. One row of the chromosome matrix contains the binary value (in gray code) of all the variables.

2.2.1 Characteristics of Genetic Algorithms

- a. Genetic algorithms can handle highly non-linear complex set of equations and constraints. The reason is that the algorithm does not try to solve the equations to find the variables. Instead it searches the entire variable range, evaluates the equations, calculates the fitness values, and decides on the variable value with the maximum fitness value as the optimum solution. All this is done without disobeying the constraints.
- b. GA is simple and easy to implement and provides a fast robust solution over a wide and probably unclear search space for difficult high-dimensional problems.

FUNDAMENTALS OF VCC AND GA

- c. Genetic algorithms can tend to settle to a local optimum value. This can be avoided by increasing the mutation rate, so that solutions outside the local range will also be considered.
- d. For a dynamic set of equations e.g. dynamic constraints, the result of the algorithm might not be optimal if it is not rapid enough to adapt to the changing equations.
- e. For this thesis, i.e. optimization of vapour compression cycle, GA would suffice. For the complexity of the equations involved, GA would serve the purpose of finding an optimal solution without much difficulty.

A basic genetic algorithm can be explained as a series of steps using the genetic operators, which searches for an optimal value of an objective within the search space specified. Before describing the evolutionary process, the initialization of genetic algorithm is as follows.

2.2.2 Population Initialization and Encoding

The potential solution of an optimization problem is an individual which can be represented by a set of variables or chromosomes. A chromosome is a binary string of variable values as defined earlier.

Binary string encoding [21] is used for its simplicity. But the use of Gray coding is preferred for overcoming the hidden representative bias in binary representation. The hamming distance between adjacent values in Gray coding is always constant.

FUNDAMENTALS OF VCC AND GA

Real value	0	1	2	3	4	5	6	7	8
Binary	0000	0001	0010	0011	0100	0101	0110	0111	1000
Gray code	0000	0001	0011	0010	0110	0111	0101	0100	1100

Table 2.1: Comparison of Binary and Gray Code

Table (2.1) shows that binary coding of real numbers is in a regular sequence. Gray coding is such that adjacent real values differ by only one bit in the gray code interpretation.

A random population of chromosomes, is generated such that, when decoded to real values, the variable values lie within their limitations. The whole generation should possibly try to include the entire range of values.

2.2.3 Objective Function and Fitness Function

From this population an initial objective function is created, which indicates the fitness of the individuals in the population array. This is the most important connection between genetic algorithm and its practical optimization application. For minimization, the individual with the lowest numerical value of objective function is fitter. The fitness function is used to transform the objective function into a linear array of individuals with varying rankings. Mathematically,

$$Fit(x) = g(f(x)) \quad (2.9)$$

where, $f(x)$ is the objective function, and $Fit(x)$ is the fitness function. $g(.)$ operator transforms the objective function to fitness function.

FUNDAMENTALS OF VCC AND GA

For transformation, linear ranking method with selective pressure of 2 can be used. The selective pressure denotes the rank range of each individual in the population. Linear ranking denotes that if the population has N elements, then the rank is equally distributed from 0-2, for N elements.

$$\begin{aligned} & \text{for } i = 0 \text{ to } N, \\ & \quad \text{Rank}(i) = 2*i/(N-1) \\ & \text{end} \end{aligned} \tag{2.10}$$

Each element in *Rank* differs from the successor element by a value of (*Selective Pressure**(1/ $N-1$)). The first element in the array *Rank* is 0, and the last element is 2(for a selective pressure of 2). The lower ranks are assigned to higher objective valued individuals and higher ranks to lower objective valued individuals.

2.2.4 Genetic Algorithm Methodology and Flowchart

The evolutionary process of GA for a population with corresponding fitness values is described as below.

Selection: Selection is the process of estimating the number of times an individual is selected as a proportion of the whole population according to the respective fitness value. The ratio of amount of individuals that have to be selected from the parent generation is called as Generation Gap.

The genetic operator in the scope of this thesis is the Roulette wheel selection. In this type of selection, individuals with higher fitness value have more probability of getting selected than individuals with low fitness value. This method can be explained with an example as shown in Figure (2.3). A random number is generated using the outer circle sector. The number generated should be from 1 to 16. Similarly, the inner

FUNDAMENTALS OF VCC AND GA

circle consists of the individuals (N elements from $I1$ to $I6$) of the population such that, the fitter individuals will get a proportionally greater portion of the inner circle. This does not rule out the weaker individuals or chromosomes, which get smaller quantities of the circle than the stronger individuals. The number generated randomly is matched to the sector of the inner circle on which it falls; thus the corresponding individual is selected.

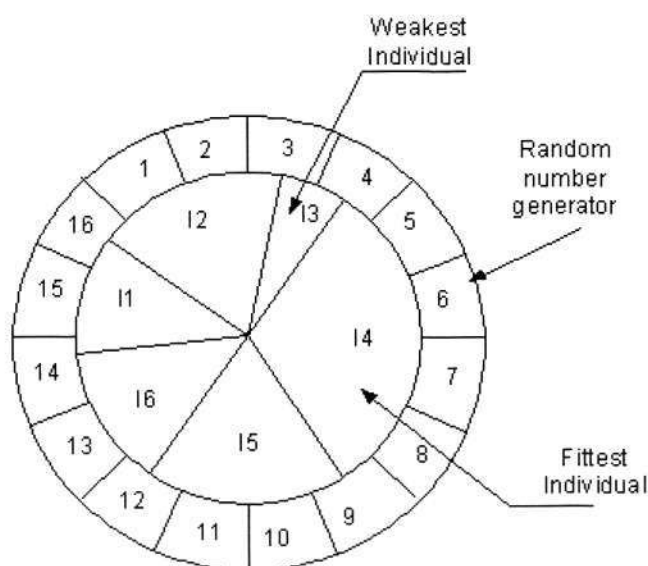


Figure 2.3: Example of Roulette Wheel Selection

Reproduction (Crossover): From the selected population, a new population of same size is generated, so that some characteristics of the parent population are absorbed by the new generation. The new population will try to converge in the range where the fitness values will be higher. The types of crossover that are generally used are one-point, two-point and uniform crossover [10]. An example of 2-point crossover is shown in Table (2.2) for individuals with length of 12. The crossover points are at the 5th bit and the 8th bit. Thus the string in-between is exchanged between the two parents to form new individuals (child 1 and child 2).

FUNDAMENTALS OF VCC AND GA

Parent 1	0000 0101 1001
Parent 2	0010 1100 0111
Child 1	0000 1100 1001
Child 2	0010 0101 0111

Table 2.2: Example of two point crossover

In this thesis, the reproduction probability is taken as 0.9

Mutation: To avoid the algorithm from getting trapped to a local optimum value, this step is required to be performed on the population. A completely random change is made in the new population, so that a very small percentage of the individuals are mutated. The individual should be totally different than its previous form and preferably not in the range of values that the current population set is in.

The mutation process can be done by changing any bit in the individual of the parent generation. For more complex types of mutation, random binary values can be added to very few individuals from the parent population. An example of the simpler type of mutation can be shown as,

Parent individual: 0 0 1 1 1 1 0 0 (Mutation at 6th bit in parent individual)

New individual: 0 0 0 1 1 1 0 0

The bit which has to be mutated is randomly selected throughout the chromosomes. If the amount of individuals that are mutated is higher, the probability of fitness value converging to an optimum becomes lesser, because the mutation probability increases the chances of destroying a fit individual. The mutation probability has to be kept at a

FUNDAMENTALS OF VCC AND GA

reasonable low value so as to make the population diverse while not destroying good individuals [8]. The mutation probability is taken as 0.023 in this thesis.

Reinsertion: In this step, fitness values of the new population (offspring) after reproduction and mutation are calculated. Based on the fitness values, the offspring are then reinserted into parent population such that, they replace the weaker individuals in the parent population.

Termination: The termination of genetic algorithm can be done in two ways.

- If the population converges to a minimum value, and stays near the minimum value for a predefined number of iterations, the genetic algorithm can be terminated.
- If the maximum generation number is reached.

In this thesis, the second termination criterion is used. The genetic algorithm is iterated till the maximum generation is reached. For each generation, a new modified population is generated. For each population, its fitness value is calculated according to the objective function. The above steps of evolution is applied on each population; and after repeating the above steps for a user defined number of times *Maxgen*, the final population is attained which will contain the required optimization solution.

Figure (2.4) briefly explains the genetic algorithm in the flowchart layout.

FUNDAMENTALS OF VCC AND GA

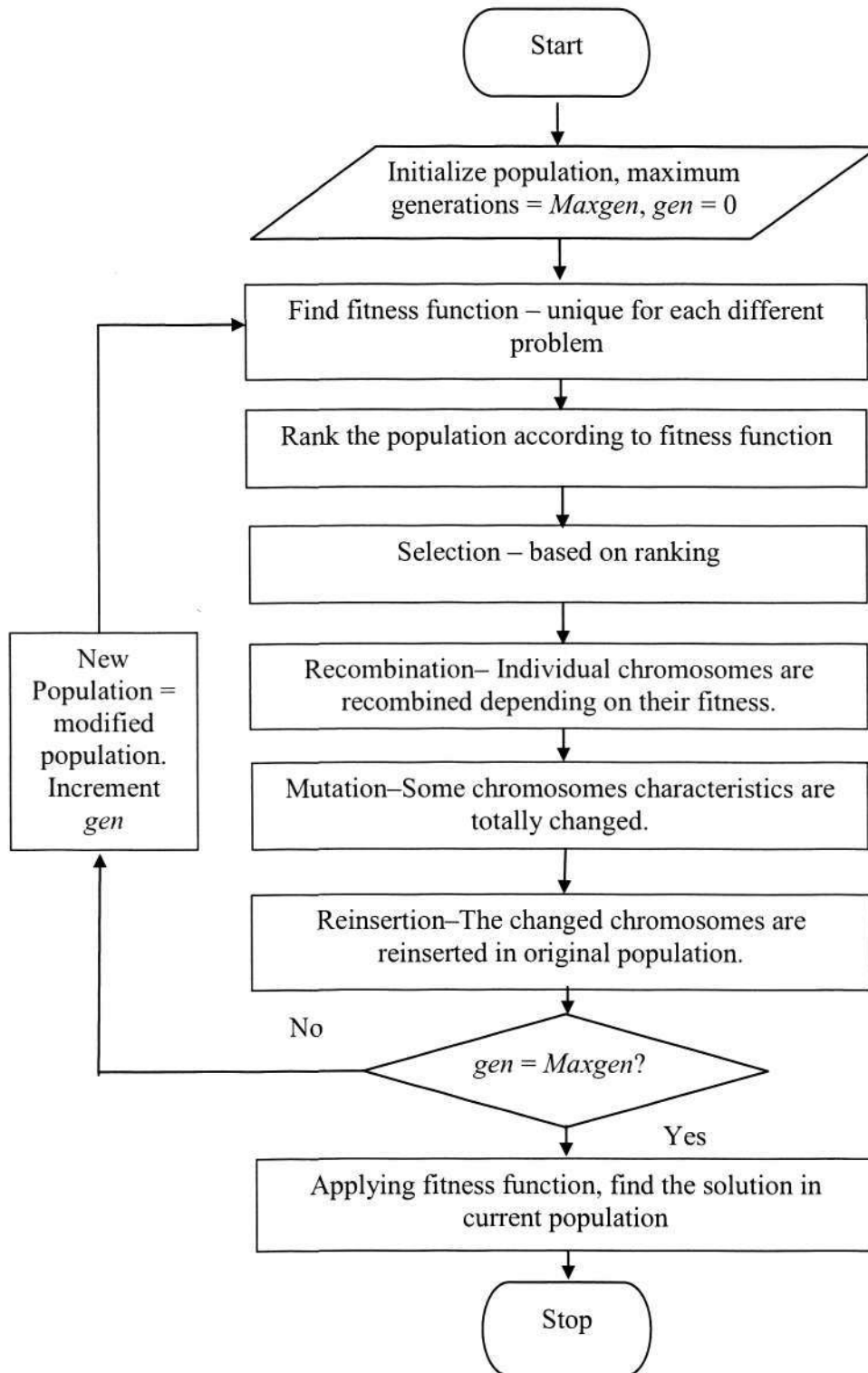


Figure 2.4: Simple Genetic Algorithm Flowchart

Chapter 3

Modelling of vapour compression cycle

The vapour compression cycle with refrigerant R134 (as discussed before in Chapter 2), consists of mainly four components – evaporator, condenser, compressor and electronic expansion valve. In this chapter, we will discuss the model used for heat transfer in evaporator, the model for heat transfer in condenser, the model for power consumed by compressor, the model for calculating mass flow rate in the vapour compression cycle using the expansion valve, and the models for condenser and evaporator fans. The corresponding constants involved in the derived models are highlighted in Appendix A.1. The rest of the process dynamics of the refrigerant are described as part of the optimization problem in Chapter 4.

3.1 Evaporator Modelling

The evaporator is synonymous to heat exchanger, which works for the purpose of absorbing heat from the surroundings. Modelling of the evaporator is very important for optimization and for performance monitoring. A simple model which can include all factors of a real evaporator is a pre-requisite for implementation of optimization on the Vapour Compression Cycle. Previous work on energy efficiency improvement

MODELLING OF VAPOUR COMPRESSION CYCLE

using model based predictive control of multiple evaporator vapour compression cycle has been done in [6].

This thesis utilizes the hybrid model for evaporator with two-phase flow [26]. The other methods available like ϵ -NTU and distributed models have their shortcomings to utilize them for real-time applications; for e.g. the ϵ -NTU method requires complete geometric details, heat transfer coefficient-area product et cetera, which are not easily computable. Thus, instead of exploring these models, we use the evaporator hybrid model. The ideology behind development of a hybrid model is:

- Formulation of basic equations of the process with energy and material balance and thermodynamic principles.
- Determining the manipulated and controllable variables for the entire process which affect the system performance.
- Representing the variables in the original equation, that cannot be simply found out without mathematical analysis.
- Correlating the equations' inputs and outputs and obtaining a single equation which can represent both the input and the output section of the system.
- Identifying unknown parameters by least squares method.

The resulting model captures all factors like the non-linear characteristics of the evaporator, and the influence that the working fluid and secondary fluid dynamics have on the heat exchange process.

The basic structure of an evaporator is shown in Figure (3.1). It consists of the heat exchanger acting as evaporator and an electronic throttling (expansion) valve. As

MODELLING OF VAPOUR COMPRESSION CYCLE

explained before, the working fluid (refrigerant R134) enters the expansion valve with temperature T_{vi} and pressure P_c and exits with temperature T_{WFi} and pressure P_e .

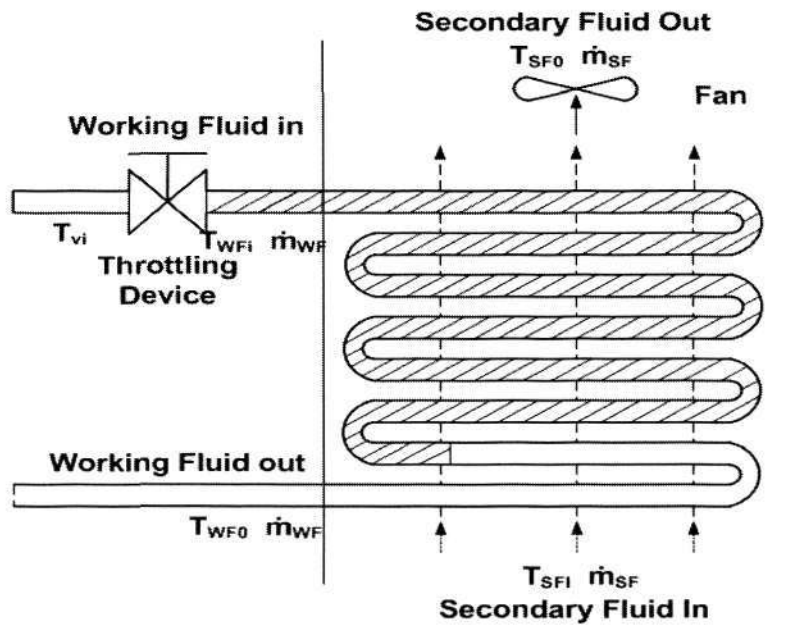


Figure 3.1: Basic Structure of Evaporator

In the secondary fluid loop, heat transfer is single phase forced convection. As the secondary fluid exits the evaporator, the temperature T_{SF} is reduced, due to heat transfer.

$$Q_{SF} = h_{SF} A_s \Delta T_{SFm} \quad (3.1)$$

where, h_{SF} is the average convective heat transfer co-efficient, which is determined by fluid properties.

ΔT_{SFm} is the average temperature difference between metal tube and secondary flow.

A_s is the average evaporator surface area

Unlike the secondary fluid loop, in the working fluid loop, the heat transfer involves phase change and heat convection.

MODELLING OF VAPOUR COMPRESSION CYCLE

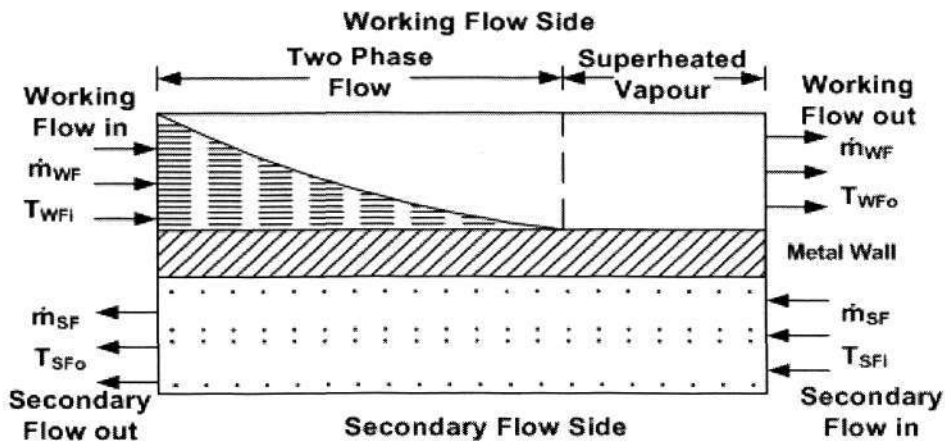


Figure 3.2: Representation of Heat transfer in Evaporator

The evaporator can thus be divided into the sections as shown in Figure (3.2).

- Two phase region
- Superheated vapour region.

From the perspective of working flow, the fluid refrigerant entering the evaporator is already a mixture of vapour and liquid, with low temperature and low pressure owing to flash evaporation in the expansion valve. In the evaporator, the working fluid absorbs heat from the secondary fluid through the metal tube wall. To completely evaporate the working fluid, Q_{WFI} amount of heat is required such that,

$$Q_{WFI} = (H_{WFi} - H_g)m_{WF} \tag{3.2}$$

where, H_g is the saturated vapour enthalpy of working fluid

H_{WFi} is the inlet enthalpy of working fluid

m_{WF} is the mass flow rate of working fluid.

After completely evaporating to vapour state, the fluid is further superheated. The heat transfer between the working fluid and the secondary fluid then becomes single phase forced convection.

MODELLING OF VAPOUR COMPRESSION CYCLE

The heat transfer Q_{WF2} can be represented by Newton's law of cooling:

$$Q_{WF2} = h_{WF2} A_{s2} \Delta T_{WF2m} \quad (3.3)$$

where, A_{s2} is surface area of section,

ΔT_{WF2m} is average difference between the evaporator outlet temperature of the working fluid and its saturation temperature.

h_{WF2} is the heat transfer co-efficient.

From energy balance, it follows that,

$$Q_{WF} = Q_{SF} = Q \quad (3.4)$$

$$Q_{WF} = Q_{WF1} + Q_{WF2} \quad (3.5a)$$

$$Q = (H_{WFi} - H_g) \dot{m}_{WF} + h_{WF2} A_{s2} \Delta T_{WF2m} \quad (3.5b)$$

Representing h as
$$h = b \dot{m}^e \quad (3.5c)$$

where, b is a constant derived from *Reynolds* and *Prandtl* number. e is independent of fluid properties, and depends on surface geometry and type of flow. Thus,

$$Q_{WF2} = b_{WF2} \dot{m}_{WF}^e A_{s2} \Delta T_{WF2m} \quad (3.6)$$

Substituting Equation (3.6) in Equation (3.5b), equating it to a modified version of Equation (3.1), and simplifying we get,

$$T_{SF_i} - T_{sat} = \frac{(Q_{WF} - (H_g - H_{WF_i}) \dot{m}_{WF})}{(b_{WF} \dot{m}_{WF}^e A_{s2})} + \frac{Q_{SF}}{b_{SF} A_s \dot{m}_{SF}^e} \quad (3.7)$$

$$Q_e = \frac{(H_g - H_{WF_i}) \dot{m}_{WF} + c_1 \dot{m}_{WF}^e (T_{SF_i} - T_{sat})}{1 + c_2 \left(\frac{\dot{m}_{WF}}{\dot{m}_{SF}} \right)^e} \quad (3.8)$$

where,

$$c_1 = b_{WF2} A_{s2}$$

$$c_2 = \frac{b_{WF2} A_{s2}}{b_{SF} A_s}$$

MODELLING OF VAPOUR COMPRESSION CYCLE

Equation (3.8) involves both secondary fluid and working fluid thermodynamics. The geometric parameters, heat transfer by forced convection and latent heat of both working flow (WF) and secondary flow (SF) are lumped in together in this equation.

Thus the heat transfer rate of the evaporator can be defined by three fundamental variables: m_{WF} , T_{SFv} , m_{SF} and three parameters T_{sat} , H_{WFv} , and H_g . c_1 , c_2 can be determined by linear least squares method when 'e' is taken as 0.8. When 'e' is taken as unknown, all three unknown parameters can be found by non-linear least squares method.

The above formulation is a simple model of evaporator derived from thermodynamics laws and energy and mass balance laws. The model involves only three variables and three parameters which can be estimated from linear or non-linear least squares method. The model predicts the actual performance of evaporator over the entire working range with an error margin of $\pm 8\%$ [26]. Thus, the model is sufficient for the purpose of vapour compression cycle

3.2 Modelling of Condenser

This section describes a simple hybrid model for condenser [27] akin to the evaporator model described in Section 3.1.

The development of the hybrid model for condenser is as follows:

- Use of basic thermodynamics laws and energy and heat transfer principles to represent the heat transfer with respect to temperature, mass flow rate etc. These

MODELLING OF VAPOUR COMPRESSION CYCLE

equations take into consideration only few important operational characteristic parameters to predict the condenser performance.

- Finding the controlled and manipulated variables which affect the system performance considerably.
- Those variables which cannot be found out by simple mathematical analysis are to be represented in the original equations.
- Correlating the inputs and outputs of the system so that they can be shown in a single equation.
- Finding the unknown parameters by least squares methods.

The schematic of condenser is as shown in Figure (3.3). It consists of two sections – working fluid loop and secondary fluid loop. The working fluid (refrigerant R134) exiting from the compressor enters the condenser in high temperature high pressure vapour state.

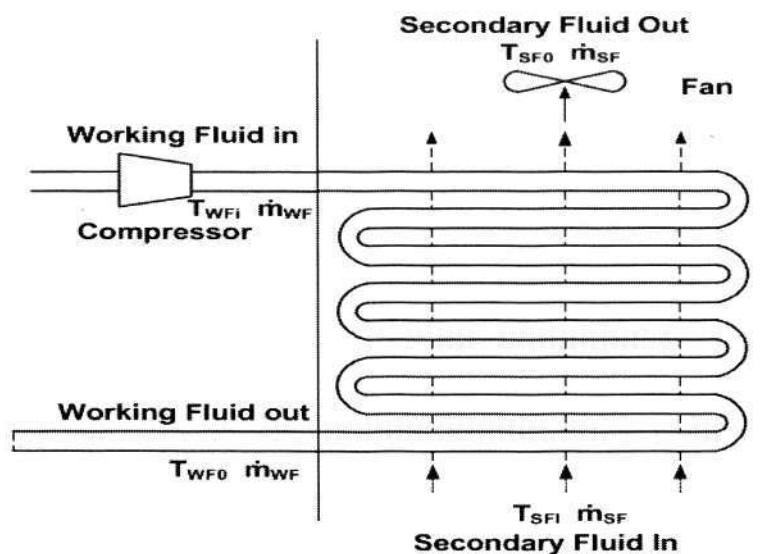


Figure 3.3: Basic Structure of condenser

MODELLING OF VAPOUR COMPRESSION CYCLE

The secondary fluid is in lower temperature than the working fluid and thus heat is transferred from the working fluid through the metal wall tube to the secondary fluid. Since the working fluid is already pressurized, it condenses to liquid state owing to the heat transfer. At the outlet of the condenser, the temperature of the working fluid reduces, and is in liquid state. In the secondary fluid loop, the heat transfer results in a higher outlet temperature than at the inlet.

In the secondary fluid loop, the heat transfer is single phase forced convection process. It is governed by the geometry of condenser, viscosity, density, thermal conductivity, expansion co-efficient, and specific heat of the fluid. The rate of heat transfer can be given by Newton's law of cooling,

$$Q_{SF} = h_{SF} A_s \Delta T_{SFm} \quad (3.9)$$

where, h_{SF} is average heat transfer co-efficient of secondary fluid.

A_s is condenser surface area.

ΔT_{SFm} is mean temperature difference between metal tube wall and secondary flow.

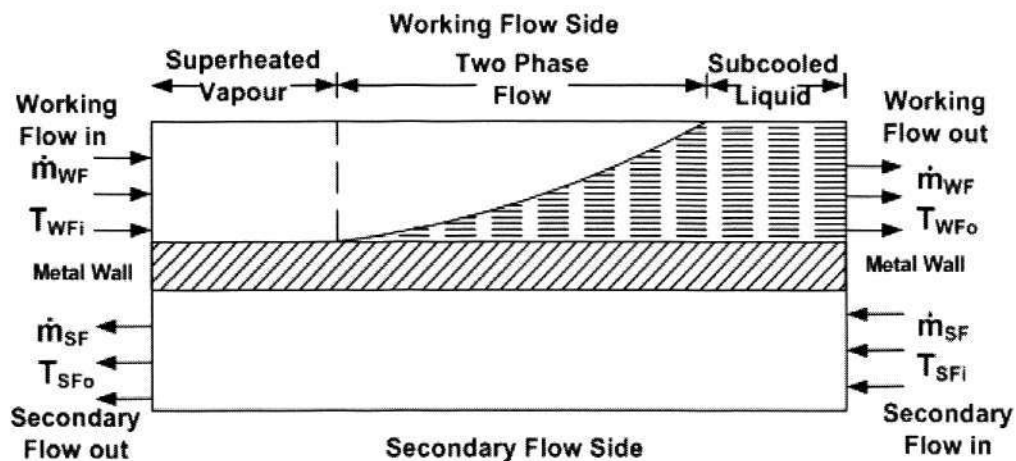


Figure 3.4: Representation of heat transfer in condenser

MODELLING OF VAPOUR COMPRESSION CYCLE

The heat transfer co-efficient can be found out as follows.

$$h_{SF} = b\dot{m}^e \quad (3.10)$$

where, b is the constant derived from the *Reynolds* and *Prandl* numbers.

In the working fluid loop, the condenser can be divided into three regions depending on the phase of the fluid: *superheated vapour region*, *two phase region*, and *liquid region* as shown in Figure (3.4). The heat transfer depends on heat convection as well as latent heat of vaporization.

The fluid entering the condenser is in superheated high pressure phase, with temperature T_{WFi} , which is higher than the saturation temperature T_{sat} . The heat transfer for the first region of the condenser can thus be represented as single phase (vapour phase) forced convection. The heat transfer results in reduction of temperature of working fluid, without condensation.

$$Q_{WF1} = C_{pg} \dot{m}_{WF} (T_{WFi} - T_{sat}) \quad (3.11)$$

At the two phase section, the temperature is reduced to T_{sat} , resulting in phase change. Thus the saturated vapour begins to condense to saturated liquid state. Heat transfer for this section can be represented as,

$$Q_{WF2} = H_{fg} \dot{m}_{WF} \quad (3.12)$$

where, H_{fg} is the latent heat of vaporization, which is the saturation enthalpy difference between the vapour and liquid.

At the third region, the working fluid is sub cooled, i.e. completely condensed to liquid state. The heat transfer then follows the forced convection single phase pattern. The heat transfer rate, Q_{WF3} is expressed by Newton's law of cooling,

MODELLING OF VAPOUR COMPRESSION CYCLE

$$Q_{WF3} = h_{WF3} A_{S3} \Delta T_{WF3m} \quad (3.13)$$

where, h_{WF3} is average heat transfer co-efficient of sub-cooled working fluid.

A_{S3} is sectional surface area.

ΔT_{WF3m} is average temperature difference between metal tube wall and saturated temperature of working fluid.

Thus, total heat transfer from the condenser is,

$$Q_{WF} = Q_{WF1} + Q_{WF2} + Q_{WF3} \quad (3.14)$$

$$Q_{WF} = C_{pg} m_{WF} (T_{WFi} - T_{sat}) + H_{fg} m_{WF} + h_{WF3} A_{S3} \Delta T_{WF3m} \quad (3.15)$$

The heat is transferred from the condenser to the surrounding secondary fluid (the environment) through the metal tube walls. By energy balance,

$$Q = Q_{WF} = Q_{SF} \quad (3.16)$$

Q is the total heat transfer rate of the condenser. Consequently, coupling together the working fluid and the secondary fluid equations, a single equation is derived which represents the thermodynamics activity of both loops. This equation will take into account the influence of fluid-interactions.

Replacing ΔT_{WF3} with $(T_{sat} - T_{wall})$ and ΔT_{SFm} with $(T_{sat} - T_{wall})$, and with some mathematical simplification and correlation,

$$T_{sat} - T_{SFi} = \frac{(Q_{WF} - C_{pg} \dot{m}_{WF} (T_{WFi} - T_{sat}) - H_{fg} \dot{m}_{WF})}{b_{WF3} \dot{m}_{WF}^{e_1} A_{S3}} + \frac{Q_{SF}}{b_{SF} A_s \dot{m}_{SF}^{e_1}} \quad (3.17)$$

Further establishing the equation as depiction of heat transfer rate,

$$Q_c = \frac{d_1 \dot{m}_{WF}^{e_1} (T_{sat} - T_{SFi}) + d_2 \dot{m}_{WF} (T_{WFi} - T_c) + H_{fg} \dot{m}_{WF}}{1 + d_3 \left(\frac{\dot{m}_{WF}}{\dot{m}_{SF}} \right)^{e_1}} \quad (3.18)$$

MODELLING OF VAPOUR COMPRESSION CYCLE

The above equation involves both secondary and primary fluid thermodynamics. The geometric parameters, heat transfer by forced convection and latent heat of both WF and SF are lumped in together in this equation.

The unknown parameters d_1 , d_2 , d_3 , and e_l have to be calculated by linear or non-linear least squares method.

3.3 Modelling of Expansion Valve

The expansion valve is modelled not for the purpose of calculating energy consumed by it, but to calculate mass flow rate in the vapour compression cycle loop. The mass flow rate is constant throughout the loop and calculated using the model for expansion valve instead of the compressor because fewer parameters are involved in the valve model.

The mass flow rate of liquid through a valve is defined as,

$$m_{WF} = C_v A_v \sqrt{(\rho v \Delta P)} = f_v \sqrt{\Delta P} \quad (3.19)$$

To find out the values of coefficients C_v , A_v , f_v in the above equation, the physical structure and design of the valve has to be known and some experimental results have to be established. For the simulated environment limited by this thesis, the MATLAB dynamic model for vapour compression cycle was used. m_{WF} was studied in relation to ΔP and an appropriate curve was fitted using the curve fitting software *TableCurve*. Thus the model used for expansion valve to calculate mass flow rate is,

$$m_{WF} = a + bu(\sqrt{\Delta P}) \quad (3.20a)$$

where,

MODELLING OF VAPOUR COMPRESSION CYCLE

$$\Delta P = P_c - P_e \quad (3.20b)$$

u is the percentage opening of the expansion valve, which changes the volumetric flow of refrigerant through the valve.

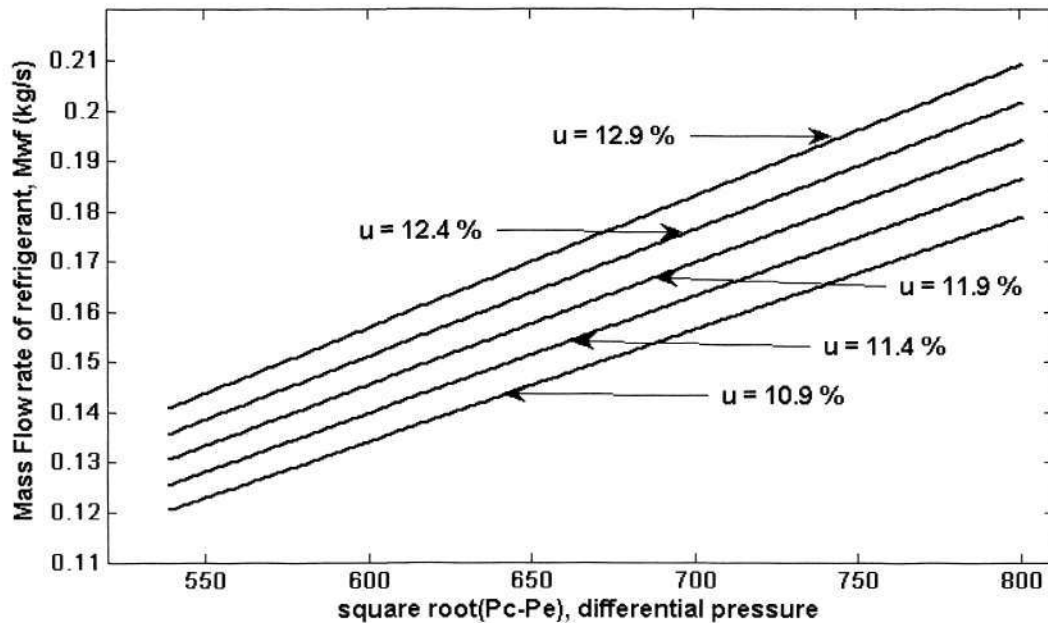


Figure 3.5: Mass flow rate Vs Differential pressure for different valve openings

The dependence of mass flow rate on pressure difference and opening area of valve is elucidated in Figure (3.5). For incrementing differential pressure, the mass flow rate increases. Also, for higher opening area of the valve, the mass flow rate is higher.

3.4 Modelling of Compressor

The compressor in the refrigeration cycle deals with pressurizing the liquid refrigerant flowing in the loop. An accurate model for of the compressor is extremely important because the power consumed by the compressor is much higher than the condenser and evaporator fans.

MODELLING OF VAPOUR COMPRESSION CYCLE

The mathematical model to correlate the power consumed by the compressor and the pressure at its inlet and outlet is determined using MATLAB's dynamic refrigeration model. W_{comp} was studied in relation to saturation pressure for evaporation, P_e and saturation pressure for condensation, P_c . The relation was curve fitted using the *TableCurve* software [1]. A polynomial model having a very low modelling error was used to attain the equation for W_{comp} .

$$W_{comp} = b_1 + b_2T_e + b_3T_e^2 + b_4T_e^3 + b_5T_c + b_6T_c^2 + b_7T_c^3 \quad (3.21)$$

To actually use this power value, we can change the rotational speed (rpm) of the compressor, so as to match the power value W_{comp} .

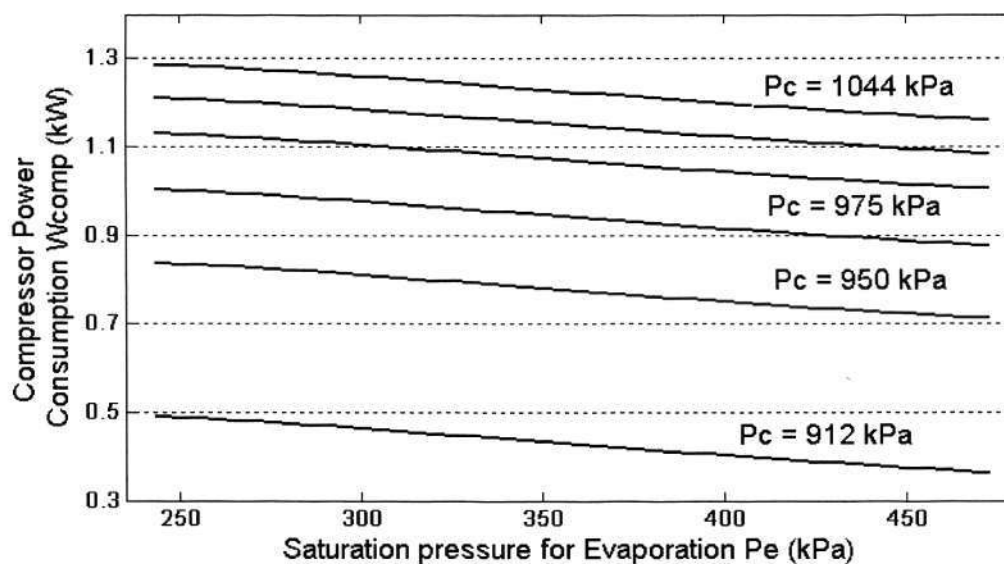


Figure 3.6: Compressor Power consumption – varying P_e

Equation (3.21) states that the power consumption of a compressor can be defined solely on the basis of T_c and T_e . Thus the power consumed by the compressor varies by changing either T_e or T_c or both. In chapter 4, T_e and T_c are explained as solely dependent on P_e and P_c respectively. For this reason, Figure (3.6) and Figure (3.7)

MODELLING OF VAPOUR COMPRESSION CYCLE

illustrate the dependency of power consumption of compressor on P_e and P_c instead of T_e and T_c .

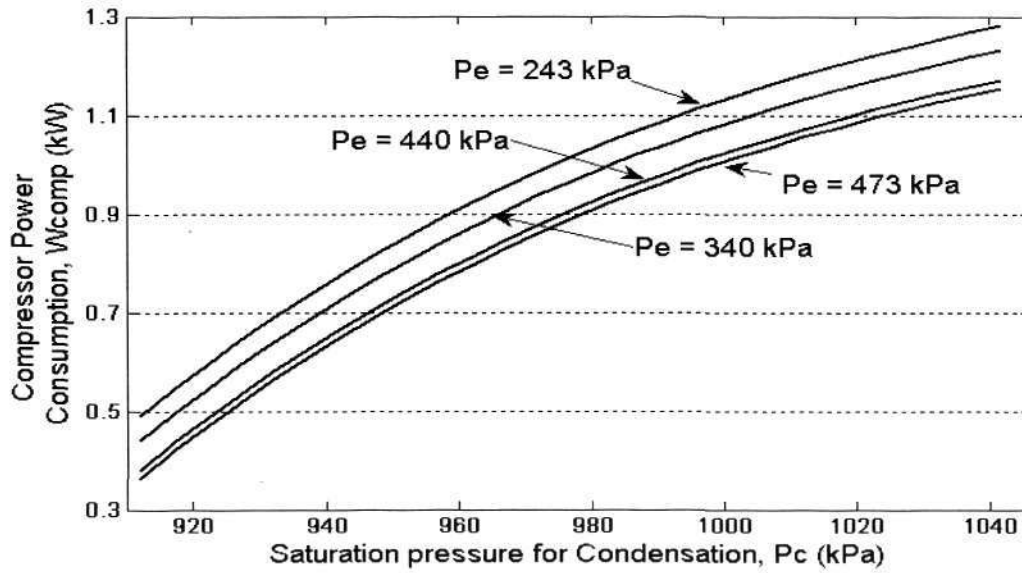


Figure 3.7: Compressor Power Consumption - varying P_c

3.5 Modelling of Evaporator and Condenser fans

For evaporators and condensers equipped with fans with VSD (variable speed drive), the power consumption are generically defined as,

$$\dot{W}_{cf} = \dot{W}_{cf,nom} \left(c_0 + c_1 \left(\frac{m_{cSF}}{m_{cSF,nom}} \right) + c_2 \left(\frac{m_{cSF}}{m_{cSF,nom}} \right)^2 + c_3 \left(\frac{m_{cSF}}{m_{cSF,nom}} \right)^3 \right) \quad (3.22)$$

$$\dot{W}_{ef} = \dot{W}_{ef,nom} \left(c_0 + c_1 \left(\frac{m_{eSF}}{m_{eSF,nom}} \right) + c_2 \left(\frac{m_{eSF}}{m_{eSF,nom}} \right)^2 + c_3 \left(\frac{m_{eSF}}{m_{eSF,nom}} \right)^3 \right) \quad (3.23)$$

where, $\dot{W}_{cf,nom}$ and $\dot{W}_{ef,nom}$ are nominal power consumption of the condenser and evaporator fans (given by the manufactures) and $m_{cSF,nom}$ and $m_{eSF,nom}$ are nominal mass flow rate of the secondary fluids across the condenser and evaporator respectively.

MODELLING OF VAPOUR COMPRESSION CYCLE

The secondary fluid across evaporator is the air in control area; and the secondary fluid across condenser is outside air. Similarly, m_{cSF} and m_{eSF} are the mass flow rates of air across evaporator and condenser. The constants C_s are determined using fan curves.

In this thesis, software *Ventil 3.1.2* [17] has been used to get the fan curves for mass flow rate of air between 0.15 to 0.65 kg/s. The compiled resulting data i.e. power consumption with corresponding mass flow rates was fitted into a curve using the 2D curve fitting software, *TableCurve* [1]. The mathematical model for fan power consumption can be modified as,

$$W_{cf} = cf_0 + cf_1 m_{cSF} + cf_2 m_{cSF}^2 + cf_3 m_{cSF}^3 \quad (3.24)$$

$$W_{ef} = ef_0 + ef_1 m_{eSF} + ef_2 m_{eSF}^2 + ef_3 m_{eSF}^3 \quad (3.25)$$

where, cf_n and ef_n are fan constants determined fan curves. If the fan specifications, like fan diameter and pressure drop are different, the constants will differ.

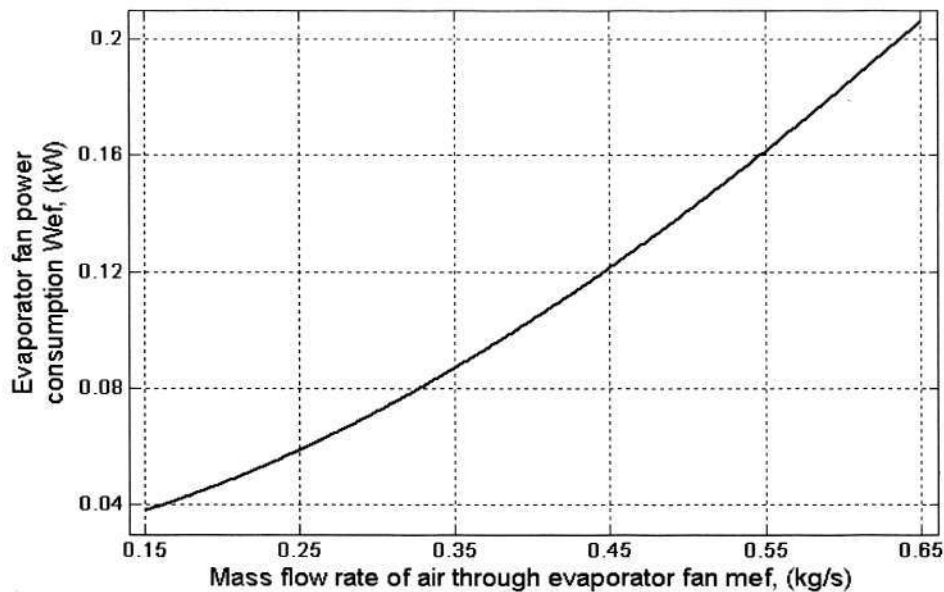


Figure 3.8: Evaporator fan Power Consumption

MODELLING OF VAPOUR COMPRESSION CYCLE

Figure (3.8) shows the relation between mass flow of air through evaporator fan and fan power consumption.

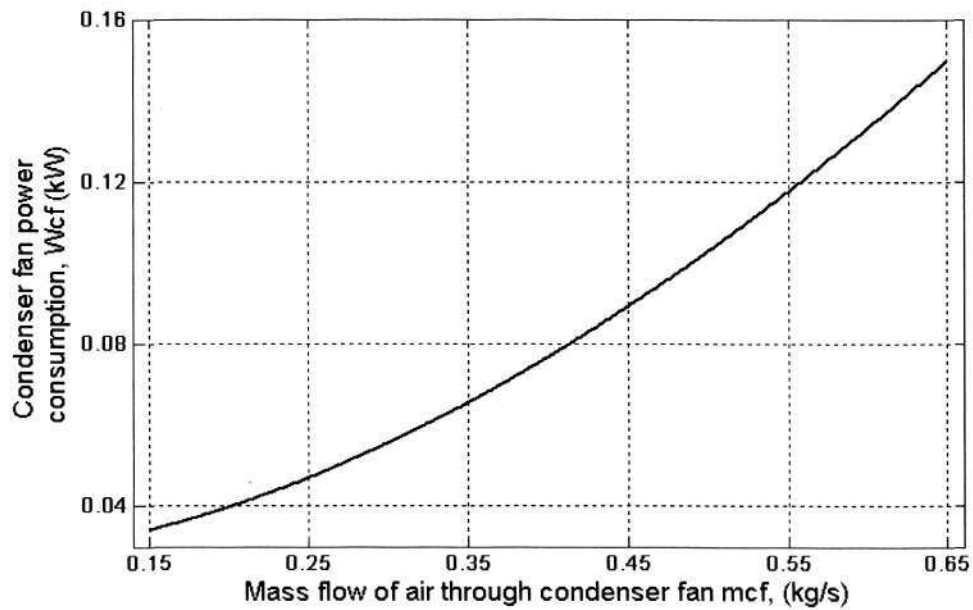


Figure 3.9: Condenser fan Power Consumption

The dependence of condenser fan power consumption on the mass flow rate of air is shown in Figure (3.9).

Chapter 4

VCC and Optimization Implementation

To apply genetic algorithm as an optimization tool on VCC, the component models as explained in previous chapter are used. This chapter discusses the optimization problem corresponding to the VCC. Later on, mechanical and irrevocable operational limits are established as the constraints. The various refrigerant properties are also discussed; the constants associated with these properties are highlighted in Appendix A.2.

4.1 Problem Definition

The foremost requirement of the problem formulation is to define the objective function. The objective function for optimization of vapour compression cycle requires that the energy consumed by the power-consuming devices, specifically the compressor, evaporator fan and the condenser fan, is minimized.

Mathematically, the requirement of the energy optimization technique is to minimize overall power consumption ($\sum W$) while successfully maintaining the reference temperature of the control area, i.e. the cold reservoir temperature $T_{cr,ref}$. The optimization problem can be stated as a function of cost function J .

VCC AND OPTIMIZATION IMPLEMENTATION

$$J = \min W_{comp} + W_{cf} + W_{ef} \quad (4.1a)$$

$$\text{Subject to } T_{cr} = T_{cr,ref} \quad (4.1b)$$

where W_{comp} : Power consumed by compressor

W_{cf} : Power consumed by condenser fan.

W_{ef} : Power consumed by evaporator fan.

The above statement can also be used as objective function for minimization of energy consumption, if the time factor is included in it.

The power consumption of compressor is given as follows:

$$W_{comp} = b_1 + b_2 T_e + b_3 T_e^2 + b_4 T_e^3 + b_5 T_c + b_6 T_c^2 + b_7 T_c^3 \quad (4.2)$$

The power consumption of evaporator and condenser fan are formulated as,

$$W_{cf} = cf_0 + cf_1 m_{cSF} + cf_2 m_{cSF}^2 + cf_3 m_{cSF}^3 \quad (4.3)$$

$$W_{ef} = ef_0 + ef_1 m_{eSF} + ef_2 m_{eSF}^2 + ef_3 m_{eSF}^3 \quad (4.4)$$

The performance of the vapour compression cycle with R134 refrigerant is dependent on various other factors, such as the physical limitations of each component, environmental conditions, and interdependencies amongst individual parameters. These factors are collectively termed as constraints. The mathematical formulations and actual explanations of these are as below.

4.1.1 Mechanical constraints

1. As W_{ef} and W_{cf} are dependent on mass flow rates m_{SF_e} and m_{SF_c} respectively, the physical limitations for these are specified by the fan manufacturer as following.

$$m_{efan,min} \leq m_{SF_e} \leq m_{efan,max} \quad (4.5)$$

$$m_{cfan,min} \leq m_{SF_c} \leq m_{cfan,max} \quad (4.6)$$

VCC AND OPTIMIZATION IMPLEMENTATION

2. The mass flow rate of working fluid is also limited for a vapour compression cycle with limited capacity.

$$m_{WF,min} \leq m_{WF} \leq m_{WF,max} \quad (4.7)$$

3. The range of condensing saturation pressure and evaporating saturation pressure for which the mathematical model replicates a real system is,

$$P_{e,min} \leq P_e \leq P_{e,max} \quad (4.8)$$

$$P_{c,min} \leq P_c \leq P_{c,max} \quad (4.9)$$

4. As per the previous point, the pressure lies between the range P_{min} to P_{max} . Subsequently, saturation temperature also lies within the range as per the relation between P and T . The relation is shown as below in Figure (4.1)

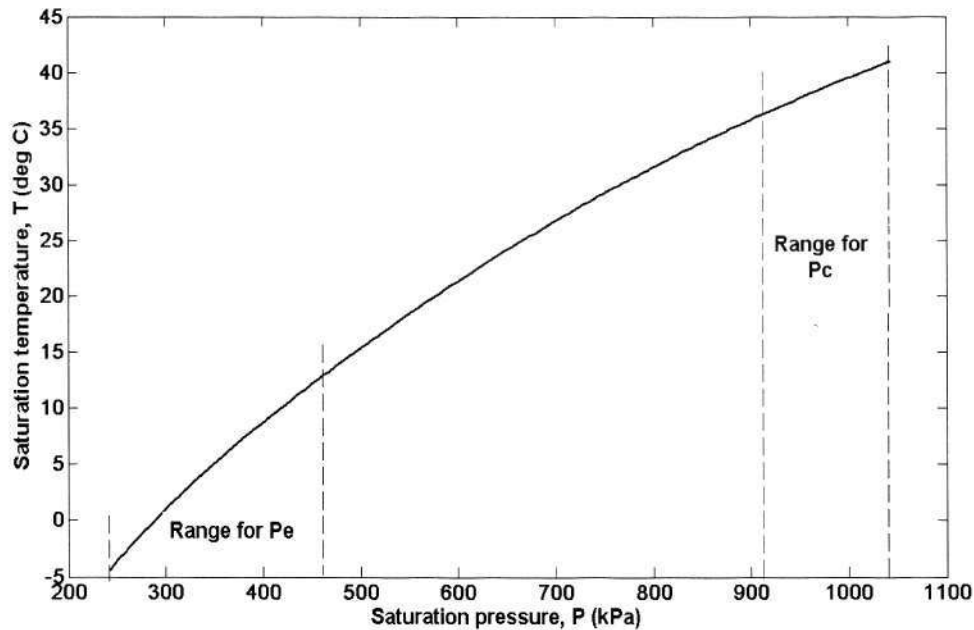


Figure 4.1: Temperature Vs Pressure Diagram

4.1.2 Operational constraints

5. Saturation evaporating temperature (T_e) and saturation condensing temperature (T_c) are limited as stated in Equation (4.10) and Equation (4.11).

VCC AND OPTIMIZATION IMPLEMENTATION

$$T_{cSF} \leq T_c \leq T_{cWF,i} \quad (4.10)$$

$$T_{eWF,i} \leq T_e \leq T_{eSF} \quad (4.11)$$

Equation (4.10) signifies that the working fluid condensing temperature should be more than the secondary fluid temperature; this is utmost important for the flow of heat to be from the condenser to the ambient air and not the other way round. Equation (4.10) also signifies that the condensing temperature should be lesser than the inlet temperature of the working fluid; this is needed for condensation to occur in the condenser.

Similarly, Equation (4.11) is to ensure that the evaporating saturation temperature inside the evaporator is higher than the inlet working fluid temperature, so as to make evaporation feasible. Also, T_e should be lesser than the surrounding air temperature so that the flow of heat is from the control area to the evaporator fluid.

6. The sub-cooled and superheated temperatures of the working fluid through the condenser and the evaporator ($T_{c,sc}$ and $T_{e,sh}$) are restricted by,

$$5K < T_{e,sh} \leq 10K \quad (4.12a)$$

$$5K < T_{c,sc} \leq 10K \quad (4.12b)$$

where,

$$T_{e,sh} = T_{eWF,o} - T_e \quad (4.13a)$$

$$T_{c,sc} = T_c - T_{cWF,o} \quad (4.13b)$$

T_e represents the temperature at which the refrigerant is saturated in the evaporator. At saturation temperature, phase transition of the refrigerant occurs. Beyond this temperature and at the corresponding pressure P_e , the refrigerant which is undergoing phase transition totally converts to vapour state. The vapour

VCC AND OPTIMIZATION IMPLEMENTATION

is superheated so that only the thermal energy is increased. The lower threshold of the superheated temperature signifies that the vapour is well beyond the saturation temperature. Effectually, the refrigerant entering the compressor is entirely converted to vapour, thus protecting the compressor from any liquid bubbles that can impair its working condition. Overheating the refrigerant beyond a certain limit can also damage the compressor. Thus the upper bound on the superheat temperature exists.

Similarly, T_c represents the temperature at which the refrigerant is saturated in the condenser. At this saturation temperature, phase transition of refrigerant occurs from vapour to liquid state. Below this temperature and at the corresponding high pressure P_c , the refrigerant which is undergoing phase transition, completely converts to liquid state. The lower threshold of the sub-cooled temperature signifies that when the refrigerant enters the valve it is liquid phase, and no vapour bubbles exist in it. In the valve, the refrigerant flash evaporates so that when entering the evaporator, it is a liquid-vapour mixture. To ascertain that this happens, the refrigerant should not be cooled much lower than the condensing saturation temperature. Thus a higher limit exists on sub-cooling temperature of refrigerant.

4.1.3 Other Important Constraints

7. The evaporator hybrid model defined in Equation (3.8) is actually a system model, on which the optimization problem is implemented. The equation is restated so as to explain this constraint.

VCC AND OPTIMIZATION IMPLEMENTATION

$$Q_e = \frac{(H_{g,e} - H_{WF,i})\dot{m}_{WF} + c_1 \dot{m}_{WF}^e (T_{SF,i} - T_e)}{1 + c_2 \left(\frac{\dot{m}_{WF}}{\dot{m}_{SF,e}}\right)^e} \quad (4.14)$$

Eq (4.14) is taken as a constraint, because one of the penalty values added to the objective function is dependent on the above model. This model is also a part of the control objective. The control objective states that the calculated Q_e should be equal to the required Q which is predefined or user-defined.

8. As per energy balance, the heat to be given out by the condenser is the amount of work done by the compressor in addition to the heat absorbed by the evaporator.

$$Q_c = Q_e + W_{com} \quad (4.15)$$

Using the above equation, the amount of heat transfer that has to occur in the condenser, is calculated.

9. The condenser hybrid model for heat transfer is as follows.

$$Q_c = \frac{d_1 \dot{m}_{WF}^{e1} (T_{sat} - T_{SF,i}) + d_2 \dot{m}_{WF} (T_{WF,i} - T_c) + H_{fg} \dot{m}_{WF}}{1 + d_3 \left(\frac{\dot{m}_{WF}}{\dot{m}_{SF,c}}\right)^{e1}} \quad (4.16)$$

Using the above equation, the actual amount of heat that is given out to the surroundings is calculated. The above relation is compared with Equation (4.15), so that if the calculated Q_c is not equal to the required amount of heat to be transferred, a second penalty value is added to the objective function.

4.2 Variable Relationships

1. The relation between saturation pressure and saturation temperature for refrigerant R134 is as follows.

VCC AND OPTIMIZATION IMPLEMENTATION

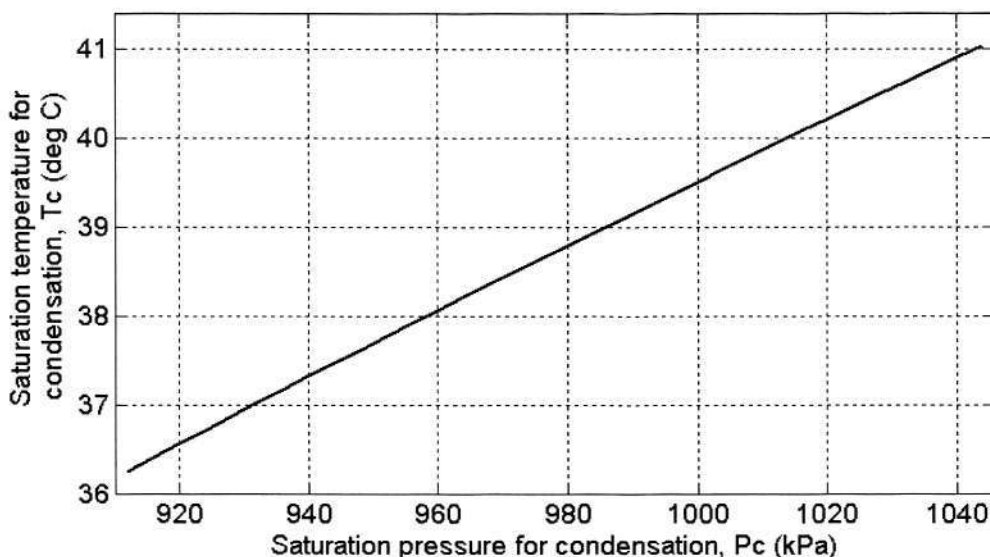


Figure 4.2: Saturation temperature T_c Vs Saturation pressure P_c

The saturation temperature T_{sat} is modelled as a 10th degree polynomial function of saturation pressure P_{sat} . Saturation temperature for evaporation and condensation are both calculated with the help of Equation (4.17).

$$T = d_1 + (d_2 + P(d_3 + P(d_4 + P(d_5 + P(d_6 + P(d_7 + P(d_8 + P(d_9 + P(d_{10} + (d_{11} * P)))))))))) \quad (4.17)$$

Since the range of pressure values for P_e and P_c are discontinuous, the graphs shown are separate. Figure (4.2) shows that for saturation pressure for condensation ranging between 912-1044 kPa, the saturation temperature of condensation ranges in 36 - 41 °C.

For saturation pressure for evaporation P_e ranging between 243 to 473 kPa, the saturation temperature of evaporation T_e ranges between -6 to 14 °C as shown in Figure (4.3).

VCC AND OPTIMIZATION IMPLEMENTATION

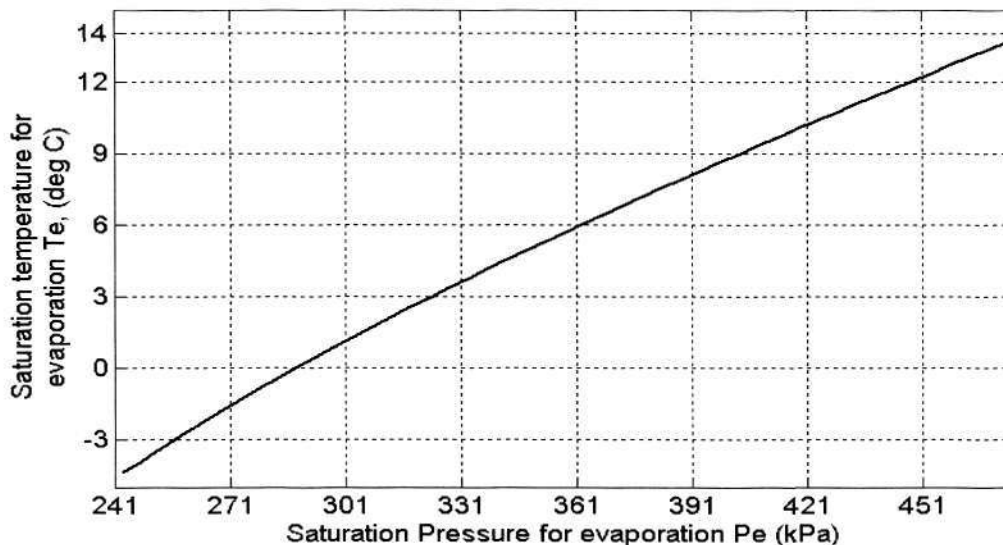


Figure 4.3: Saturation temperature T_e Vs Saturation pressure P_e

- Heat exchanged in the evaporator is depended on the enthalpy of refrigerant as shown in Figure (4.4). As explained before, the heat transfer involves two elements, the latent heat and the superheat. The latent heat to convert liquid vapour refrigerant to vapour is,

$$Q_{latent} = (H_{g,e} - H_{e,i})\dot{m}_{WF} \tag{4.18}$$

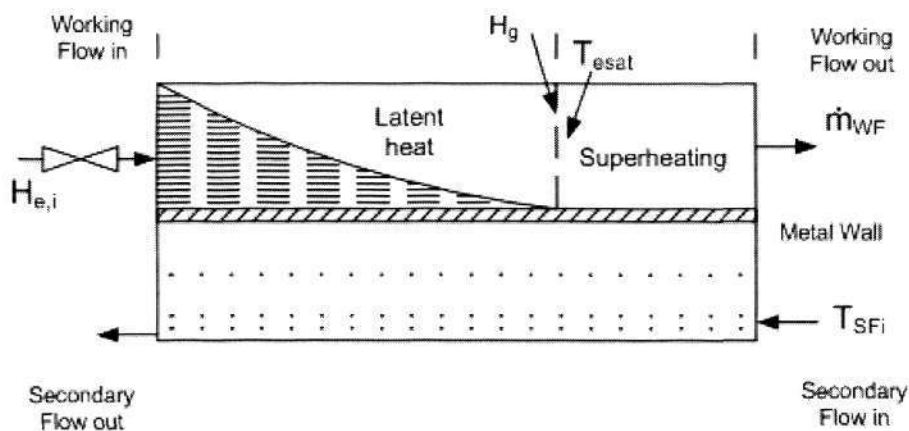


Figure 4.4: Enthalpies Involved in evaporation

Vapour Enthalpy $H_{g,e}$ depends exclusively on the saturation pressure for evaporation, P_e . It is defined as a 10th order polynomial as follows.

VCC AND OPTIMIZATION IMPLEMENTATION

$$H_{g,e} = e_1 + (e_2 + P_e(e_3 + P_e(e_4 + P_e(e_5 + P_e(e_6 + P_e(e_7 + P_e(e_8 + P_e(e_9 + P_e(e_{10} + (e_{11} * P_e)))))))))) \quad (4.19)$$

For P_e ranging between 243 to 473 kPa, $H_{g,e}$ varies between 396 J/kg to 406J/kg, as shown in Figure (4.5).

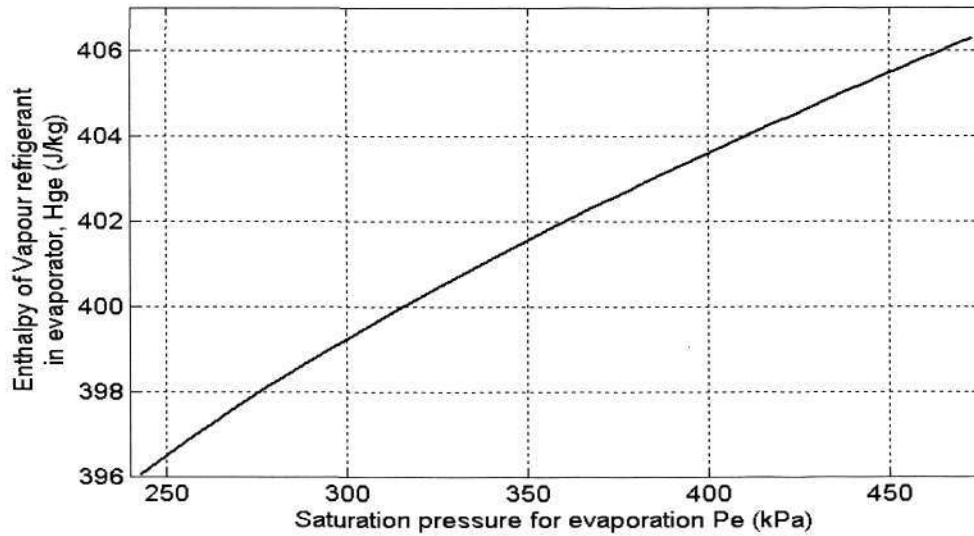


Figure 4.5: Vapour enthalpy of refrigerant in evaporator

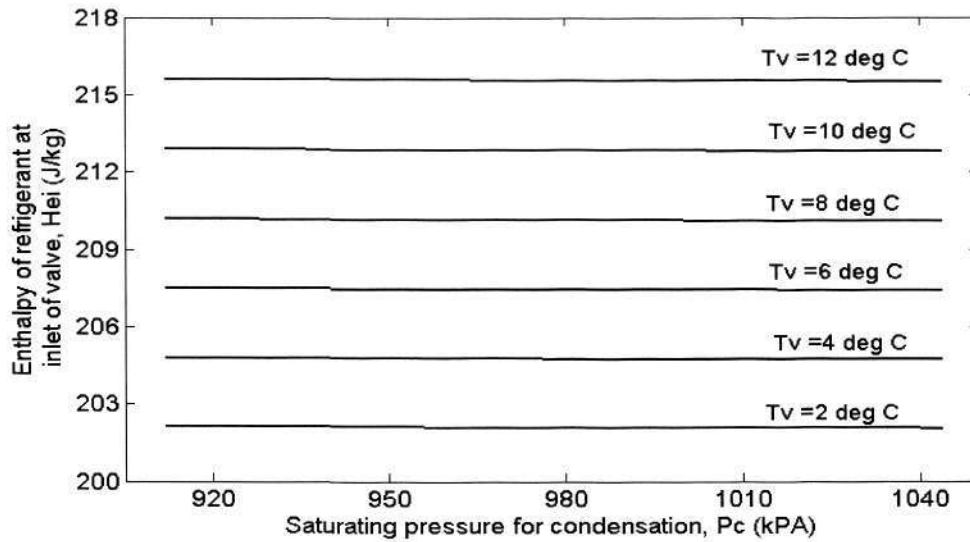


Figure 4.6: Liquid Enthalpy $H_{e,i}$ Vs Saturation pressure P_c

VCC AND OPTIMIZATION IMPLEMENTATION

$H_{e,i}$ is the enthalpy of liquid refrigerant that enters the valve. It depends on two parameters, condensing pressure P_c and valve inlet temperature, T_v . The value of $H_{e,i}$ with change in P_c , varies very faintly, for a constant T_v .

$$H_{e,i} = a_0 + P_c(a_1 + P_c(a_2 + P_c a_3)) + T_v(a_4 + T_v(a_5 + T_v a_6)) + P_c T_v(a_7 + a_8 P_c + a_9 T_v) \quad (4.20)$$

Figure (4.6) shows the relation as $H_{e,i}$ plotted against P_c for different values of T_v .

- To calculate the heat transfer in condenser, the latent heat H_{fg} is required. H_{fg} is the enthalpy of the two phase refrigerant at the intermediary region shown in Figure (3.4). As Equation (4.21) states, it is calculated as the difference in enthalpy of liquid refrigerant H_f and enthalpy of vapour refrigerant H_g . Figure (4.7) plots the enthalpy values.

$$H_{fg} = H_{gc} - H_{fc} \quad (4.21)$$

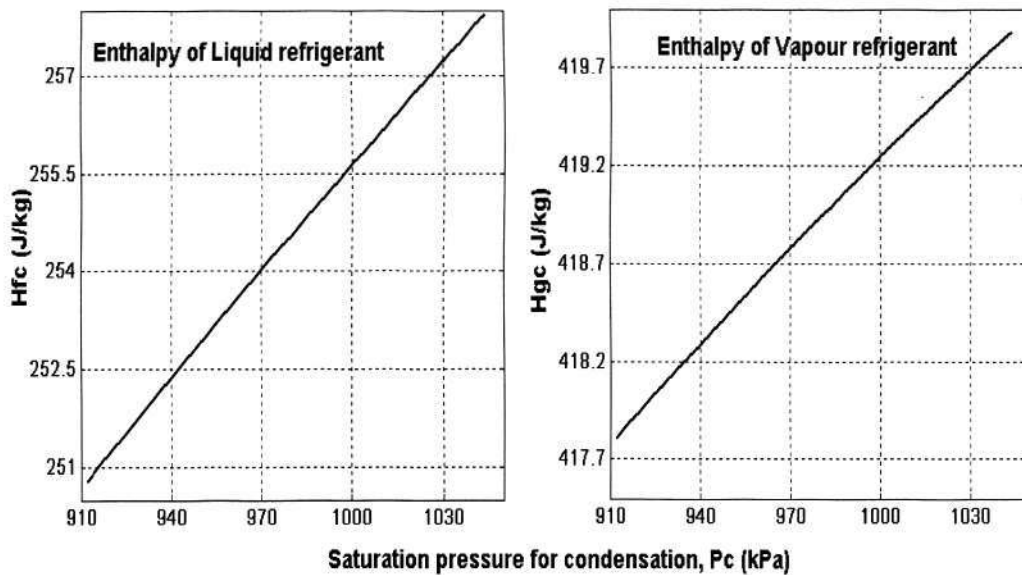


Figure 4.7: Enthalpy of liquid-vapour mixture in Condenser

4.3 Model based Optimization-Vapour Compression Cycle

The design of model based optimization system is based [12] on the distributed control system where there are different levels of controls. The cross-couplings and interactions in the process are managed by the local controllers. The high-end controllers govern the process and calculate the model parameter accordingly. The advantage of having a distributed control system over a centralized one is that, there are fewer parameters involved in each level process system making it easier for the control system to control the subsystems.

The main optimization part covered in this thesis is the set-point optimization. The objective function(s) have to be declared foremost, when defining a problem for optimization. As per the scope of this thesis, there is only one objective function, which is to minimize the power consumption of the vapour compression cycle. To be called as online set-point optimization, the optimization algorithm has to run and calculate the optimal set points continuously.

Set-point optimization lies on top of the distributed control system. It calculates the work points (or set-points) for optimized control of the process. As shown in Figure (4.8), the set-point optimization section can be divided into 3 subgroups,

- Model based adaptation
- Steady state prediction model
- Steady state optimization

VCC AND OPTIMIZATION IMPLEMENTATION

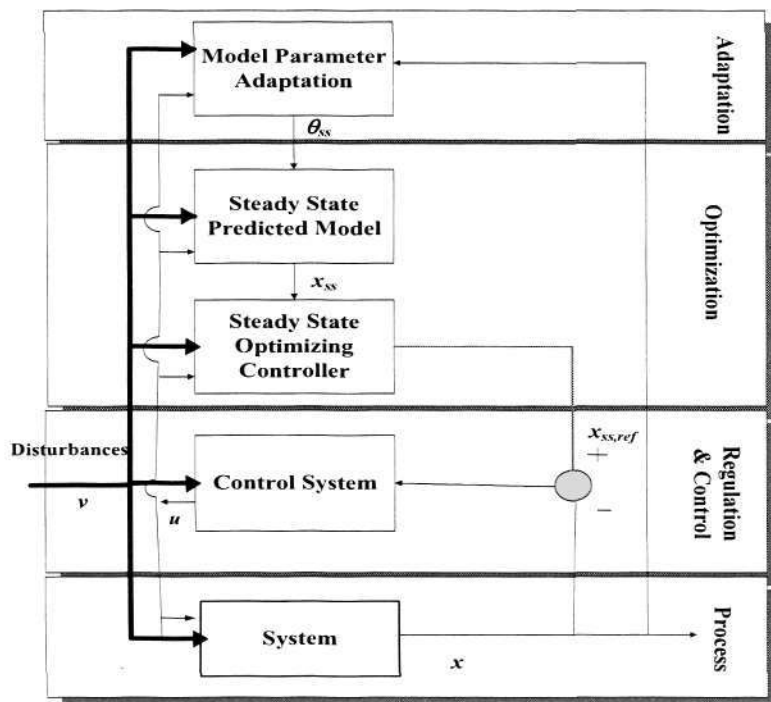


Figure 4.8: Control Structure for Optimization

The steady state model is used by the steady state optimization block to drive cost function J' to a minimum. The steady state model is regularly adapted to outside disturbances by the model parameter adaptation, thus reducing prediction error. For the system to work accurately the prediction error should be minimized; thus the model should try to capture the maximum characteristics of the actual system.

The control system at the regulation and control section, involves the dynamic optimization strategy. This part controls the fast disturbances as part of the regulatory level.

Moving up the hierarchy level, control parameters vary less frequently than the dynamic optimization block. Thus, the distributed control system can be divided according to the frequency [12]. The dynamical optimization is handled at the regulatory/control level whereas the set-point optimization is handled by the

VCC AND OPTIMIZATION IMPLEMENTATION

optimization level. Due the regulatory nature of dynamic optimization at the regulatory level, the involvement of the set-point optimization is reduced in the process level.

This thesis is limited to simulation of set-point optimization of Vapour compression cycle. Thus, real-time modelling adjustments and dynamic optimization control is not discussed beyond this section.

4.3.1 Optimization Algorithms

The main control objective for optimization is to meet the set point temperature of the room i.e. control area. The difference between the present temperature and the set point temperature can be converted to equivalent heat, that has to removed so that the room temperature is brought down to equal the set-point. Mathematically, it can be represented as,

$$Q_{SF} = C * \Delta T_{SFm} \quad (4.22)$$

where, C is a constant containing factors such as the average convective heat transfer co-efficient and heat exchange surface area.

ΔT_{SFm} is average temperature difference between metal tube of heat exchanger and secondary air-flow.

Thus, if the temperature has the brought down from for e.g. 35 °C to 22 °C, the equivalent heat to be removed is Q . When the refrigerator starts cooling the room, the room temperature decrease thus the cooling load Q also reduces.

Hence the algorithm has to be made useful for different cooling loads. The independent variables and the set-points of different components in the refrigerator

VCC AND OPTIMIZATION IMPLEMENTATION

vary for altering cooling loads. These variables and set-points are calculated using the algorithm described as below along with the subroutine described in Section 4.3.2.

1. Initialization: Various genetic Algorithm parameters are defined. The parameters are population $NIND$, generation gap $GGAP$, number of iterations $MaxGen$, number of variables $NVAR$ and precision of binary numbers $PREC$.
2. Outside air temperature T_{SFc} and room temperature T_{SFe} are predefined or given.
3. The cooling load Q corresponding to T_{SFc} and T_{SFe} are also predefined.
4. Actuator variables ranges are defined.
5. A gray-coded number matrix $Chrom$ of $NIND$ rows and $PREC*NVAR$ columns is randomly generated.
6. The base value $Chrom$ is converted into real value, for use in the subroutine algorithm. The result is an array of randomly generated actuator variable values such that they are always in the range specified in Step 4.
7. The fitness function of each row of $Chrom$ is calculated, using the subroutine, Section 4.3.2.
8. The initial generation is defined as, $Gen = 0$, and increased by 1 for each of the following iteration until $Gen = MaxGen$.
 - a. The fitness function matrix is ranked from a range of 0-2. Here, a rank of 2 means that the fitness value is lesser than the rest of the population. And a lower rank means that the fitness value is higher than the rest of the population.
 - b. A predefined percentage of the population is selected according to roulette wheel method using the ranks assigned to each of the individual in the population.

VCC AND OPTIMIZATION IMPLEMENTATION

- c. Recombination is done on the individuals of the selected population, such that the changed population contains some characteristics of the original population.
 - d. A part of the selected population is again invoked in mutation, that is, a percentage of population are modified such that their characteristics are completely changed. Effectively this means that the search direction is altered a bit, so that solutions are searched in all the possible search regions.
 - e. The subroutine algorithm is used to find the objective function value of the new population - which is a combination of the modified version of the old population and a percentage of new individuals.
 - f. Using the fitness value array of objective function, the individuals from the modified population are reinserted such that the weaker individuals of the old population are more probably replaced by stronger counterparts in the modified population.
 - g. Simultaneously, the fitness value is also stored along with the new population.
 - h. A generation is thus completed and a new generation begins from the Step number (8.a.) using the population achieved in the predecessor generation
 - i. The above loop is broken if the generation $Gen = MaxGen$.
9. It is natural to assume that the last generation contains the best fit individual; in effect the best solution to the objective function is contained in this population.
 10. For the final population, the fitness values are calculated.
 11. The individual whose fitness value is lesser than the rest of the population is settled as the individual with best fitness.
 12. For this individual, the rest of the parameters are calculated.

VCC AND OPTIMIZATION IMPLEMENTATION

4.3.2 Subroutine

1. The foremost requirement is the objective function which is defined as follows.

$$J = \min(W_{comp} + W_{cf} + W_{ef}) \tag{4.23a}$$

$$\text{Subject to } Q = Q_{load} \tag{4.23b}$$

The optimization problem requires that the sum of power consumed by the energy consuming devices, i.e., compressor (W_{comp}), evaporator fan (W_{ef}) and the condenser fan (W_{cf}) is minimized. The objective function should be minimized while meeting the control objective, i.e. the amount of heat Q removed from the control area should be equal to cooling demand Q_{load} . In this thesis, the genetic algorithm as described in Figure (4.10) and Figure (4.11) are used to solve Equation (4.23).

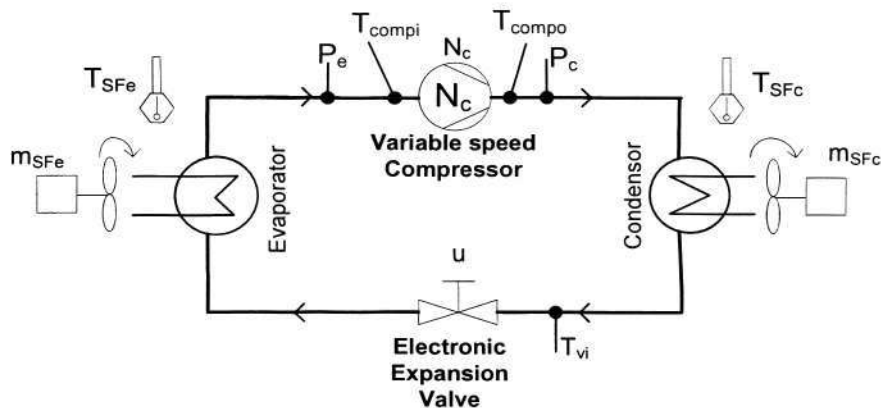


Figure 4.9: VCC with parameters

Figure (4.9) illustrates the temperature parameters involved in VCC.

These parameters will be used in the following explanation. In case of simulations, the initial parameters (T_{SFe} and T_{SFc}) that cannot be calculated are assumed. If measured, the parameters are captured by temperature probes placed appropriately to capture the right information.

VCC AND OPTIMIZATION IMPLEMENTATION

If the optimization is working on a real system, the parameters values are measured and updated every once a while as per user definition. Since the implementation is for set-point optimization, continuous measurement of these variables is not required.

2. $P_e, P_c, m_{SF_e}, u, m_{SF_c}$ are taken as the manipulated variables. Random values of P_e and P_c are generated within a range of the operational limits such that $P_c > P_e$ always. The expression of $P_c > P_e$ satisfies the basic constraint for the operation of VCC. In reality the pressure values are manipulated using the compressor and electronic expansion valve. Mass flow rate of air in control area must always fall in the following range (previously in Equation (4.5)).

$$m_{SFmin} < m_{SF_e} < m_{SFmax} \quad (4.24)$$

Mass flow rate of air at the condenser fan outlet must be in the following range (previously shown in Equation (4.6)).

$$m_{SFmin} < m_{SF_c} < m_{SFmax} \quad (4.25)$$

3. Mass flow rate of working flow is calculated using Equation (3.20) as the model of expansion valve. For this purpose, parameters P_e, P_c , and percentage opening of valve 'u' are required.
4. Other values such as $H_{g,e}, H_{e,i}, T_e, T_c$ are calculated using appropriate models.
5. Using the mass flow rate of air across evaporator m_{SF_e}, T_v is calculated using Equation (4.14) such that the initial requirement, Q_{load} is met.

$$W_{penalty\ 1} = e^{|(Q_e - Q_{load})| * 10} \quad (4.26a)$$

$$if\ |Q_e - Q_{load}| > 0 \quad (4.26b)$$

VCC AND OPTIMIZATION IMPLEMENTATION

6. By measuring T_{compi} and T_{compo} , we find H_{compi} and H_{compo} and use it to find the effective work done by the compressor W_{com} , which would be less than the power consumed by it.
7. As per energy balance, Q_{cl} is the required heat to be given out to the surroundings Q_{cl} can be calculated from Equation (4.15).
8. The condenser inlet temperature is calculated Using Equation (4.16) and Equation (4.15).

$$W_{penalty\ 2} = e^{|(Q_c - Q_{cl})| * 10} \quad (4.27a)$$

$$if\ |Q_c - Q_{cl}| < 0 \quad (4.27b)$$

9. Since all the constraints are satisfied, the cost function can now be calculated
10. Using the mass flow rates, the power utilization of the fans is calculated.
11. The fan power consumption along with the compressor power consumption and penalty values $W_{penalty\ 1}$ and $W_{penalty\ 2}$ represent the fitness function W_f .

$$W_f = W_{comp} + W_{ef} + W_{cf} + W_{penalty\ 1} + W_{penalty\ 2} \quad (4.28)$$

4.3.3 VCC Optimization Flowcharts

The algorithm described in Section 4.3.1 for application of GA as optimization tool is depicted in flowchart Figure (4.10). Figure (4.11) illustrates the subroutine involved for application of GA on the VCC model further describing Section 4.3.2.

VCC AND OPTIMIZATION IMPLEMENTATION

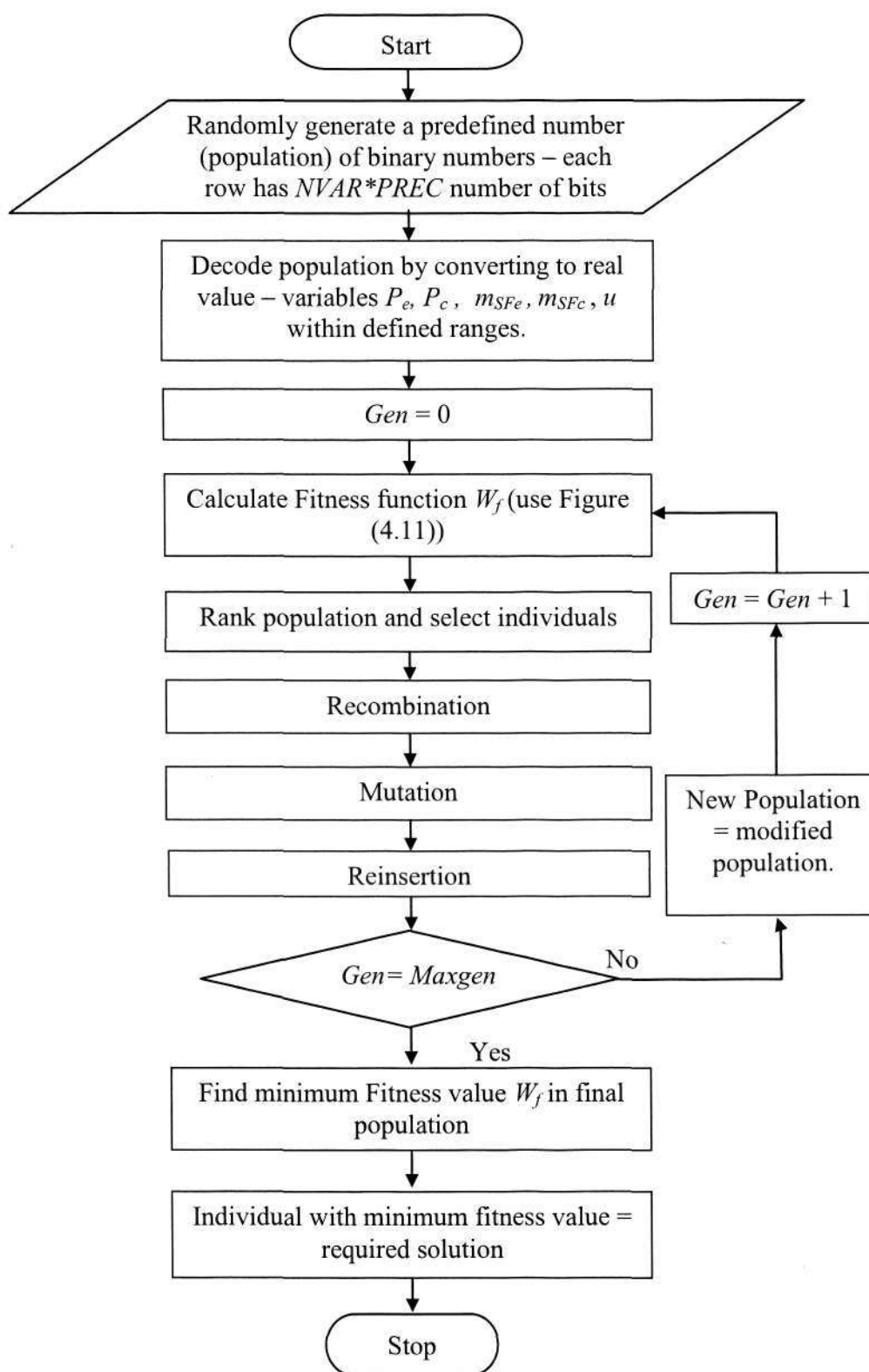


Figure 4.10: Flowchart for application of GA on optimization problem

VCC AND OPTIMIZATION IMPLEMENTATION

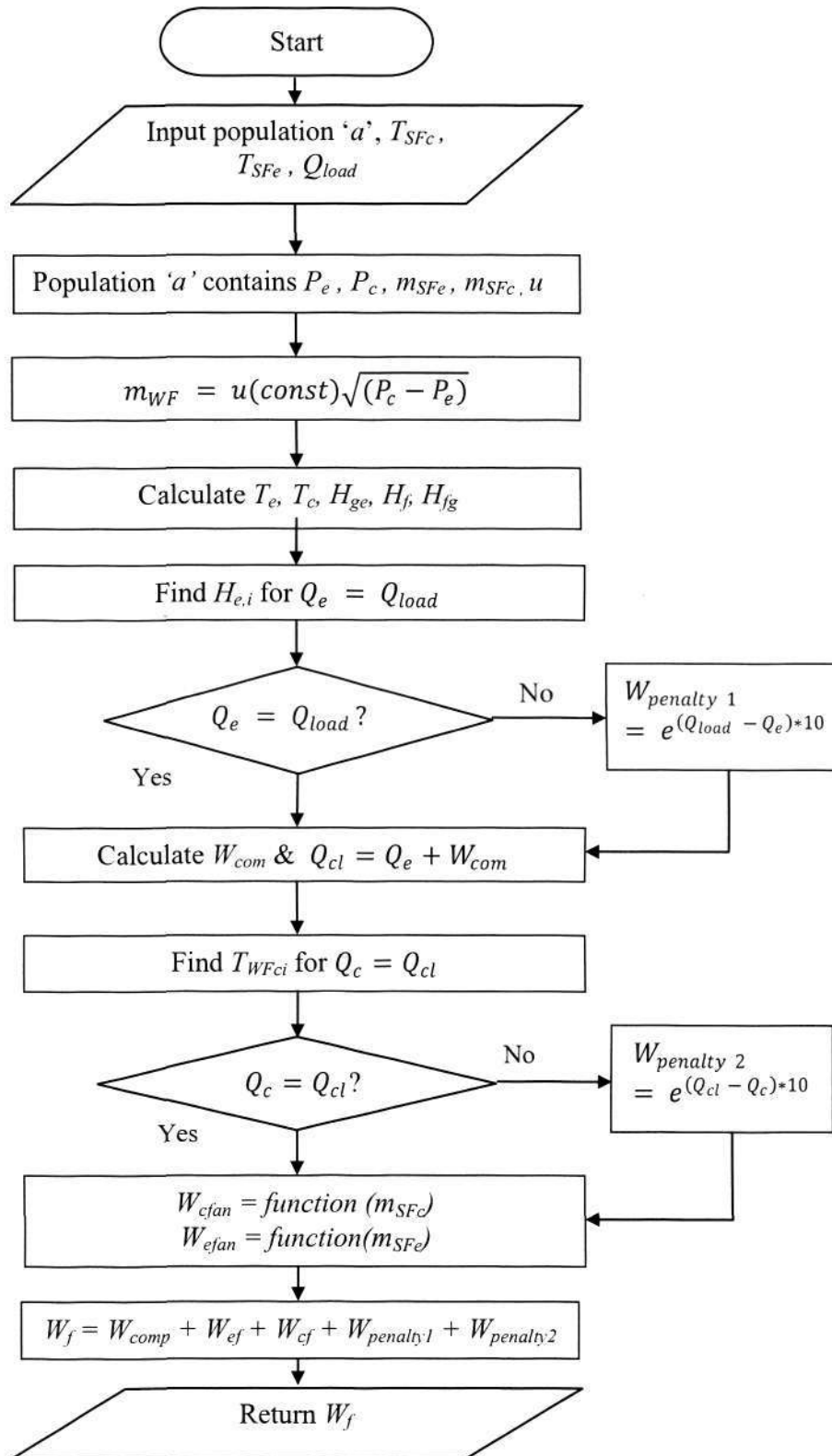


Figure 4.11: Subroutine – VCC Model and objective function

VCC AND OPTIMIZATION IMPLEMENTATION

4.3.4 Explanation of penalty functions

The above algorithms contain two penalty terms. These penalty terms are the determining factor in ascertaining that the control objective is always obeyed prior to minimizing the objective function. In the case of optimization of vapour compression cycle, the first important factor is $Q_e = Q_{load}$; that is, the amount of required heat to be removed from the control area is actually absorbed by the working fluid in the refrigeration loop. If this does not happen, the result of optimization would be baseless.

Another determining factor is that the heat absorbed by the working fluid in the refrigerant loop should be given out to the surroundings, i.e. the heat removed by the VCC from the control area which is in low temperature, should be rejected to another region whose ambient temperature is higher.

By following the energy balance law, we get the relationship shown in Figure (4.12).

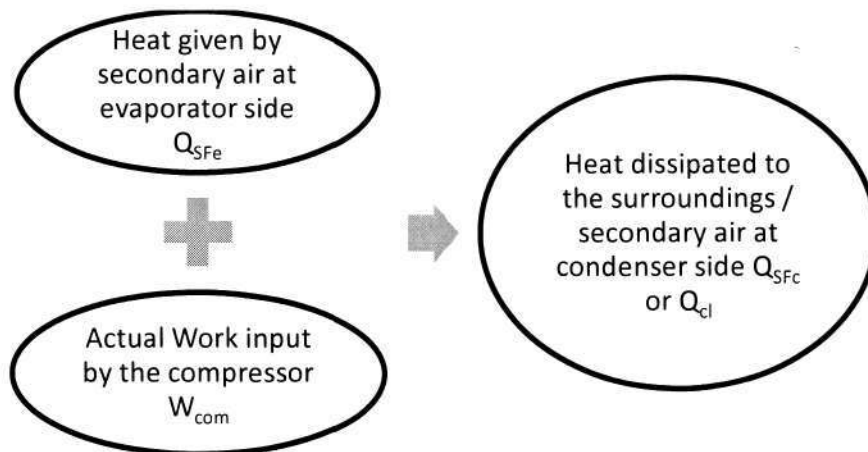


Figure 4.12: Heat flow diagram in VCC

VCC AND OPTIMIZATION IMPLEMENTATION

Hence, if this amount of heat Q_{SF_c} is not dissipated to the surroundings, the cycle is not completed, and the target of maintaining the temperature of the control area will not be met. Thus a second penalty function is added if $Q_c = Q_{cl}$.

Chapter 5

Implementation and Results

This chapter is divided into two main sections. Section (5.1) comprises of the basic optimization results. Section (5.2) covers the comparison of optimization algorithm with a base-case method.

5.1 Basic Optimization Results

This section describes the optimization implementation and results of GA on the vapour compression cycle model as a simple case. It does not include any comparison with any other method.

5.1.1 Initialization and Assumptions

Before discussing the results of optimization, the prerequisites are the inputs assumptions which are necessary for the objective function, and initialization of the genetic parameters which are mandatory for the search algorithm.

Since the thesis is limited to studying VCC optimization in a simulated environment, variables such as cooling load, room temperature and outside air temperature are assumed as they cannot be calculated or measured

IMPLEMENTATION AND RESULTS

Cooling load range for control objective:

$$Q_{load} = [0.95, 1, 1.03, 1.07, 1.1, 1.15, 1.18, 1.21, 1.25, 1.3]$$

For the above-mentioned cooling load range, we are assuming two input profiles as following.

Input Profile 1: T_{SFc} constant and T_{SFe} increasing

Outside Air (or secondary flow at condenser side) Temperature, in °C

$$T_{SFc1} = [32, 32, 32, 32, 32, 32, 32, 32, 32, 32]$$

Room air (or secondary flow at evaporator side) Temperature, in °C

$$T_{SFe1} = [24, 24.2, 24.4, 24.6, 24.8, 25, 25.2, 25.4, 25.6, 25.8]$$

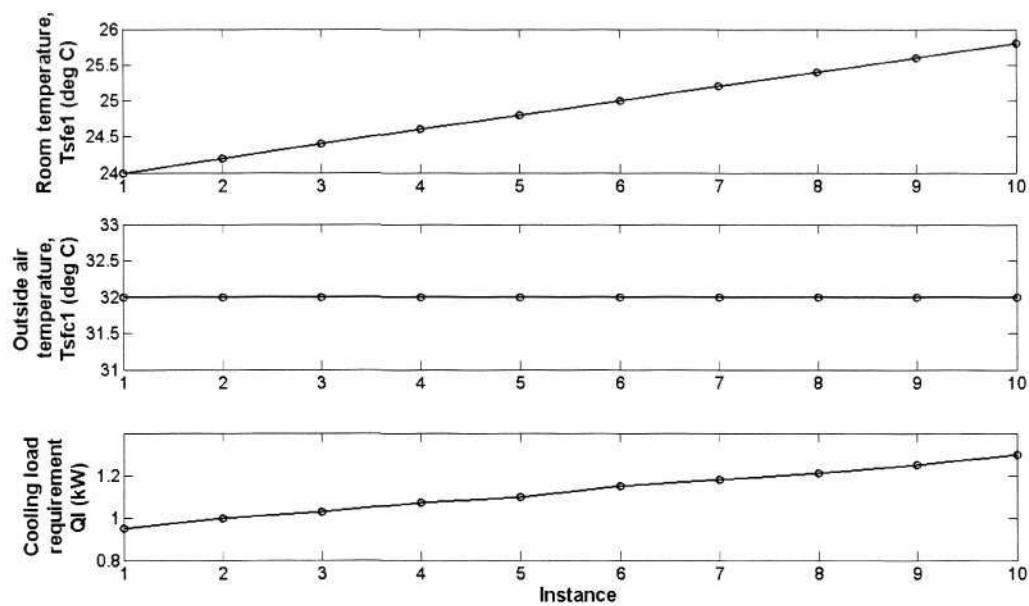


Figure 5.1a: Input profile 1, T_{SFe1} , T_{SFc1} , Q_{load}

Figure (5.1a) is a plot of the inputs' (T_{SFe1} , T_{SFc1} , Q_{load}) which forms the base profile for the implementation of the optimization algorithm.

Input Profile 2: T_{SFc} increasing and T_{SFe} constant

Outside Air (or secondary flow at condenser side) Temperature, in °C

$$T_{SFc2} = [29, 29.3, 29.6, 29.9, 30.2, 30.5, 30.8, 31.1, 31.4, 31.7]$$

IMPLEMENTATION AND RESULTS

Room air (or secondary flow at evaporator side) Temperature, in °C

$$T_{SF_{e2}} = [25, 25, 25, 25, 25, 25, 25, 25, 25, 25]$$

Figure (5.1b) is a plot of inputs' ($T_{SF_{e2}}$, $T_{SF_{c2}}$) which forms another base profile for the optimization algorithm.

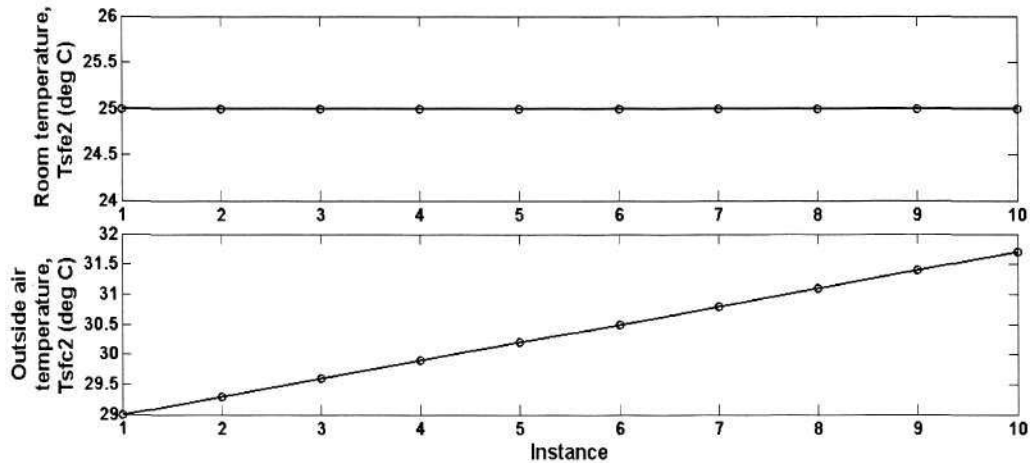


Figure 5.1b: Input profile 2, $T_{SF_{e2}}$, $T_{SF_{c2}}$

Manipulated Variables' Ranges:

The manipulated variables used for optimization are mass flow rate of air through evaporator m_{SF_e} and condenser fans m_{SF_c} , saturation pressure for evaporation P_e and condensation P_c , and expansion valve opening u . Since these values are incorporated in the VCC model, the range of these variables are defined as following for cooling load range between 0.95 to 1.3 kW.

1. Mass flow rate of air through fans:

$$0.15 \text{ kg/s} < m_{SF} < 0.65 \text{ kg/s}$$

2. Saturation pressure for evaporation,

$$243 \text{ kPa} < P_e < 473 \text{ kPa}$$

3. Saturation pressure for condensation,

IMPLEMENTATION AND RESULTS

$$912 \text{ kPa} < P_c < 1044 \text{ kPa}$$

4. Expansion valve percentage opening,

$$10.9 \% < u < 12.9 \%$$

5.1.2 GA implementation and Results

The GA optimization is applied on the mathematical formulation of VCC model. The operational constants that are defined foremost are shown in Table (5.1).

Population size per generation, <i>Nind</i>	100
Precision of individual (chromosome) for base conversion, <i>Prec</i>	12
Maximum number of generations, <i>Maxgen</i>	80

Table 5.1: Genetic Algorithm Constants

It was noted that *Maxgen* needs to be a minimum of 60 for the genetic algorithm to converge without much variation. For a larger population, the probability of finding an optimal solution increases. But setting it higher than the value of 100 makes the algorithm sluggish. The chromosome size needs to be a minimum of 8 for accurate values of the objective function. To be on the safer side, it was set equal to the value defined in Table 5.1.

For each value of input parameters (shown in Figure (5.1a and 5.1b)), GA is implemented so that the resultant variable values are achieved. For every set of input parameters, corresponding manipulated variables are calculated which when implemented will give an optimized objective function W_f .

IMPLEMENTATION AND RESULTS

Input Profile 1 - $T_{SFc1} = 32\text{ }^{\circ}\text{C}$						
Inputs		Variables for optimization				
Cooling Load, Q_{load} (kW)	Room Temperature, T_{SFc1} ($^{\circ}\text{C}$)	Saturation pressure for evaporation, P_{e1} (kPa)	Saturation pressure for condensation, P_{c1} (kPa)	Percentage opening of expansion valve, u_1 (%)	Air mass flow rate - condenser fan, m_{SFc1} (kg/s)	Air mass flow rate - evaporator fan, m_{SFc1} (kg/s)
0.95	24	406.8926	920.8	11.3269	0.6485	0.2811
1	24.2	410.3187	937.8198	12.6353	0.5837	0.1741
1.03	24.4	399.7595	934.0484	12.3681	0.6451	0.2407
1.07	24.6	400.6581	941.2689	12.877	0.6397	0.2423
1.1	24.8	351.7937	952.97	12.5904	0.6141	0.1919
1.15	25	326.4066	958.1919	12.8814	0.6406	0.1769
1.18	25.2	251.1441	969.0549	11.28	0.6483	0.2393
1.21	25.4	313.0391	971.9238	12.8565	0.6317	0.2257
1.25	25.6	290.1795	977.6938	12.8526	0.6496	0.2285
1.3	25.8	294.3358	998.8073	12.8531	0.5913	0.3355

Table 5.2a: Input profile 1 - Variable values for optimized operation of VCC

Input Profile 2 - $T_{SFc2} = 25\text{ }^{\circ}\text{C}$						
Inputs		Variables for optimization				
Cooling Load, Q_{load} (kW)	Outside Air Temperature, T_{SFc2} ($^{\circ}\text{C}$)	Saturation pressure for evaporation, P_{e2} (kPa)	Saturation pressure for condensation, P_{c2} (kPa)	Percentage opening of expansion valve, u_2 (%)	Air mass flow rate - condenser fan, m_{SFc2} (kg/s)	Air mass flow rate - evaporator fan, m_{SFc2} (kg/s)
0.95	29	440.5922	912	12.3022	0.3109	0.2096
1	29.3	433.8523	912	12.8375	0.3636	0.2239
1.03	29.6	426.7192	912	12.8985	0.4172	0.2692
1.07	29.9	383.5275	912	12.8883	0.4898	0.2147
1.1	30.2	381.0562	912	12.8419	0.5614	0.2935
1.15	30.5	356.7924	920.8	12.8839	0.6152	0.3157
1.18	30.8	310.2308	934.822	12.4111	0.6281	0.2821
1.21	31.1	301.6935	945.1048	12.751	0.6471	0.2454
1.25	31.4	294.5043	960.4484	12.8878	0.6488	0.2677
1.3	31.7	261.0855	991.748	12.6343	0.5954	0.2781

Table 5.2b: Input profile 2 - Variable values for optimized operation of VCC

IMPLEMENTATION AND RESULTS

For the required amount of cooling load, room temperature and outside air temperature, an optimized objective function is searched in the limited exploration area and the manipulated variables P_e , P_c , u , m_{SFe} , m_{SFC} , corresponding to the optimized objective function are determined. For input profile 1, i.e. Q_{load} , T_{SFe1} , ($T_{SFC1} = 32$), the generated values of the manipulated variables for optimized working of VCC is as shown in Table (5.2a). As observed, all the values lie within their respective ranges.

For the input profile 2, Q_{load} , T_{SFC2} , ($T_{SFe2} = 25$ °C), the generated values of the manipulated variables for optimized working of VCC is as shown in Table (5.2b).

For the calculated optimized results, the various parameters are enumerated as below.

1. Heat transfer in evaporator:

Direction of heat transfer in the evaporator is from the secondary flow (air) to the working flow (refrigerant). For the set of variables P_c , P_e , m_{SFe} , m_{SFC} , and u , other intermediate variables are calculated to find the actual heat removed by the evaporator, so that it matches the cooling load requirement.

To ascertain that the calculated (or actual) amount of heat transfer in evaporator Q_e is equal to the cooling load, Q_{load} , the penalty function $W_{penalty1}$ is used.

$$\text{If } \text{abs}(Q_{load} - Q_e) > 0.015 \quad (5.1a)$$

$$W_{penalty1} = e^{(|Q_e - Q_{load}| * 10)} \quad (5.1b)$$

The genetic algorithm tries to satisfy the control objective $Q_{load} = Q_e$, as close as a difference of 0.015; if unsuccessful in doing so, a penalty value $W_{penalty1}$ is included in the cost function $ObjF$.

IMPLEMENTATION AND RESULTS

Figure (5.2) shows the result of the optimization; the evaporator fulfils the cooling load requirement with an error margin of about 1.6%. For both input profiles, the evaporator matches the cooling load, in a very similar manner.

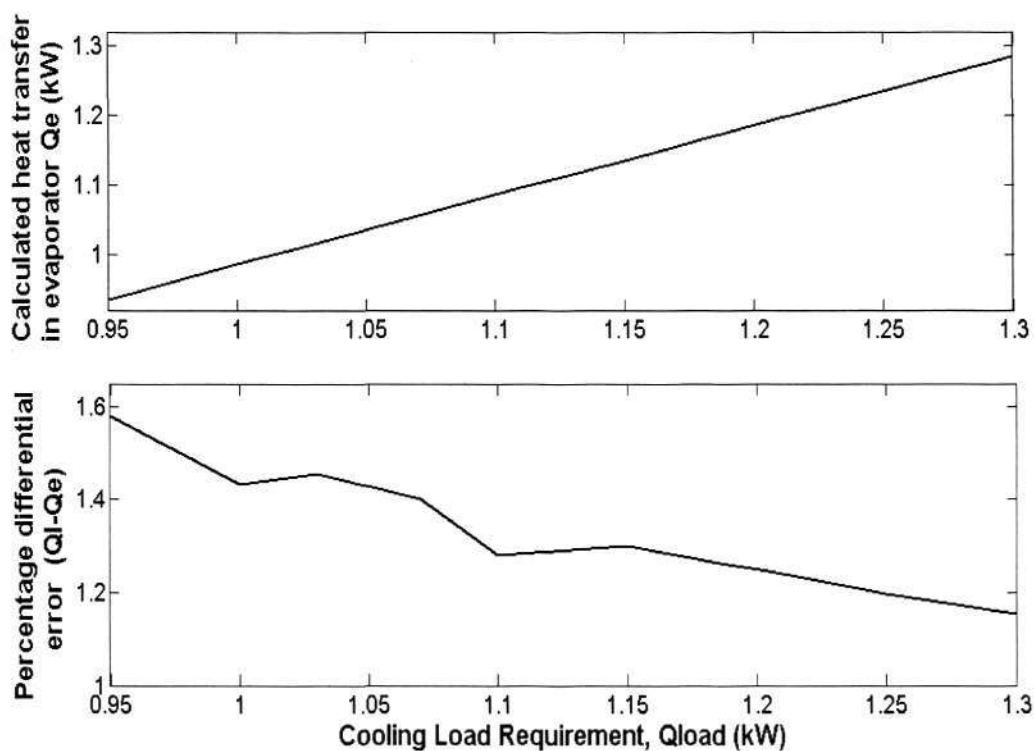


Figure 5.2: Heat transfer in evaporator

2. Heat transfer in condenser:

Direction of heat transfer in the condenser is from the working flow (refrigerant) to the secondary flow (air). For the set of variables P_c , P_e , m_{SF_e} , m_{SF_c} , and u , other intermediate variables are calculated to find the actual heat Q_c rejected by the condenser, so that it matches the required amount of heat Q_{cl} to be removed.

IMPLEMENTATION AND RESULTS

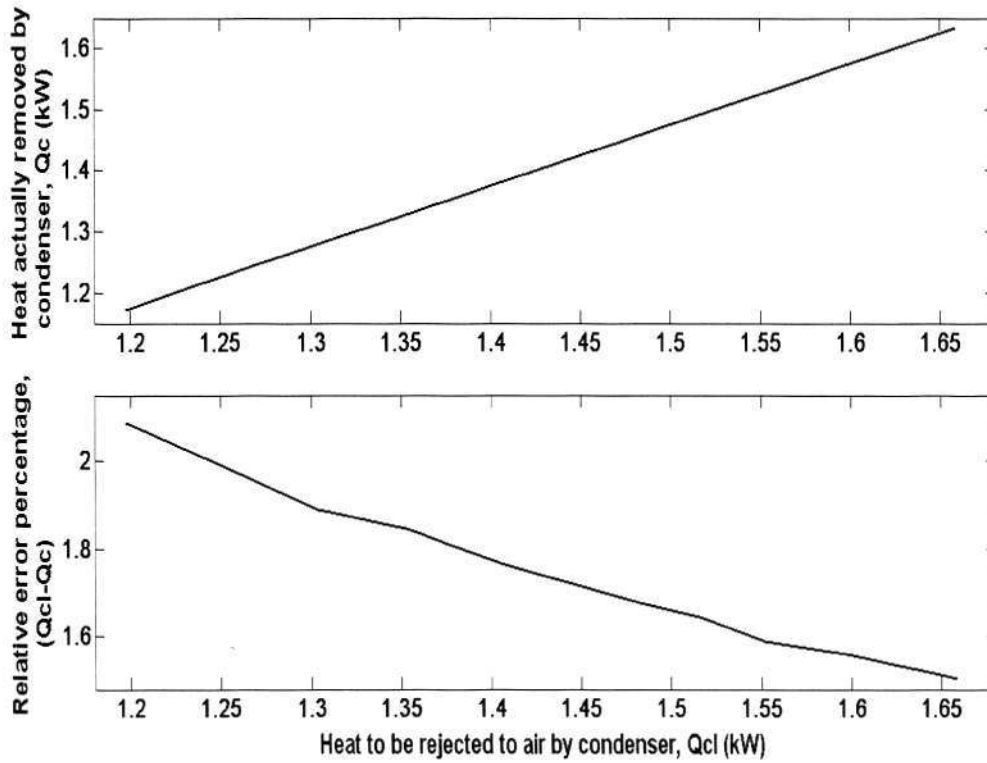


Figure 5.3: Heat transfer in condenser

To ascertain that the calculated (or actual) amount of heat transfer in condenser Q_c is the same as Q_{cl} , penalty function $W_{penalty2}$ is used.

$$\text{If } \text{abs}(Q_{cl} - Q_c) > 0.015 \quad (5.2a)$$

$$W_{penalty\ 2} = e^{|(Q_{cl}-Q_c)|*10} \quad (5.2b)$$

The genetic algorithm tries to satisfy the control objective $Q_c = Q_{cl}$, as close as feasible; if not a penalty value $W_{penalty2}$ is included in the cost function $ObjF$.

Figure (5.3) shows the result of the optimization (for both the input profiles, the results are alike); the condenser fulfils the load requirement with an error margin of about 1.6%. The load requirement, Q_{cl} is calculated by the energy balance equation i.e.

$$Q_{cl} = Q_e + W_{com} \quad (5.3)$$

IMPLEMENTATION AND RESULTS

where, W_{com} is the work done by compressor on the refrigerant and is calculated using the enthalpy of working fluid at its inlet and the outlet and the mass flow rate of the refrigerant.

$$W_{com} = m_{WF}(H_{compo} - H_{compi}) \quad (5.4)$$

3. Objective Function:

The optimization algorithm minimizes the objective function to its utmost extent.

From Equation (4.22),

$$ObjF = W_{comp} + W_{ef} + W_{cf} + W_{penalty\ 1} + W_{penalty\ 2} \quad (5.5)$$

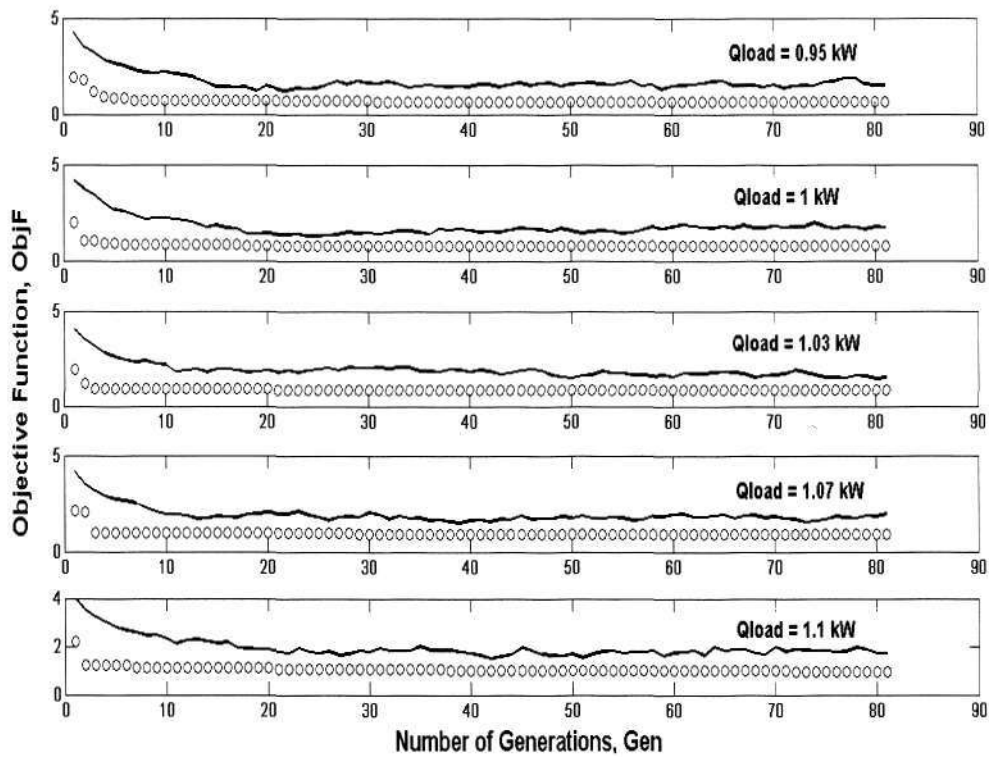


Figure 5.4a: Objective Function Convergence – Q_{load} - 0.95kW to 1.1 kW

IMPLEMENTATION AND RESULTS

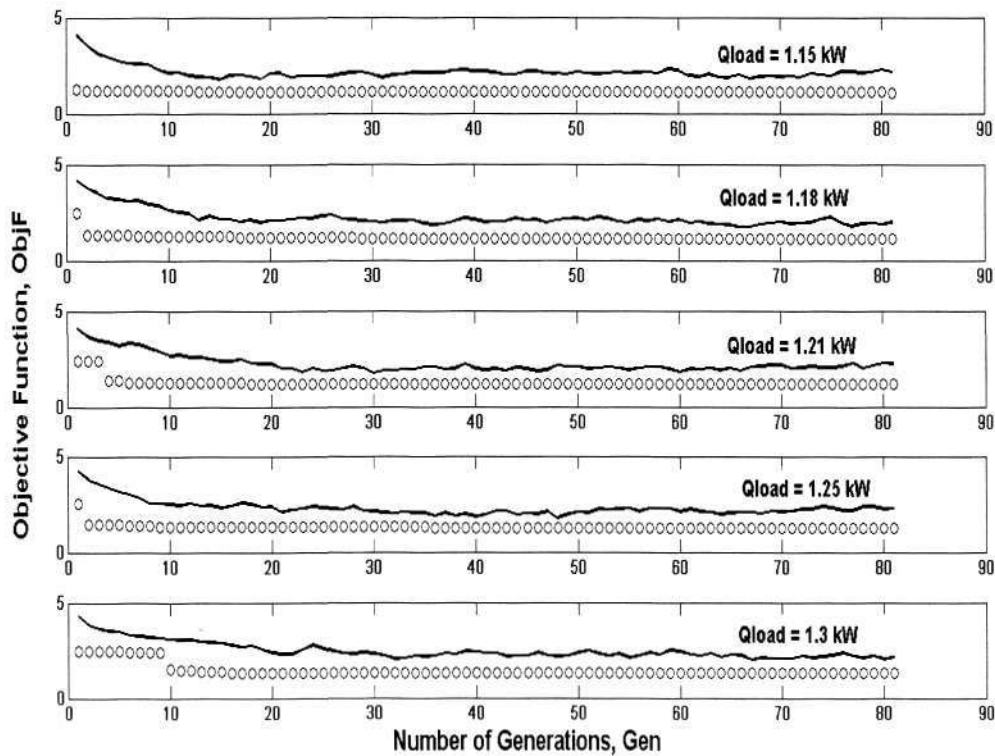


Figure 5.4b: Objective Function Convergence – Q_{load} – 1.15 kW to 1.3 kW

In each subplot in Figure (5.4a) and (5.4b), two graphs are plotted. The dark line shows the average of objective function $ObjF$ of all individuals in the population for each generation. The other value is the minimum value of objective function amongst all individuals in the population for each generation. The second plotted value is considered as the optimal power consumed by all the components of vapour compression cycle, because it nullifies the penalty values in Equation (5.5).

4. Power Consumption:

Since the purpose of optimization is to minimize the power consumed by the Vapour compression cycle while meeting the control objective, the resulting

IMPLEMENTATION AND RESULTS

objective function of the final iteration of the GA implementation, should be equal to the summation of power consumed by individual components.

$$W_{total} = W_{comp} + W_{ef} + W_{cf} \quad (5.6)$$

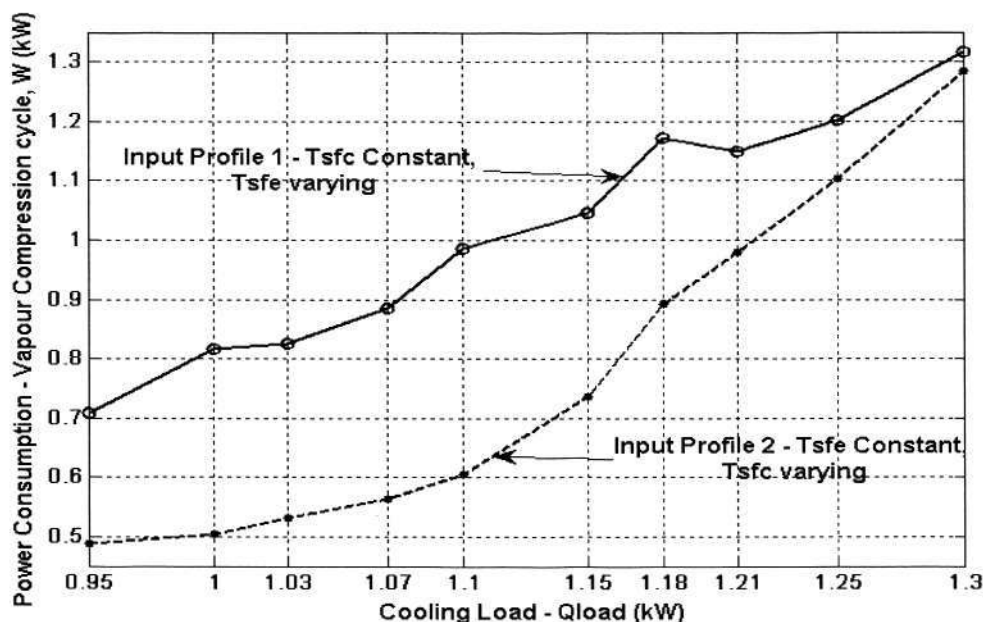


Figure 5.5: Vapour compression cycle power consumption

Figure (5.5) shows that for input profile 1, the power consumption for the given Q_{load} ranges between 0.7 to 1.3 kW; for input profile 2, the power consumption varies between 0.5 to 1.3 kW.

The power consumption value can be broken down to individual elements, W_{ef} , W_{cf} and W_{comp} as shown in Figure (5.6). As observed, the influence of compressor power consumption over objective function is more prominent than the evaporator and condenser fans. Consequentially, for increasing cooling load, the W_{comp} plot gradually rises, while W_{ef} and W_{cf} appear random.

IMPLEMENTATION AND RESULTS

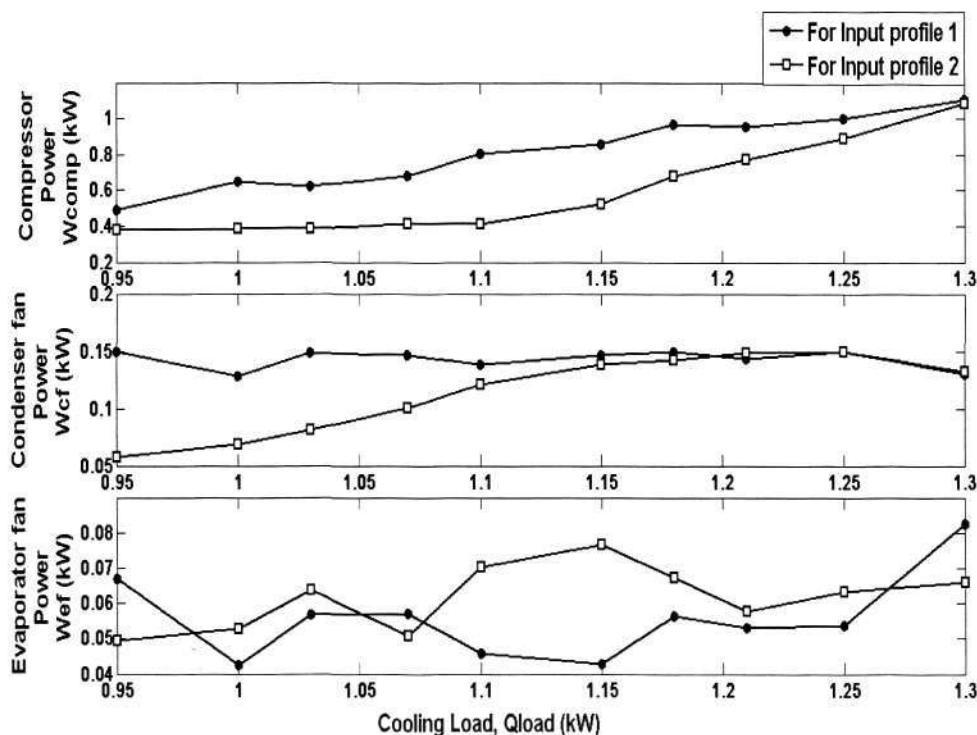


Figure 5.6: Power consumption – Compressor, Condenser fan, Evaporator fan

5.2 Comparison with ON-OFF Control

The ON-OFF control is used predominantly in simple refrigeration systems, such as the air-conditioning units in residential buildings. The comparison of the above explained optimization algorithm with a simple ON-OFF control is required to show advantages of GA based control, if any. Thus, we first delve into the basics of ON-OFF control. We then, discuss the input profile that we will use for the comparison of both control methodologies. Later in section (5.2.4), we would see the difference in the two methods.

IMPLEMENTATION AND RESULTS

The assessment is based on the amount of energy consumed in 24 hours by the vapour compression cycle, in case of ON-OFF control and the energy consumed by the system in case of optimization control. This is calculated in kilowatt-hours.

5.2.1 Comparison Base - Input Profile

To carry on with the comparison between the two controls methodologies, we need to develop a base-case for comparison. A temperature profile for 24 hours is assumed, with the corresponding heat content of the room. These values are used so as to make the comparison viable (the vapour compression cycle model employed in this thesis has the capacity to remove heat between 0.95 to 1.3 kW). Thus, the room equipped with the air-conditioning system has temperature varying between 23 °C to 27 °C. Also, the heat load, Q_{load} varies between 0.95 to 1.3 kW, but the profile is different for each room temperature value. The maximum power drawn by the refrigeration system is taken as 1.5 kW.

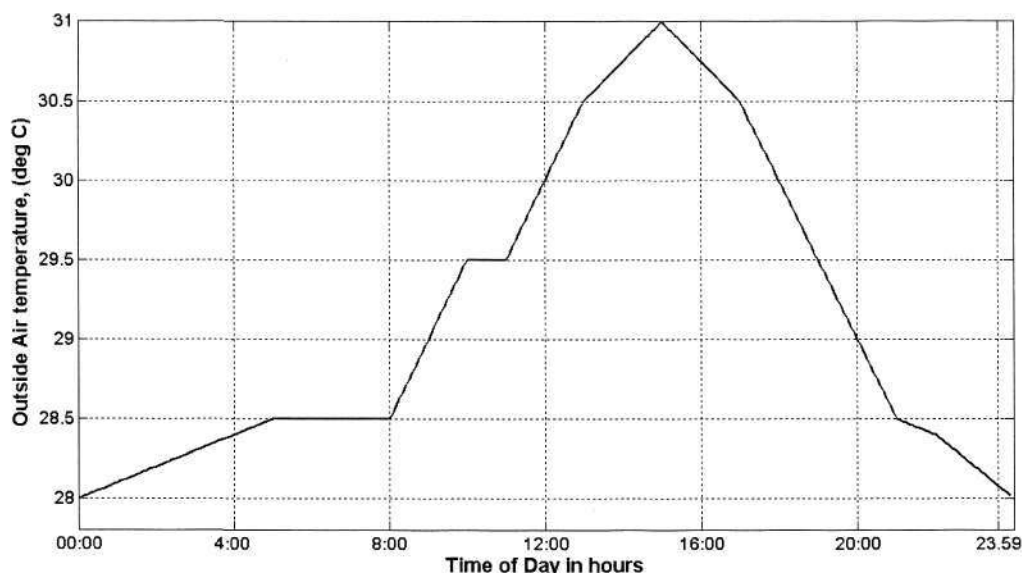


Figure 5.7: Outside Air temperature profile

IMPLEMENTATION AND RESULTS

Assuming the temperature varies in a manner described below for a time frame of 24 hours, in particular, 00:00 hours to 23:59 hours, the heat load will also vary in a similar way. Figure (5.7) shows an example for outside air temperature variation.

This profile is just an example, and may be different for different regions and geographies. Corresponding to the above outside air temperature profile, the cooling load for the room (with temperature control) varies in a similar manner. For a particular room temperature, the cooling load requirement or the heat content to be removed from the room is low at off-peak hours and increases during daytime.

Since the cooling load for the model considered can vary only between 0.95 to 1.3 kW, we cannot consider loads greater than 1.3 kW.

Thus for a room of 100 m³ volume, and for room temperature 23°C, the cooling load variation throughout the day is shown in Figure (5.8).

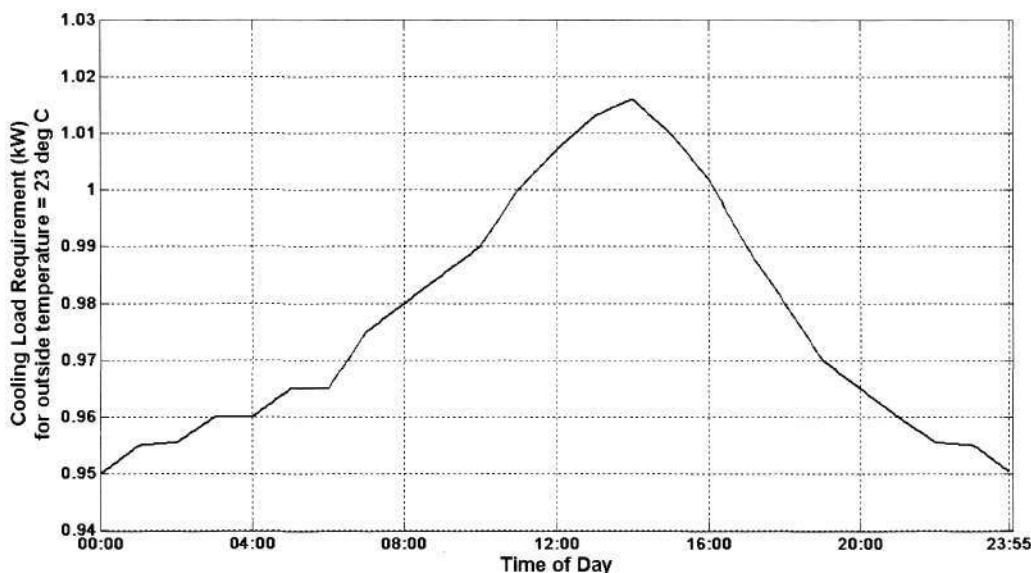


Figure 5.8: Cooling load requirement of room for outside air temperature 23°C.

IMPLEMENTATION AND RESULTS

While calculating time for temperature to decrease or to calculate temperature, after particular time duration, we use the profile shown in Figure (5.8). The plot is an example of the cooling load profile. For ON-OFF control and optimization control, we use a set of similar profiles to calculate other parameters that are required.

The parameter used in common for both algorithms is the cooling load profile for respective room temperatures, which we will delve in further sections. The air density in the room is taken as 1.184 kg/m^3 . Also, the specific heat capacity of air, C_p is taken as equal to $1.012 \text{ kJ/kg/}^\circ\text{C}$.

5.2.2 ON-OFF Control – Base Case Study

In the ON-OFF control methodology, a temperature range is defined and the room temperature has to be maintained in this temperature range. This is done by switching the air-conditioning on and off depending on the current reading of temperature.

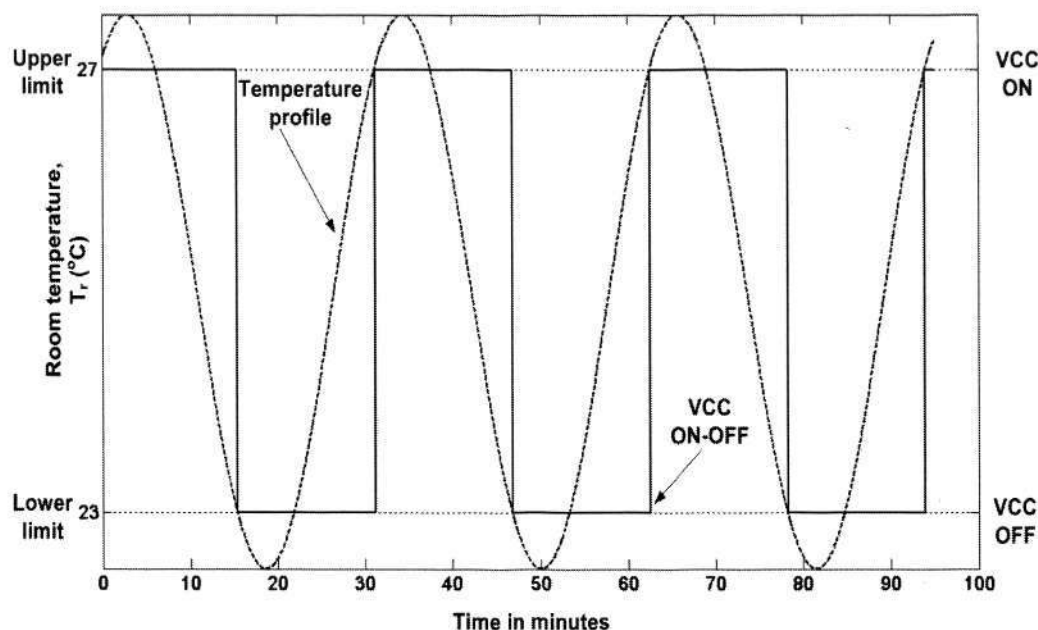


Figure 5.9: Explanation for ON-OFF Control

IMPLEMENTATION AND RESULTS

The ON-OFF method can be explained as below with the help of Figure (5.9). When the room temperature exceeds the upper limit, that is, 27°C, the VCC is switched on. Once turned on, the VCC extracts heat from the room and rejects it to the outside air or surroundings. Thus the temperature starts decreasing. When the room temperature goes below the lower limit, that is, 23°C, the VCC is switched off. Now because of natural heat convection and higher heat content in surroundings, the room temperature starts increasing. Until the temperature reaches the upper limit again, the VCC is off. Then the same cycle as explained is repeated.

The time t_{Tdec} required for the temperature to decrease from 27°C to 23°C when the VCC is switched on, is calculated as,

$$t_{Tdec} = \frac{\text{Mass of air in room} * C_p * (27 - 23)}{W_q - Q_{23}(t)} \quad (5.7)$$

where, W_q is the heat removal capacity of the vapour compression cycle = 1.3 kW. $Q_{23}(t)$ is the heat content of the room for temperature to be equal to 23°C, at the time of calculation, t (refer to Figure (5.8)).

The maximum power drawn by the vapour compression cycle, is taken as

$$W_f = W_{comp} + W_{ef} + W_{cf} \approx 1.5kW \quad (5.8)$$

W_f is the power drawn by the VCC, when on.

The time t_{Tinc} required for the temperature to increase from 23°C to 27°C when the VCC is switched off is calculated as,

$$t_{Tinc} = \frac{\text{Mass of air in room} * C_p * (27 - 23)}{Q_{27-23}(t)} \quad (5.9)$$

where, $Q_{27-23}(t)$ is heat content difference in the room, when the temperature rises from 23°C to 27°C.

IMPLEMENTATION AND RESULTS

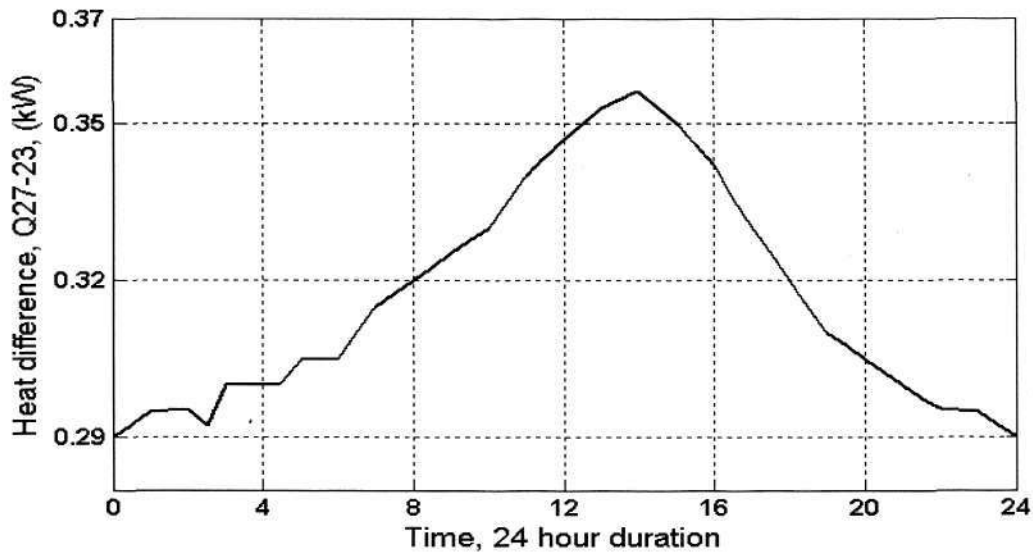


Figure 5.10: Difference in heat content between 27°C and 23°C

Q_{27-23} is the difference between the heat load at 27°C and the base heat value of room at 23°C, which is taken as 0.98kW. Thus, the heat content difference increases during daytime, and then decreases as shown in Figure (5.10).

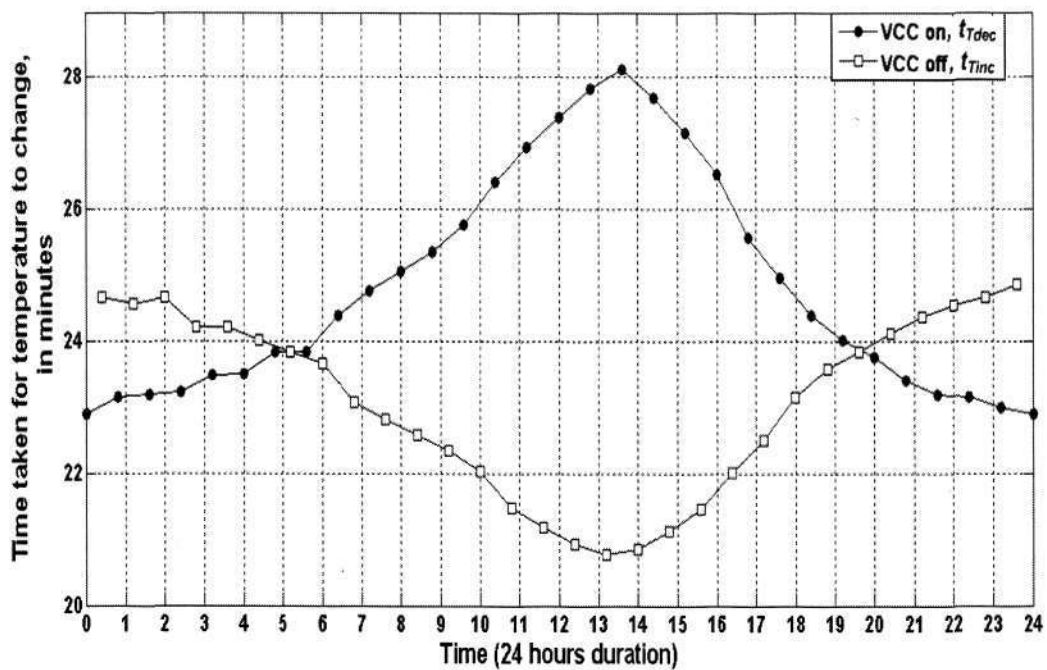


Figure 5.11: Time taken for temperature to change, with VCC on and off

IMPLEMENTATION AND RESULTS

Figure (5.11) shows that the time taken for the temperature to increase naturally (VCC off); t_{Tinc} decreases during peak hours, as the outside air heat content is higher and thus the flow of heat from room (at 23°C) to surroundings is faster.

The time taken for the temperature to reduce (VCC on), t_{Tdec} increases during daytime, as the outside air temperature and humidity also increases; thus the removal of heat requires a little extra effort than at the night-time or before daybreak. Figure (5.11) shows the change in t_{Tdec} and t_{Tinc} throughout 24 hours.

Figure (5.12) plots the power consumption pattern of the Vapour compression cycle, throughout 24 hours. Since the control is by turning VCC alternately on and off, the power consumption also switches between 1.5 kW when temperature T_{room} reaches 27 °C; and 0 kW when T_{room} decreases to 23 °C.

IMPLEMENTATION AND RESULTS

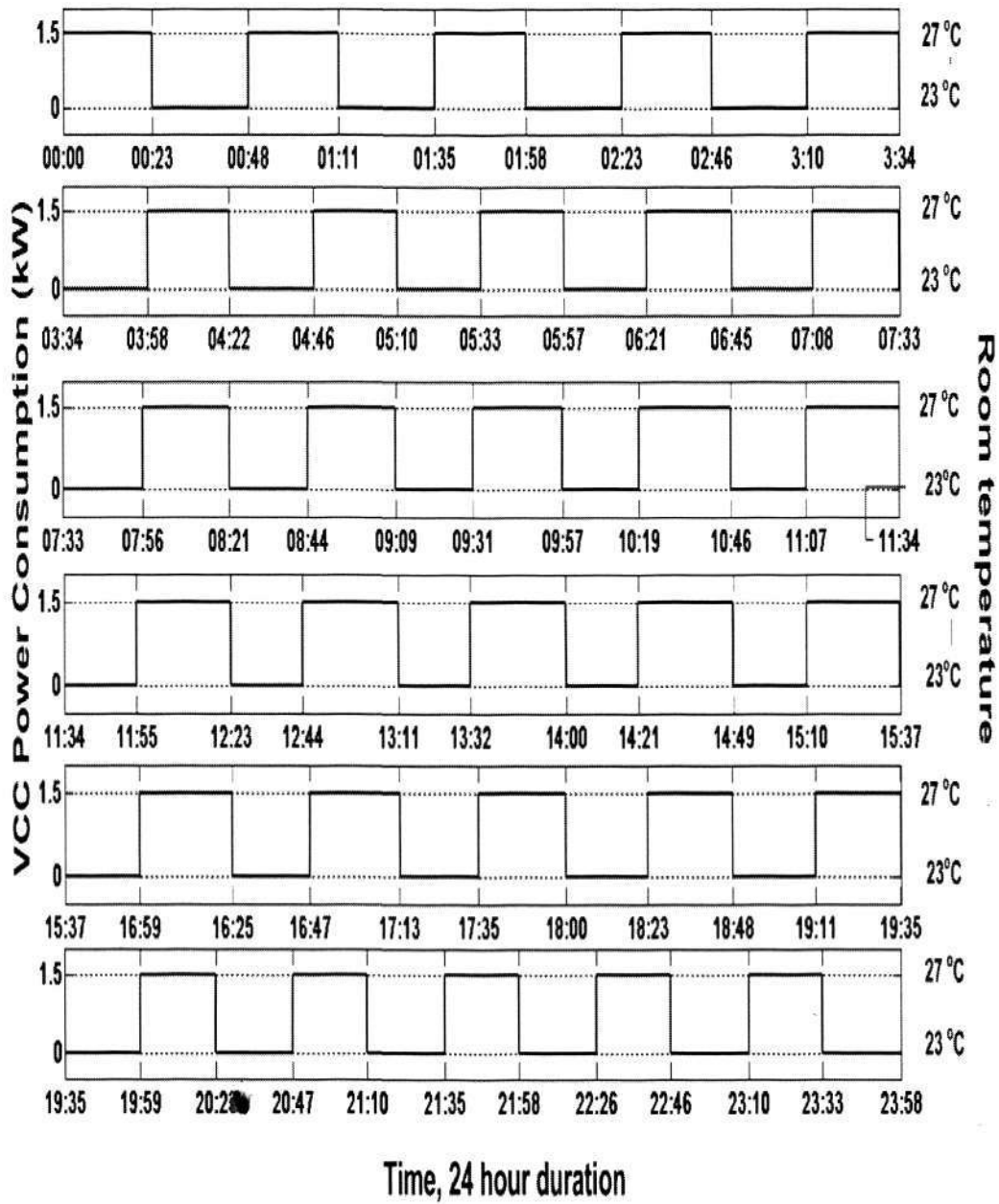


Figure 5.12: Power consumption of VCC in 24 hours

The energy consumed by the vapour compression cycle, is estimated as,

$$E_{Whour} = W_f * t_{Tdec} \quad (5.10)$$

IMPLEMENTATION AND RESULTS

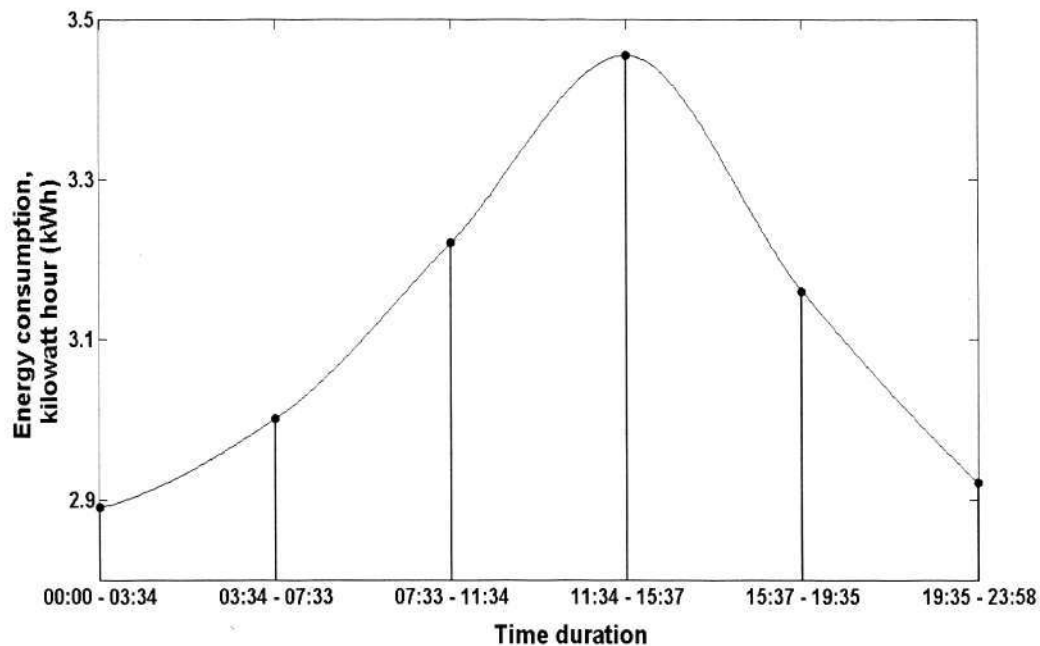


Figure 5.13: VCC energy consumption in 24 hours

Figure (5.13) illustrates the energy consumption for different durations in one whole day. As observed, at peak hours in the afternoon, the consumption is higher; it is lesser during night time and early morning. For the duration of 24 hours the energy consumed when the VCC is operated by on-off control is,

$$E_{Onoff} = 18.654 \text{ kWh} \quad (5.11)$$

5.2.3 GA optimization Control

Based on the input profile discussed in Section 5.2.1, the optimization strategy is implemented as a control method on the vapour compression cycle. In optimization based (genetic algorithm) control methodology, a new set of manipulated variables is sent to the VCC controller in predefined intervals. This is unlike on-off control method, where the VCC is turned to either full load or zero- load depending on the upper and lower temperature limits.

IMPLEMENTATION AND RESULTS

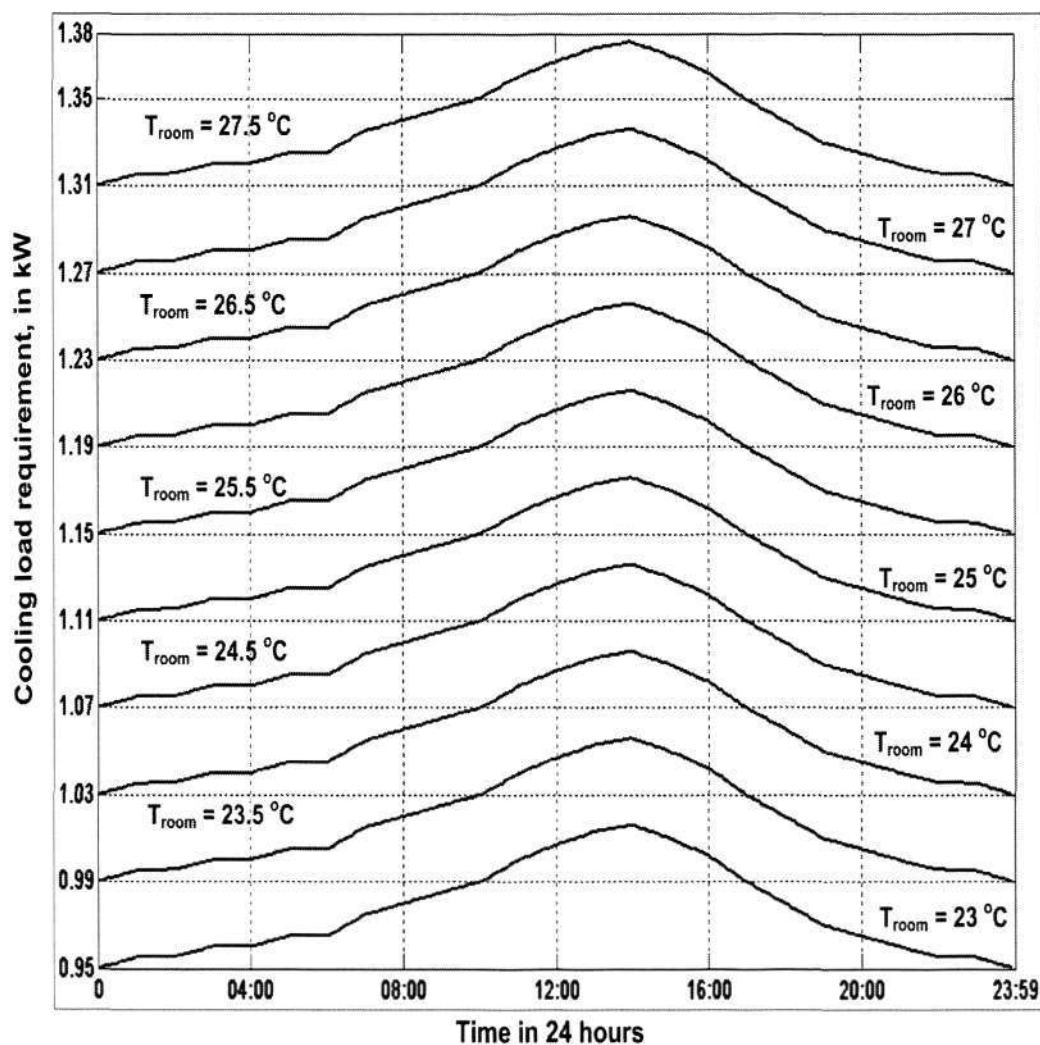


Figure 5.14: Cooling load profiles for varying room temperature

The prerequisites for GA optimization control of VCC for duration of 24 hours are.

- Outside air temperature profile, as shown in Figure (5.7).
- Set point temperature $T_{SP} = 25$ °C.
- Heat content / cooling load Q_{SP} corresponding is T_{SP} is shown in Figure (5.15)
- Room temperature range,

$$T_{room} = [23 \ 23.5 \ 24 \ 24.5 \ 25 \ 25.5 \ 26 \ 26.5 \ 27 \ 27.5]$$

- Heat content graph Q_{load} corresponding to T_{room} is shown in Figure (5.14).

IMPLEMENTATION AND RESULTS

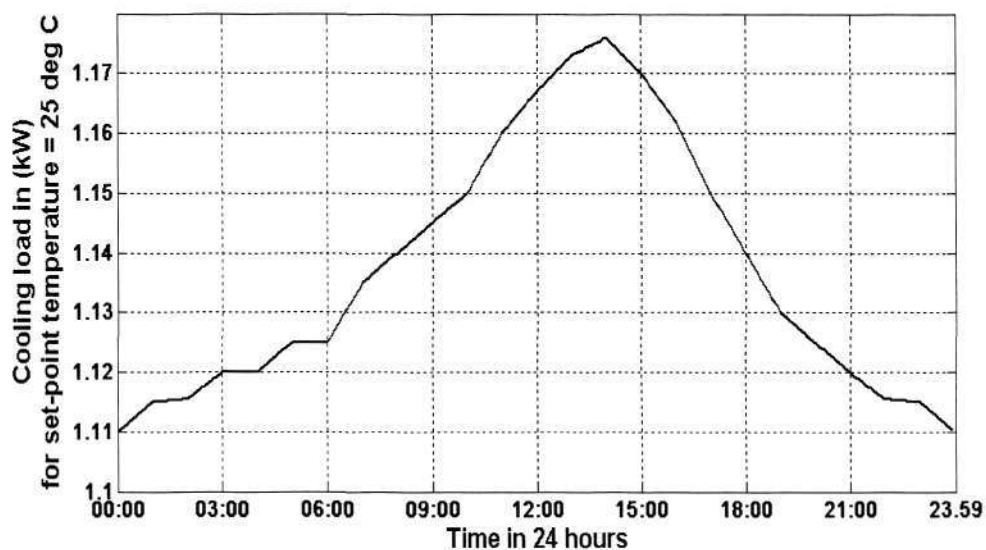


Figure 5.15: Cooling load profile for $T_{SP} = 25$ °C, in 24 hours.

Algorithm Description:

The algorithm for optimization based control of VCC for temperature control can be explained as below.

The algorithm is started at $t = 0$ hours and is implemented every 5 minutes during the whole cycle of 24 hours. The room temperature $T_{room}(t)$ is initially assumed to be 27 °C. The energy consumption $E_{opt}(t = 0)$ is equal to 0.

1. The Q_{load} graph corresponding to $T_{room}(t)$ is estimated from Figure (5.15)
2. GA based optimization algorithm from Sections 4.3.1 and 4.3.2 are implemented for $Q_{load}(t)$, $T_{SFc} = T_{air}(t)$ and $T_{SFc} = T_{room}(t)$. The GA algorithm outputs values of manipulated variables matrix $workpoint(t)$, and power consumed $W(t)$.
3. For current room temperature, $T_{room}(t)$, the corresponding Q_{Troom} is the median value of the heat content at that temperature. This value is time invariant and only changes when the room temperature varies.

IMPLEMENTATION AND RESULTS

4. The change in temperature due to removal of heat by the vapour compression cycle is represented as,

$$\text{del}T = \frac{((Q_{T_{room}} - Q_{SP}(t)) * 5 * 60)}{(\text{Air Mass in room} * C_p)} \quad (5.12)$$

The above change in temperature is at the end of the 5 minute cycle. Thus the new room temperature after 5 minutes is,

$$T_{room} \left(t + \frac{5}{60} \right) = T_{room} (t) - \text{del}T \quad (5.13)$$

5. The energy consumption, $E_{opt}(t)$ is calculated every 5 minutes.

$$E_{opt} \left(t + \frac{5}{60} \right) = E_{opt} (t) + W(t) * \frac{5}{60} \quad (5.14)$$

6. Time t is incremented by 5 minutes and the above algorithm from Step number 1 is repeated. The procedure is continued for one whole day, i.e. until $t = 24$ hours.

The result $E_{opt}(t=24)$ is the energy consumed by vapour compression cycle for one whole day. The simulation of VCC with optimal set-point control for 24 days can be explained as a flowchart shown in Figure (5.16).

IMPLEMENTATION AND RESULTS

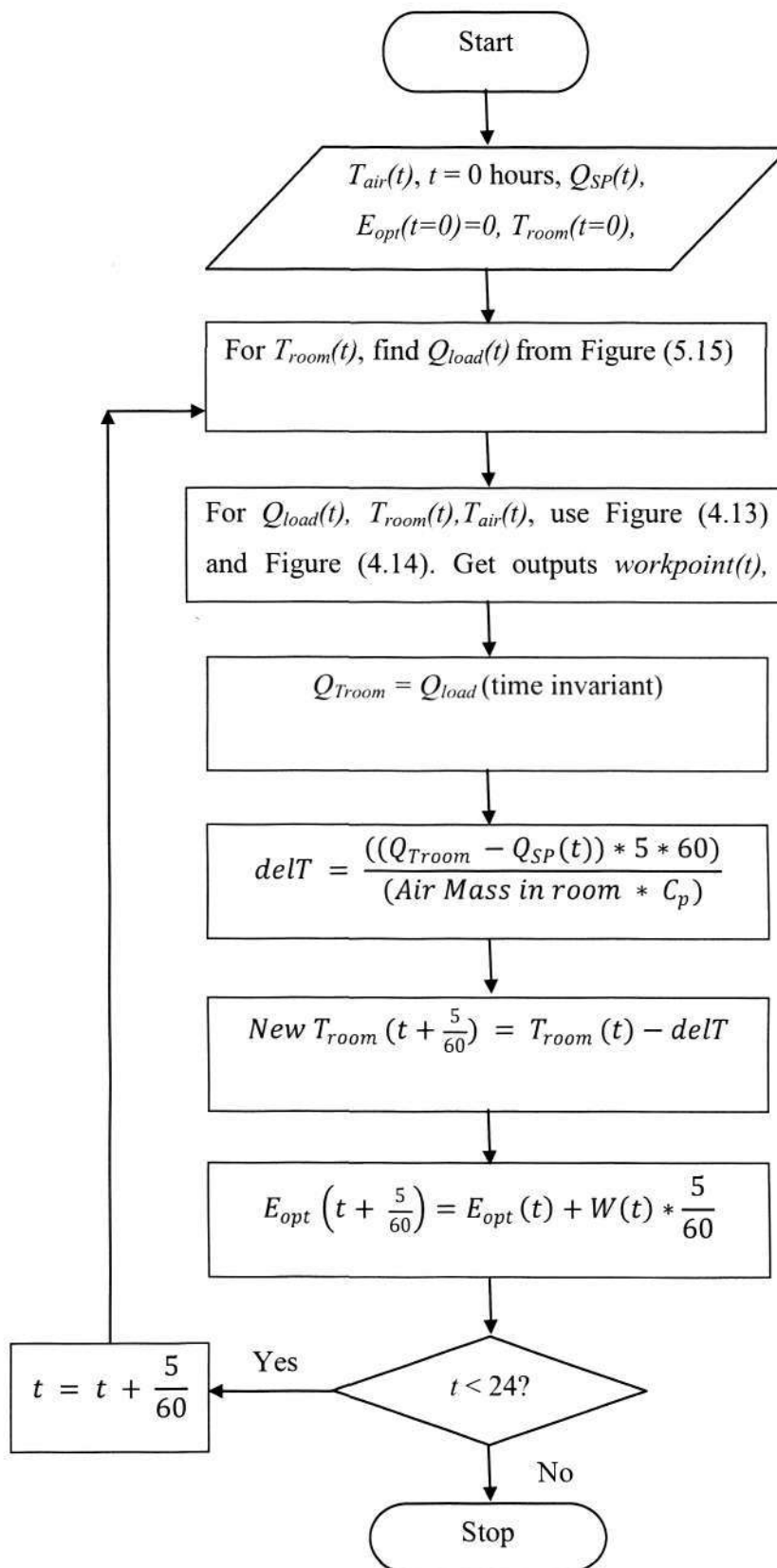


Figure 5.16: Flowchart for optimization based control of VCC for one whole day

IMPLEMENTATION AND RESULTS

By implementing the GA based optimization control, the power consumed by the vapour compression cycle for the inputs and initial conditions as mentioned above, is shown in Figure (5.17).

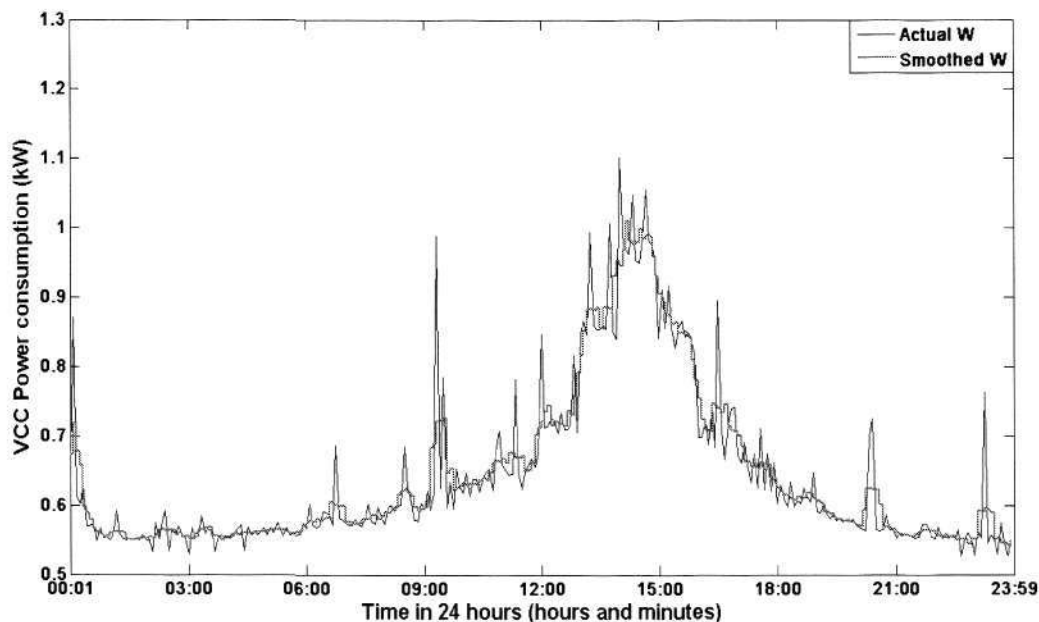


Figure 5.17: VCC power consumption for 24 hours

As observed the power consumption reaches the peak in the afternoon, and is lesser during early hours and night-time. This is in the same manner as the cooling load profile and outside air temperature profile, which peaks during the day and reduces at night time.

The set point temperature T_{SP} is kept at 25°C . The actual temperature, T_{room} is calculated by the above algorithm and is plotted in Figure (5.18). The room temperature lies within 24.5°C to 25.5°C . Due to higher heat content and outside air temperature the temperature is higher during peak hours.

IMPLEMENTATION AND RESULTS

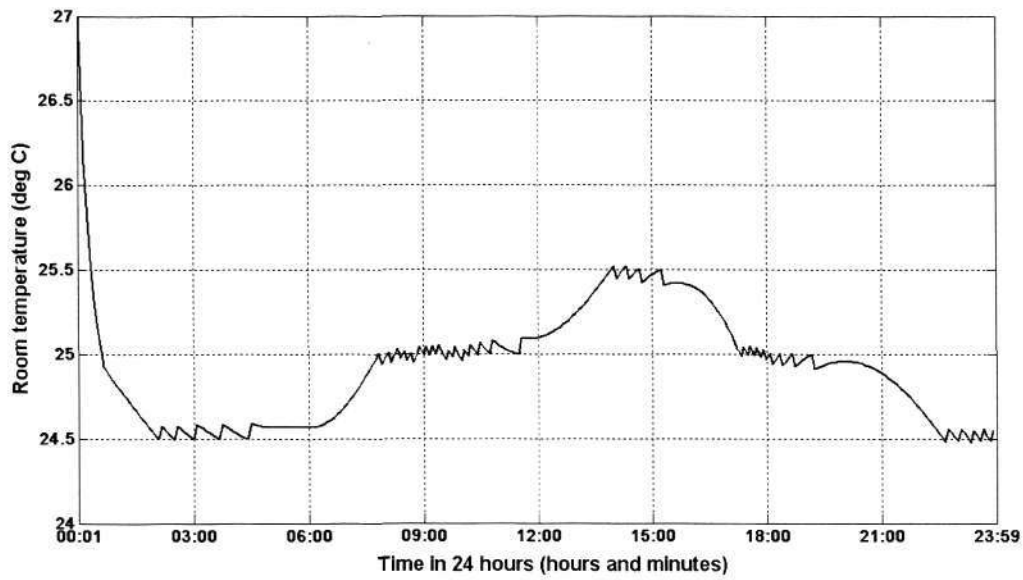


Figure 5.18: Room temperature in the course of 24 hours

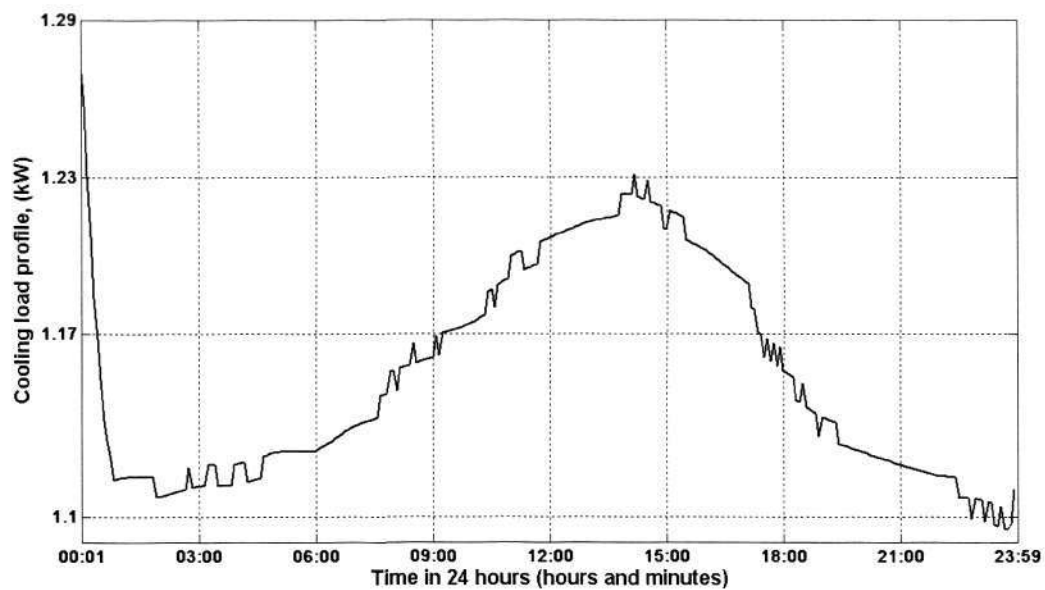


Figure 5.19: Calculated Cooling load for 24 hours

Depending on the room temperature, the cooling load for the next iteration (5 minute later) is estimated using Figure (5.15). The cooling load - temperature graph is spaced evenly for every 0.5 °C. Therefore, if the room temperature changes as a multiple of 0.5 °C, the corresponding curve is chosen and the cooling load value for that time

IMPLEMENTATION AND RESULTS

instant is taken for further calculations. The calculated cooling load for 24 hours is plotted as shown in Figure (5.19).

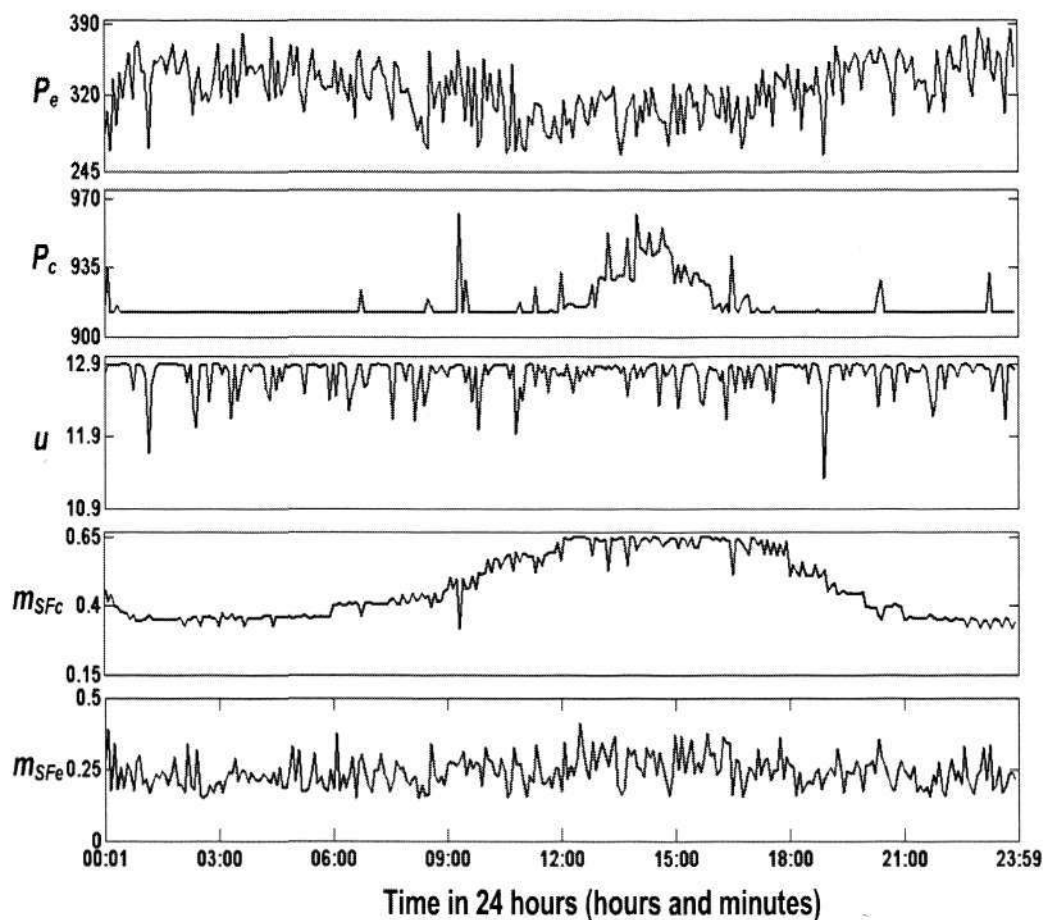


Figure 5.20: Manipulated variables values- P_e , P_c , u , m_{SF_c} , m_{SF_e} for 24 hours

The outcome of genetic algorithm based optimization is *workpoint*. The *workpoint* array includes values of manipulated variables for energy-optimal performance of vapour compression cycle. The manipulated variable as listed below are plotted in Figure (5.20), for a period of 24 hours.

- Saturation pressure for evaporation P_e
- Saturation pressure for condensation P_c
- Percentage opening of expansion valve, u

IMPLEMENTATION AND RESULTS

- Mass flow rate of air through condenser fan, m_{SF_c}
- Mass flow rate of air through evaporator fan, m_{SF_e}

The energy consumption E_{opt} is calculated by Equation (5.14). In Figure (5.21), the calculated energy consumed by VCC is illustrated for every 3 hours.

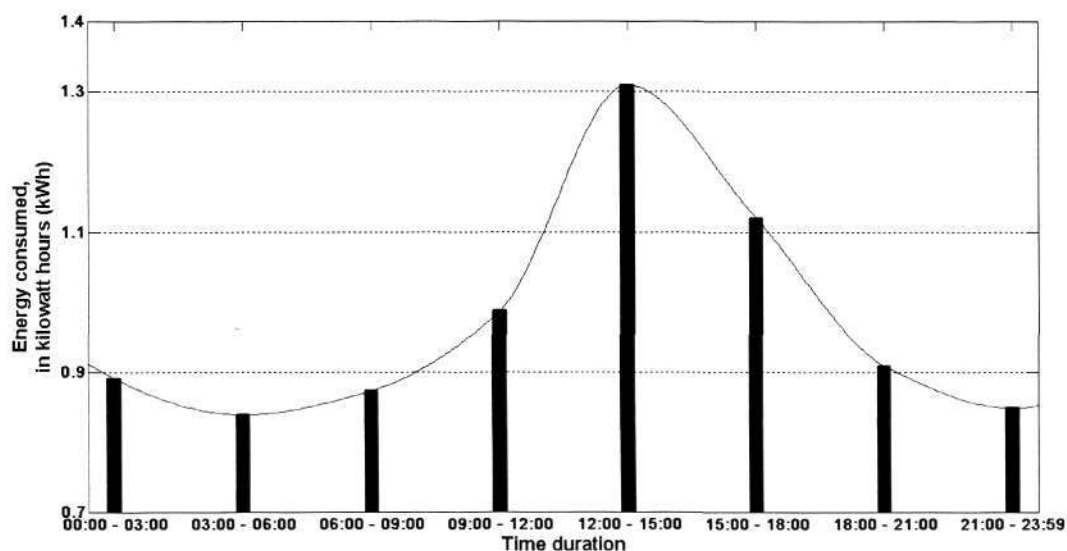


Figure 5.21: Energy consumption of VCC (optimized control) in 24 hours

The calculated energy consumption by the vapour compression cycle when controlled by genetic algorithm based optimization method for duration of 24 hours is,

$$E_{opt_day} = 15.464 \text{ kW} \quad (5.15)$$

5.2.4 Comparison

To give a quantitative idea of the possibility of any improvement in the performance, i.e. reduction in energy consumption, the on-off control was simulated for the same set of inputs and basic factors which were used in the genetic algorithm based set-point optimization method. Thus, the on-off control method which acts as the base-case is compared with the method proposed in this thesis to give a measure of the

IMPLEMENTATION AND RESULTS

amount of reduction of energy the optimization method can afford. Figure (5.22) compares VCC energy consumption when the on-off control is implemented, with set-point optimization control.

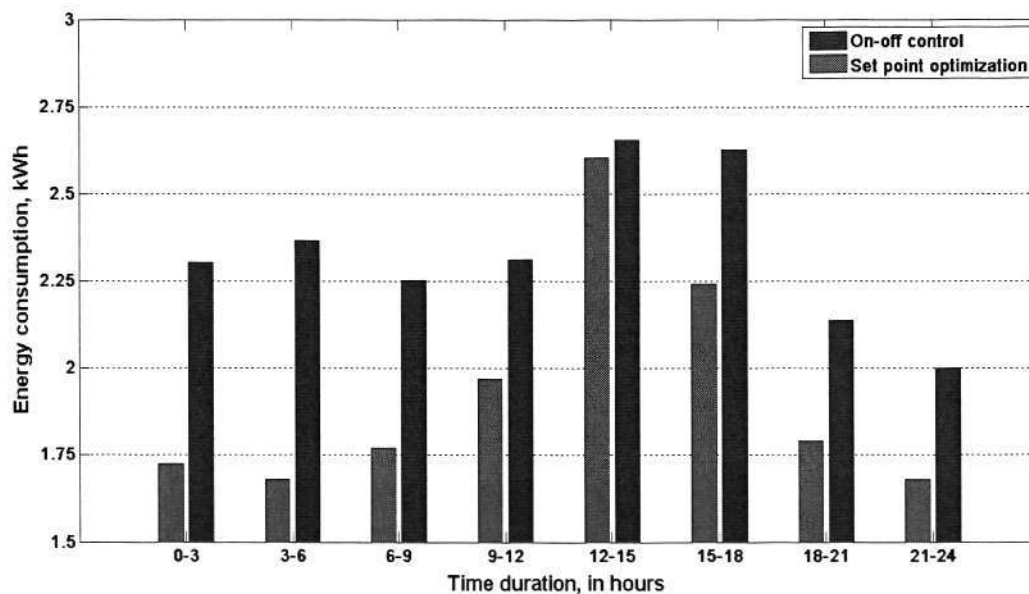


Figure 5.22: VCC Energy consumption– for every 3 hours (on-off Vs optimization)

The percentage reduction in energy consumption by VCC in 24 hours, when controlled by optimization algorithm with respect to on-off control is,

$$E_{rel} = \frac{(E_{onoff} - E_{opt_day})}{E_{onoff}} * 100 \quad (5.16)$$

From Equation (5.11) and (5.15), E_{rel} is calculated as

$$E_{rel} = \frac{(18.654 - 15.464)}{18.654} * 100 = 17.10\%$$

Thus the percentage reduction in energy consumed offered by optimization based control method is 17.10%. The value, E_{rel} is only applicable to the model used and for the inputs assumed in the thesis. If implemented on a real system, the value may vary.

IMPLEMENTATION AND RESULTS

The comparison between the energy consumed by VCC in 24 hours, when on-off control method is applied and set-point optimization is employed is shown in Figure (5.23)

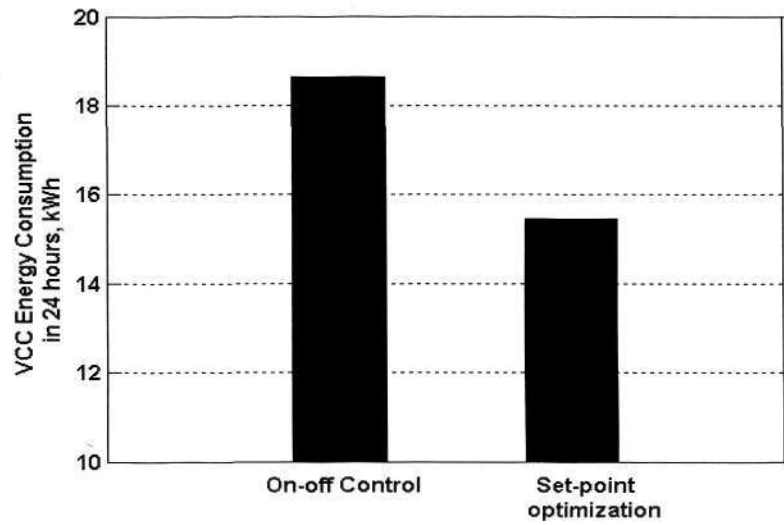


Figure 5.23: VCC Energy consumption for 24 hours duration, in kWh

Chapter 6

Conclusion and Future Scope

6.1 Conclusion

Set-point optimization of the vapour compression cycle forms the basis of the thesis. An easy to use optimization method, based on genetic algorithm was developed for the vapour compression cycle. The simplicity and straightforward implementation can offer a great advantage over other advanced control methods and also over traditional methods such as on-off and manual control.

The works done in the thesis can be summarized as below.

1. Mathematical Model Development:

The mathematical representation of the vapour compression cycle is a combination of individual models. In the hybrid representations of evaporator and condenser, the dynamics of air in the room, outside air and the working fluid (refrigerant) are taken together thus simplifying the implementation of optimization on the whole model of vapour compression cycle. The models are determined with the help of simulated version of vapour compression cycle developed in *Simulink*®. The mathematical models used have an unique

CONCLUSION AND FUTURE SCOPE

advantage, because it includes both working fluid and secondary fluid, therefore eliminating many of the intermediate parameters which are generally associated with the vapour compression cycle.

2. Development of Genetic Algorithm based optimization technique:

Genetic algorithm is used as optimization tool because it is efficient and simple to use. The various genetic tools were studied and used for the purpose of optimization of vapour compression cycle. As discussed in chapter 4 and 5, the use of genetic algorithm leads to convergence of the cost function value within a hundred iterations. The cost function in the case of optimization is the addition of power consumed by the various components in vapour compression cycle and the penalty functions which oversee the constraints.

3. Implementation of optimization on vapour compression model:

The optimization algorithm was implemented on the vapour compression cycle model. The inputs, namely, outside air temperature, room temperature and cooling load were assumed in two separate cases. In the first case, the outside air temperature was taken as constant while the room temperature is increasing and in the second case, the outside air temperature was taken as linearly increasing while the room temperature was taken as constant. For both instances, the cooling load is varied between 0.95 to 1.3 kW. The results calculate the power consumed by the vapour compression cycle while conforming to the objective function which requires that the required amount of heat is removed from the room to maintain the temperature at a reference value.

CONCLUSION AND FUTURE SCOPE

4. Comparison: on-off and GA based optimization control:

The on-off control is still widely used because it is straightforward and satisfies the control objective of maintaining the temperature within a set-point range. Since this method is widely used, and easy to implement as well, this method was taken as the base case. The comparison results show that the percentage reduction in energy consumed offered by optimization based control method is 17.10%.

6.2 Discussions and Future Scope

In the following section, ideas for future work and research are stated.

1. The vapour compression cycle used in the thesis can take a heat load of 0.95 to 1.3kW. Although here the optimization is limited only for this range, it will almost certainly be advantageous for whatever range it is adopted for. The percentage improvement provided by the implementation might vary for different ranges, and that should be studied for a wider understanding of this optimization technique.
2. In this thesis, the implementation of genetic algorithm based optimization control is done in MATLAB on a mathematical model of vapour compression cycle. It would be worthwhile to use the optimization algorithm on a test-bed. A real system will throw in more complexities, like vapour compression cycle efficiency, heat transfer loss in evaporator and condenser, modelling errors et-al. In addition, the inputs assumed for the simulated environment, like air temperature and load demand may be actually measured and calculated

CONCLUSION AND FUTURE SCOPE

- accordingly. This may lead to a real view of the advantage the optimization algorithm might command over traditional methods.
3. The method discussed in the thesis is set-point optimization of vapour compression cycle. Referring to section 2.2.2, set-point optimizer calculates the set-points values for which the system will run in energy-optimal mode. For a more complicated and stricter environment like pharmaceutical factories, dynamic optimizing control can also be implemented along with the investigated set-point optimizer.
 4. The implementation in the thesis is for a simple vapour compression cycle. For a wider domain, this should be further incorporated in Heating Ventilation and Air Conditioning systems. In an HVAC system, the secondary flow in evaporator is the chilled water and the secondary flow in condenser is the condenser water. Both of them if already controlled by interacting controllers, will affect the operation and may increase the complexity in control algorithm for the vapour compression cycle (chiller system).

BIBLIOGRAPHY

Bibliography

- [1] Automated Curve Fitting Analysis, *TableCurve 2D*®,
URL: <http://www.sigmaplot.com/downloads/download.php>
- [2] Building and Construction Authority, Green Building Design Guide – Air conditioned buildings,
URL: <http://www.bca.gov.sg/GreenMark/others/ggenergy.pdf>
- [3] Building and Construction Authority, Media release - 27 April 2009,
URL: <http://www.bca.gov.sg/Newsroom/others/pr270409.pdf>.
- [4] Choi J.M., Kim Y.C. (2003) , *Capacity modulation of an inverter-driven multi-air conditioner using electronic expansion valves* *Energy*, 28 (2), pp. 141-155,
- [5] Dossat, R. J. (2002). *Principles of refrigeration*. Prentice Hall.
- [6] Elliott M.S. and Rasmussen B.P. (2008). *Model-based predictive control of a multi-evaporator vapor compression cooling cycle*. 2008. Seattle, WA, United states: Institute of Electrical and Electronics Engineers Inc.
- [7] Gen, M. (2000). *Genetic algorithms and engineering optimization*. Wiley.
- [8] Goldberg D.E., (1989), *Genetic Algorithms in Search Optimization and Machine Learning*. Reading, MA: Addison-Wesley.
- [9] He X.-D., et al. (1998), *Multivariable control of vapor compression systems*. HVAC and R Research, 4(3): p. 205-230.
- [10] Holland J.H., (1975), *Adaptation in Natural and Artificial Systems*, Cambridge, MA: MIT Press.

BIBLIOGRAPHY

- [11] Leducq D., Guilpart J., and Trystram G. (2006), *Non-linear predictive control of a vapour compression cycle*. International Journal of Refrigeration, 29(5): p. 761-772.
- [12] Larsen L. F. S (2005), *Model Based Control of Refrigeration Systems*, Department of Control Engineering. Denmark, Aalborg University. Ph.D thesis.
- [13] Lu, L., W. Cai, et al. (2005). *Global optimization for overall HVAC systems-- Part I problem formulation and analysis*. Energy Conversion and Management 46(7-8): 999-1014.
- [14] Lu, L., W. Cai, et al. (2005). *Global optimization for overall HVAC systems-- Part II problem solution and simulations*. Energy Conversion and Management 46(7-8): 1015-1028.
- [15] Lu, L., W. Cai, et al. (2004). *HVAC system optimization--condenser water loop*. Energy Conversion and Management 45(4): 613-630.
- [16] Lu, L., W. Cai, et al. (2005). *HVAC system optimization--in-building section*. Energy and Buildings 37(1): 11-22.
- [17] *Nicorta Ventil Selection program*, URL: <http://www.nicotra.co.uk/>
- [18] Onwubiko, C. O. (1984). *Introduction to engineering design optimization* Prentice-Hall.
- [19] Outtagarts, A., P. Haberschill, and M. Lallemand (1997), *The transient response of an evaporator fed through an electronic expansion valve*. International Journal of Energy Research, 1997. 21(9): p. 793-807.
- [20] Potter, M. C. (2006). *Schaum's outline of thermodynamics for engineers* McGraw-Hill.

BIBLIOGRAPHY

- [21] R.B. Holstein (1971), *Artificial Genetic adaptation in computer control systems*, Department of Computer and Communication Sciences, University of Michigan Ann Arbor, PhD thesis.
- [22] Shah R., Rasmussen B.P., and Alleyne A.G. (2004), *Application of a multivariable adaptive control strategy to automotive air conditioning systems*. International Journal of Adaptive Control and Signal Processing, 2004. 18(2): p. 199-221.
- [23] Sonntag, R. E., C. Borgnakke and G. J. Van Wylen (1998), *Fundamentals of Thermodynamics(5th edn)*. John Wiley and Sons,
- [24] Vanderplaats, G. N. (1984). *Numerical optimization techniques for engineering design : with applications*, McGraw-Hill.
- [25] Venkataraman, P.,(2002). *Applied optimization with MATLAB programming* Wiley.
- [26] Xudong Ding, W. Cai, Lei Jia, Changyun Wen (2008), *Evaporator modeling – A hybrid approach*, Applied Energy 86: 9.
- [27] Xudong Ding, W. Cai, Lei Jia , Changyun Wen (2008). *A hybrid condenser model for applications in steam ejector air-conditioning systems*, IEEE Conference on Industrial Electronics and Applications, ICIEA 2008 6.
- [28] Yeh, T.J., et al. (2009), *Incorporating fan control into air-conditioning systems to improve energy efficiency and transient response*. Applied Thermal Engineering, 2009. 29(10): p. 1955-1964.

APPENDIX

Appendix A

A.1 Component Models

In Chapter 3, various mathematical formulations associated with the components of vapour compression cycle were described. The constants for each of the formulation are as below.

1. Evaporator Model:

$$Q_e = \frac{(H_g - H_{WF_i})\dot{m}_{WF} + c_1 \dot{m}_{WF}^e (T_{SF_i} - T_{sat})}{1 + c_2 \left(\frac{\dot{m}_{WF}}{\dot{m}_{SF}}\right)^e} \quad (\text{A.1})$$

where,

$$c_1 = 0.8683$$

$$c_2 = 2.6722$$

$$e = 0.8639$$

2. Condenser Model:

$$Q_c = \frac{d_1 \dot{m}_{WF}^{e_1} (T_{sat} - T_{SF_i}) + d_2 \dot{m}_{WF} (T_{WF_i} - T_c) + H_{fg} \dot{m}_{WF}}{1 + d_3 \left(\frac{\dot{m}_{WF}}{\dot{m}_{SF}}\right)^{e_1}} \quad (\text{A.2})$$

where,

$$d_1 = 0.7516$$

$$d_2 = 4.1258$$

$$d_3 = 30.64$$

$$e_1 = 0.5133$$

APPENDIX

3. Expansion Valve:

$$m_{WF} = a + bu(\sqrt{\Delta P}) \quad (\text{A.3})$$

where,

$$a=1.70727808565465e-05;$$

$$b=1.89412548453991e-05$$

4. Compressor

$$W_{comp} = b_1 + b_2T_e + b_3T_e^2 + b_4T_e^3 + b_5T_c + b_6T_c^2 + b_7T_c^3 \quad (\text{A.4})$$

where,

$$b_1 = -110.3260269$$

$$b_2 = -0.005995987$$

$$b_3 = -0.000318031$$

$$b_4 = 1.34357E-05$$

$$b_5 = 7.508483311$$

$$b_6 = -0.169097785$$

$$b_7 = 0.001276775$$

5. Evaporator and condenser fans

$$W_{cf} = cf_0 + cf_1m_{cSF} + cf_2m_{cSF}^2 + cf_3m_{cSF}^3 \quad (\text{A.5})$$

$$W_{ef} = ef_0 + ef_1m_{eSF} + ef_2m_{eSF}^2 + ef_3m_{eSF}^3 \quad (\text{A.6})$$

where,

$$cf_0 = 0.026235$$

$$cf_1 = 0.002044$$

$$cf_2 = 0.346676$$

$$cf_3 = -0.0878$$

APPENDIX

$$ef_0 = 0.022008$$

$$ef_1 = 0.040252$$

$$ef_2 = 0.463528$$

$$ef_3 = -0.13714$$

A.2 Parameter Models

In chapter 4, various intermediate parameters such as saturation temperature, heat content value etc. are described. The constants associated with each of the parameters are as follows.

1. Saturation temperature from saturation pressure

$$T = d_1 + (d_2 + P(d_3 + P(d_4 + P(d_5 + P(d_6 + P(d_7 + P(d_8 + P(d_9 + P(d_{10} + (d_{11} * P)))))))))) \quad (\text{A.7})$$

where,

$$d_1 = -61.9767581773210411$$

$$d_2 = 0.483195082161747998$$

$$d_3 = -0.0017089610080956366$$

$$d_4 = 4.00093331735781744e-06$$

$$d_5 = -5.82736136954912233e-09$$

$$d_6 = 5.41707378842884822e-12$$

$$d_7 = -3.26576795419137016e-15$$

$$d_8 = 1.27001414459248502e-18$$

$$d_9 = -3.0716006692643237e-22$$

$$d_{10} = 4.1994175180710371e-26$$

APPENDIX

$$d_{11} = -2.47842942570640414e-30$$

2. Enthalpy from fluid temperature and saturation pressure

$$H_f = a_0 + P(a_1 + P(a_2 + Pa_3)) + T(a_4 + T(a_5 + Ta_6)) + PT(a_7 + a_8P) + a_9T \quad (A.9)$$

where, depending on the state of fluid, the constants differ.

Constant	Liquid	Vapour
a ₀	199.9623578	384.0611964
a ₁	-0.000531434	-0.018011617
a ₂	1.3373623	0.704649858
a ₃	-2.05517e-08	-5.48028e-06
a ₄	0.001436755	0.000650721
a ₅	-1.18893e-05	0.000246613
a ₆	6.42513e-12	-4.06979e-10
a ₇	1.48352e-05	2.30827e-06
a ₈	-9.85185e-08	-1.41516e-06
a ₉	7.9041e-10	5.78982e-08

Table A.1: Enthalpy constants for Equation (A.9)

3. Vapour Enthalpy from saturation pressure

$$H_g = e_1 + (e_2 + P(e_3 + P(e_4 + P(e_5 + P(e_6 + P(e_7 + P(e_8 + P(e_9 + P(e_{10} + (e_{11} * P)))))))))) \quad (A.8)$$

where,

$$e_1 = 360.0380668$$

APPENDIX

$$e_2 = 0.308067288$$

$$e_3 = -0.001107571$$

$$e_4 = 2.58481e-06$$

$$e_5 = -3.75956e-09$$

$$e_6 = 3.49178e-12$$

$$e_7 = -2.10384e-15$$

$$e_8 = 8.17818e-19$$

$$e_9 = -1.97734e-22$$

$$e_{10} = 2.70276e-26$$

$$e_{11} = -1.59486e-30$$

4. Liquid enthalpy from saturation pressure

$$H_f = f_1 + (f_2 + P(f_3 + P(f_4 + P(f_5 + P(f_6 + P(f_7 + P(f_8 + P(f_9 + P(f_{10} + (f_{11} * P)))))))))) \quad (\text{A.10})$$

where,

$$f_1 = 120.6556422$$

$$f_2 = 0.603210171$$

$$f_3 = -0.00208711$$

$$f_4 = 4.8726e-06$$

$$f_5 = -7.08752e-09$$

$$f_6 = 6.58368e-12$$

$$f_7 = -3.96722e-15$$

$$f_8 = 1.5423e-18$$

$$f_9 = -3.72925e-22$$

$$f_{10} = 5.0976e-26$$

APPENDIX

$$f_{11} = -3.00807e-30$$